

*Author:*
**Payne, Ruth**

*Title:*
**Chemical Variations in Cryoconite Hole Meltwaters in Antarctica During the Seasonal Freezing Process**

# CHEMICAL VARIATIONS IN CRYOCONITE HOLE MELTWATERS IN ANTARCTICA DURING THE SEASONAL FREEZING PROCESS

Ruth Payne

A dissertation submitted to the University of Bristol in accordance with the requirements for award of the degree of Master of Science by Research in the Faculty of Science

School of Geographical Sciences

August 2018

Word Count: 25,517

**Abstract**

Cryoconite holes are small, quasi-cylindrical meltwater features that form on the surface of glaciers. In Antarctica, due to the harsh surface conditions, they form lids of refrozen ice, which separate the meltwaters from the atmosphere. The freezing process is not well-documented in Antarctic cryoconite holes because of the challenges associated with direct sampling techniques. This study presents geochemical modelling as a suitable alternative, using data from Bagshaw *et al,* (2007) and Fortner *et al.,* (2005) to examine important changes in meltwater chemistry as the seasonal cryoconite hole freeze-up takes place. In the high melt season, lidded cryoconite holes are more alkaline than their open counterparts. However, when calcite begins to precipitate at approximately 90% Freezing, pH collapses in lidded cryoconite holes. By contrast, atmospheric equilibrium in terms of $pCO_2$ in open cryoconite holes buffers the reduction in pH, decreasing the magnitude of change. pH in closed cryoconite holes therefore undergoes a transition from moderately-alkaline to moderately-acidic. $pCO_2$ is forced to remain at equilibrium in open cryoconite holes, but in lidded cryoconite holes, $pCO_2$ increases to values above atmospheric levels, as $CO_2$ is squeezed into the headspace from the meltwater as the volume of meltwater decreases at a slower rate than the volume of the headspace. This leads to the build up of gas pressure in the headspace. The large range of conditions that an Antarctic cryoconite hole experiences throughout the freezing process are likely to provide further stress to psychrotolerant species inhabiting the microenvironment.

Abstract word count: 245

**Acknowledgements**

I would like to thank Martyn Tranter for his supervision throughout this project. His guidance was invaluable during the whole process, and made it great fun, even when the end seemed far.

I would also like to thank my family and friends; those who have listened to my questions and ramblings. It may not have made sense to them, but it helped it make sense to me.

## Author’s Declaration

I declare that the work in this dissertation was carried out in accordance with the requirements of the University's *Regulations and Code of Practice for Research Degree Programmes* and that it has not been submitted for any other academic award. Except where indicated by specific reference in the text, the work is the candidate's own work. Work done in collaboration with, or with the assistance of, others, is indicated as such. Any views expressed in the dissertation are those of the author.

SIGNED: Ruth Payne

DATE: 29.08.18

## Table of Contents

## List of Tables

## List of Figures

# 1.0 Literature Review

## 1.1 The Supraglacial Ecosystem

### 1.11 – Glacier Surfaces

The harsh conditions that glacier ice experiences and exerts, particularly in polar regions, ensured that, until relatively recently, the cryosphere was thought to be devoid of life. More recently, ice sheets have been recognised as part of an important biome, within which a diverse network of microorganisms has been found to exist (Anesio and Laybourn-Parry, 2012). The glacier surface has been found to be of particular importance to the cryospheric biome. Anesio *et al.* (2007) found viral and bacterial abundances to be significantly larger in surface ice than further at depth. The viability of the glacier surface as a habitat is attributed to the provision of liquid water as well as the supply of organic matter and nutrients (Hodson *et al.,* 2008), a high proportion of which are thought to be delivered onto the supraglacial ice from both local and distal sources, through aeolian transport (Cook *et al.,* 2015).

There are several key habitats that exist on glacier surfaces: wet snow, supraglacial streams, moraines, ponds and cryoconite holes (Hodson *et al.,* 2008). Of these, cryoconite holes are of particular importance because the sediment they contain is in direct contact with meltwater, which in turn is, in some cases, in contact with the atmosphere. This potentially allows a chain of biogeochemical processes to develop, through which nutrients can be scavenged to support the ecosystem present (Tranter *et al.,* 2004), largely within the sediment (Anesio *et al.,* 2009). The hydrogeochemical conditions within the cryoconite holes make them refugia for life (Steinbock, 1936), and the biota commonly found within cryoconite holes have been found to catalyse chemical weathering reactions, including carbonate dissolution and sulphide oxidation (Hodson *et al.*, 2010). Present knowledge of these and other biogeochemical processes within cryoconite holes is limited (Cook *et al.,* 2015), particularly when considering changes occurring within freeze-thaw cycles, and so this study will focus entirely on these features.

### 1.12 Cryoconite Holes: Definition

Cryoconite holes are vertical, cylindrical, water-filled depressions found on surface ice in the ablation area of glaciers (Wharton Jr *et al.*, 1985). These phenomena were first observed by polar explorer A.E. Nordenskjold during his 1870 Greenland expedition (Gerdel and Drouet, 1960), which resulted in his naming of the holes as

‘cryoconite’, meaning ‘ice dust’ (Leslie, 1879). Nordenskjold’s naming of cryoconite holes was more appropriate than he may have realised; only more recently has it been established that a large proportion of the sediment which initiates cryoconite hole formation is likely to be deposits of aeolian dust (Nagatsuka *et al*., 2014; Dong *et al.,* 2016). As such, cryoconite holes structure generally takes the form of a thin layer of inorganic and organic sediment at the bottom, overlain with meltwater, which commonly fills the hole in the high melt season, and undergoes freezing in winter (Gerdel and Drouet, 1960)

Since Nordenskjold first documented the existence of cryoconite holes, they have been observed in the Antarctic (e.g. Wharton Jr *et al.*, 1981), Arctic (e.g. Säwström *et al*., 2002) and in lower-latitude glaciated regions (e.g. Takeuchi, 2000) and are therefore accepted as a feature found on supraglacial ice. Cryoconite holes are generally found at these high latitudes and altitudes because the ambient air temperatures and reception of shortwave solar radiation are low, which maintains low melt rates at the surface, enabling sediment to remain on the surface of the ice for long enough to ensure the formation and development of cryoconite holes (MacDonell and Fitzsimons, 2008).

## 1.2 Properties and Formation

### 1.21 Arctic and Lower-Latitude Cryoconite Holes

Cryoconite holes in the Arctic and mid-latitudes are commonly less than 1m in diameter, and less than 50cm deep (Anesio *et al.*, 2009). These holes form when aggregations of biotic and abiotic sediment, often termed cryoconite debris, gather in depressions in the ice surface (Mueller *et al.*, 2001), having been transported onto the ice by wind (e.g. Bøggild *et al.,* 2010). The sediment melts the underlying ice preferentially due to its lower albedo, as the particles absorb further solar radiation than that absorbed by the surrounding glacier ice, and conduct shortwave radiation into the ice immediately below (Fountain *et al.*, 2004). The cryoconite material continues to melt downwards through the surface ice until it reaches equilibrium depth, whereby surface ablation rate is equal to the downwards ablation rate of the hole floor caused by the lower albedo (Gribbon, 1979). There is frequent emptying of these features in much of the Arctic and lower-latitudes, because the relatively high melt rate, when compared to glaciers in Antarctica, allows a hydraulic network

to develop throughout the melt season, allowing the transfer of both meltwater and sediment downstream (Cook *et al.,* 2015).

### 1.22 Antarctic Cryoconite Holes

In the McMurdo Dry Valleys, Antarctica, cryoconite holes have been found to have diameters ranging from <5cm to 145cm, and depths of 4-56cm, with sediment thicknesses of approximately 0.8cm (Fountain *et al.,* 2004; Bagshaw *et al.,* 2013). However, the melt season in Antarctica is 20-40 days shorter than in the Arctic (Bagshaw *et al.,* 2016). This is because for much of the year, there is very little downward shortwave radiation, with a short period of intense downward shortwave radiation flux in the austral summer (Hatzianastassiou *et al.,* 2005). This leads to average annual air temperatures of -15-30°C with summer temperatures close to 0°C (Doran *et al*., 2002). As a result, a large proportion of cryoconite holes in Antarctica exhibit different characteristics from those found elsewhere in the cryosphere. Crucially, Antarctic cryoconite holes have been observed to be enclosed by an ice lid at the surface, up to 36cm in thickness (Fountain *et al.*, 2004), with a gas headspace, of 1-10cm depth, separating the ice lid from the meltwater below (Tranter *et al.*, 2004).

Cryoconite holes in Antarctica initially form when wind-blown sediment melts into the ice, similarly to holes in other regions, as described in Section 1.21. The meltwater then experiences surface refreezing due to the advection of cold katabatic winds at the glacier surface, causing the sediment to become entombed beneath the ice surface (Fountain *et al.*, 2008). The refrozen ice lid of the cryoconite hole is transparent, as solutes are rejected from the crystalline structure when freezing occurs (Richardson, 1976). As a result, the albedo of the cryoconite hole remains to be lower than that of the surrounding ice, with the cryoconite surface albedo of approximately 0.5, in comparison to the ice surface albedo of approximately 0.65 (Fountain *et al.,* 2004).

The lower albedo of the cryoconite hole surface causes preferential absorption of shortwave radiation compared with the surrounding glacier surface. This energy is conducted through the ice to the low-albedo cryoconite debris, which in turn conducts thermal energy to the surrounding colder ice (Fountain *et al*., 2004; MacDonell and Fitzsimons, 2008). This promotes subsurface melt while the advection of cold surface winds maintains a high sublimation rate, which preserves the ice lid (Lewis *et al.*, 1995). Overall, this combination of factors leads to a subsurface water layer overlying the cryoconite material, with isolation from the

atmosphere as well as from further melt input, owing to the presence of a thick ice lid (Fig. 1) These cryoconite holes can remain in this state, with liquid water below the surface of the ice, for 1-3 months during austral summers (Foreman *et al.,* 2007).

Figure 1 - Schematic of cryoconite hole evolution, sourced from Fountain et al. (2008).

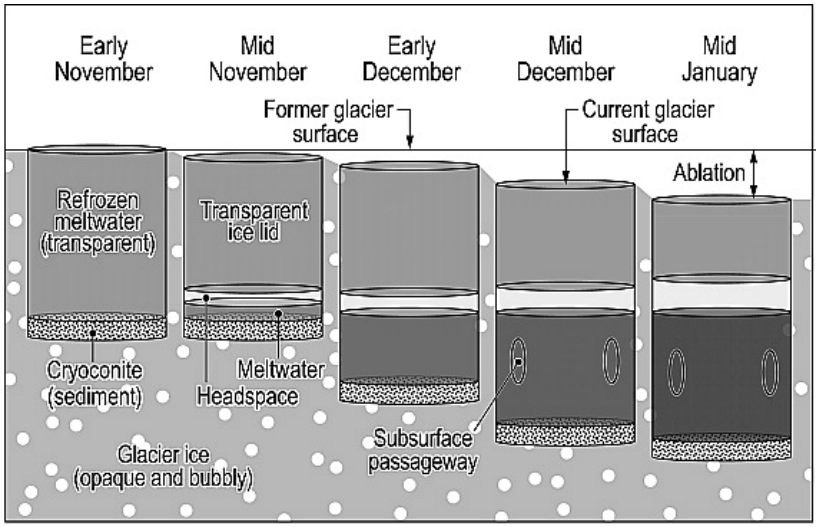


A cryoconite hole melts and refreezes on a number of timescales with fluctuations in incoming solar radiation (Bagshaw *et al.,* 2011). For the purposes of this study, we will consider seasonal melting and freezing processes to be of the highest importance, as it is this timescale over which biogeochemical processes will leave the greatest footprint. Furthermore, Antarctic cryoconite holes have been observed to completely freeze in the winter season, and melt from the entombed sediment layer outwards in the austral summer, ensuring that a significant number retain an ice lid year-round (Bagshaw *et al.,* 2013).

Cryoconite hole formation in Antarctica is widely accepted to initially generate holes that are hydrologically isolated, but as the hole matures, often it develops hydrological connections to a wider supraglacial drainage system (Fountain *et al.,* 2004). 44% of cryoconite holes on Canada Glacier at the time of sampling in the 1998/9 austral summer were found to be hydrologically isolated from their surroundings (Fountain *et al.*, 2004). The duration of isolation, determined using Chloride concentration of the meltwaters as a tracer, dated the isolated cryoconite holes as having been segregated for 1-11 years (Fountain *et al*., 2004). This isolation has the potential to greatly impact on the chemical conditions present within the cryoconite holes. The solute content of cryoconite hole meltwater, which steadily accumulates across freeze-thaw cycles, is derived from ice melt as well as

dissolution of aerosols and debris (Tranter *et al.*, 2004). Hydraulic isolation prevents further input of solutes into the freshwater.

In addition to providing a steadily more concentrated solution, the isolation of cryoconite holes for long periods may facilitate the development of microbial communities within the sediment, with organisms tolerant of their surroundings (Irvine-Fynn *et al.,* 2011).

## 1.3 Structural Components

### 1.31 Sediment

Cryoconite sediment is comprised of a combination of biotic and abiotic material (Cook *et al.,* 2016). The inorganic fraction is largely formed of mineral fragments, which in the McMurdo Dry valleys, is sourced from aeolian dust, blown onto the ice sheet surface by katabatic winds, and originates from the surrounding valley floor and sides (Lyons *et al.,* 2003). The organic component is thought to consist of both allochthonous and autochthonous material, of which the allochthonous material is also thought to be aeolian in source (Pearce *et al.,* 2009), and the survival of microorganisms in the atmosphere may increase the likelihood of survival on the ice sheet surface, due to similar temperature and nutrient stresses. Cryoconite debris has been found to contain substantially more organic carbon than exists in marginal soils, despite them being thought to be sourced from these soils (Bagshaw *et al.,* 2013). This may indicate that cryoconite holes are a site of organic carbon production, and supporting the presence of autochthonous organic matter. Indeed, cryoconite holes in Antarctica are more reliant on autochthonous organic carbon than those in the Arctic and lower latitudes, despite them having lower abundance and productivity (Cook *et al.,* 2016). Furthermore, Antarctica receives solar radiation at a low angle of incidence, so shortwave radiation may in some cases be unable to penetrate to the base of the cryoconite hole. Heat released during respiration, termed biothermal energy, may therefore be an important contributor to the seasonal melting of cryoconite holes (McIntyre, 1984).

### 1.32 Meltwater, and sediment-meltwater interaction

Cryoconite hole meltwater is of key importance to the ecosystem, which is largely found within the sediment. The meltwater is the sole source of liquid water for the microbial community. Direct sampling of cryoconite hole meltwater in the McMurdo

Dry Valleys has demonstrated that the meltwater has unique and extreme characteristics, such as pH (Tranter *et al.,* 2004). Cryoconite granules display heterogeneous clustering of microbes within them, with indications of microbial presence at the surface (Langford *et al.,* 2010). Bacteria in particular actively take up nutrients in cryoconite holes (Anesio *et al.,* 2007). Overall, cryoconite hole meltwaters are known to be extreme in their hydrochemistry, and micro-organisms are known to be active, and in contact with that meltwater. It is therefore important to fully understand the conditions that meltwater exerts on life forms residing within the cryoconite hole, as organisms survive within those holes across freeze-thaw cycles, with further input of allochthonous organic matter prevented by the ice lid.

The solute content of cryoconite hole meltwaters has two primary contributors: solute scavenged from the surrounding ice upon melt into the hole; dissolution of solute from the cryoconite debris when the sediment causes the surrounding ice to melt (Tranter *et al.,* 2004). Electrical conductivity, a crude measure of solute concentration, has been observed to peak when initial melting occurs above the sediment, which supports scavenging from the surrounding ice as a source of solute (Bagshaw *et al.,* 2016). Furthermore, longer periods of hydrological isolation have been linked to further enrichment of solutes, since the residence time of the water in contact with the cryoconite material allows further solute dissolution to occur (Bagshaw *et al.,* 2013). As a result, the source of the cryoconite sediment, prior to aeolian transport onto the glacier surface, can have a chemical footprint in the meltwater (Bagshaw *et al.,* 2007). Overall, continued scavenging of solute as well as further dissolution of solute from the sediment ensures that solute concentrations rise as the cryoconite hole matures, which only ceases when there is hydrological or atmospheric connectivity (MacDonell and Fitzsimons, 2008).

Hydrologic and atmospheric isolation enables Antarctic cryoconite hole meltwater solute chemistries to be used as proxies for biological activity. The initial composition of the meltwater is dictated by the sediment source as well as the solute content of the surrounding ice. Further changes to the concentrations of species will be caused partly by the activity of the microbial community, as well as through the melt of additional surrounding ice and the continued reaction of sediments with the water as discussed above, though the latter may itself be microbially-mediated (MacDonell and Fitzsimons, 2008). As a result, consideration of solute chemistry alone as a proxy for biological activity is most suitable for changes within the austral summer, during the period in which the hole is at equilibrium depth, as this limits the addition of solute from ice melt. One such consideration is that higher initial biomass,

dependent on microbial abundance within the sediment source area, results in increased photosynthesis and increases solute concentrations (Porazinska *et al.,* 2004).

### 1.33 Ice Lid

The ice lids of cryoconite holes are thought to be primarily physical in purpose, as they contain solute concentrations approximately 2.5 times more dilute than the meltwaters they enclose (Bagshaw *et al.,* 2007). Therefore, whilst not entirely inert, they are not considered to be of chemical importance themselves. However, their physical presence, with approximate thickness of 20cm, has two key effects (Fountain *et al.,* 2008). Firstly, the ice lids are a key component of the formation of cryoconite holes in Antarctica, as described in Section 1.22. They operate as 'solar greenhouses': transparent, insulating barriers from the outside world, facilitating melt as well as protecting the ecosystem (Foreman *et al.,* 2007). Secondly, the presence of this physical barrier between the cryoconite hole and the surrounding environment creates a closed system. The freezing of the meltwater, as well as the 'freeze-squeeze' of gases into and out of solution may generate unique meltwater chemistry, with potentially extreme pH values in particular, as well as contributing to the observed high gas pressures in headspaces (Tranter *et al.,* 2004; Fountain *et al.,* 2004).

The formation and persistence of ice lids on cryoconite holes is thought to be controlled by the ambient air temperature at the surface (Fountain *et al.,* 2004). In particularly warm austral summers, when ambient air temperature rises above 0°C, the ice lids melt into the holes. Bagshaw *et al.* (2007) calculated the isolation ages of cryoconite hole meltwaters sampled on Canada Glacier during the austral summer of 2005-6. All the holes were dated to have been isolated for less than 5 years. The 2001-2 austral summer was particularly warm, which suggests that the extreme warmth may have resulted in the melt-in of ice lids (Bagshaw *et al.,* 2007). The transfer of gas between solution and the atmosphere is made possible in such circumstances, by the absence of a physical barrier (MacDonell and Fitzsimons, 2008). As a result, the system becomes open. When examining the changes a cryoconite hole may experience over time, it is therefore important to acknowledge that the system may be open or closed to the atmosphere depending on hole maturity and the temperature conditions.

### 1.34 Headspace

The difference in density between ice and water, with ice being less dense than water, means that when melting occurs, the parcel of water that had been in solid form occupies a smaller volume when it is in the liquid phase. As a result, a headspace develops at the top of the cryoconite hole, between the meltwater and the ice lid, as observed by Tranter *et al.* (2004). These voids are filled with gas, which are trapped within the ice as bubbles, and are released upon melt, existing preferentially within the headspace rather than the meltwater (Fountain *et al.*, 2008; Bagshaw *et al.,* 2011). Further additions of gas into the headspace are generated immediately when melting occurs close to the sediment layer, as photosynthetic organisms release oxygen and solute during photosynthesis (Fountain *et al.,* 2008).

Comparatively little research has been conducted concerning cryoconite hole headspaces, partly because of the challenges associated with sampling them. However, Tranter *et al.* (2004) found Antarctic cryoconite meltwaters to have highly unusual chemical signatures. Processes resulting in the release or consumption of preferentially gaseous chemical species are known to occur within cryoconite holes, including photosynthesis, respiration and carbonate precipitation/dissolution (e.g. Fountain *et al.,* 2008). This is therefore likely to impact upon gas concentrations in the headspace, and may indeed be the cause of observed high gas pressures within headspaces. Fountain *et al.* (2004) observed jets of water 1-2m high when they pierced holes in the lids of cryoconite holes in the McMurdo Dry Valleys.

Bagshaw *et al.* (2011) investigated the build-up of oxygen pressure within the headspace through a model of headspace-water interaction using Henry's Law. An approximate factor of 3 decrease in meltwater volume, if there was no interaction with headspace, would be expected to correspond to an increase of similar magnitude in the concentration of a given chemical species. However, they calculated that there was an increase in dissolved oxygen of only 56%. This suggests that, in reality, the presence of the headspace allows partitioning of oxygen into the gas phase, resulting in a build up of air pressure within the headspace (Bagshaw *et al.,* 2011).

## 1.4 Chemical features of interest

### 1.41 pH

Antarctic cryoconite holes have been recorded to contain meltwaters with extremely high pH values of up to 10.99 (Tranter *et al.,* 2004), whereas at other latitudes the pH is much lower, for example with pH=3.9 in White Glacier cryoconite holes in the Canadian Arctic (Mueller *et al.,* 2001). In general, cryoconite hole meltwaters tend towards slightly alkaline pH values, which has been suggested to be a reflection of photosynthetic activity (Foreman *et al.,* 2007). Conversely, more acidic pH in cryoconite holes has been correlated with low rates of bacterial production and an absence of invertebrates (Porazinska *et al.,* 2004). pH is therefore a feature which can be used to provide a crude estimate of net primary production, as described in Section 1.34, with lower pH indicating a lack of biological activity (Bagshaw *et al.,* 2013). Recent measurements of pH on Canada Glacier suggest that net primary production occurs in cryoconite holes (Tranter *et al.,* 2004), but other studies find a state of net respiration to be prevalent (Bagshaw *et al.,* 2011). In reality, it is likely that primary production and respiration are fairly balanced, at least on longer timescales, with the dominant process dependent upon local physical and biogeochemical conditions (Bagshaw *et al.,* 2011).

The specific impact of cryoconite hole freeze-up on pH is as yet unknown. When the cryoconite hole is fully melted, in the summer, the pH is extreme, even 'seemingly inhospitable' (Tranter *et al.,* 2004, pp. 386). Solute concentrations increase when freezing occurs (Richardson, 1976), so pH will also change. Organisms survive within the cryoconite holes between summers, as photosynthesis occurs when thawing begins, despite the ice lid providing a barrier to input of further microorganisms (e.g. Bagshaw *et al.,* 2007; Fountain *et al.,* 2008). It is therefore important to quantify the change in pH during freeze-thaw cycles in order to fully understand the tolerance of the communities within cryoconite holes to potentially extreme chemical conditions.

### 1.42 Carbon

Carbon in meltwater can take two forms: dissolved organic carbon (DOC), largely composed of by-products of respiration, and dissolved inorganic carbon (DIC), which consists of carbonic acid, $CO_2$, $HCO_3^-$ and $CO_3^{2-}$ (Hedges, 1992; Stumm and Morgan, 1970). Carbon in cryoconite holes in the McMurdo Dry Valleys has been measured as 60-76% inorganic, with the remainder being DOC (Bagshaw *et al.,*

2013). The onset of melt initiates a state of net photosynthesis, which transforms DIC into organic matter (Fountain *et al.,* 2008). Net respiration is caused by the subsequent freezing, which causes DIC to return into solution, in addition to some DOC (Bagshaw *et al.,* 2007). The balance of DIC and DOC can therefore be used to estimate net primary production.

It is possible to use the concentration of $CO_2$ within cryoconite hole meltwaters as a crude proxy for net primary production, in a similar way to pH, as $CO_2$ is used up in photosynthesis. This is unsurprising, since pH is a function of the partitioning of DIC species in solution. As a result, low $pCO_2$ values in meltwater are associated with net primary production, and high $pCO_2$ with net respiration (Edwards *et al.,* 2011). Bagshaw *et al.* (2013) also found that on all three glaciers sampled in Taylor Valley: Taylor, Canada and Commonwealth glaciers, the enrichment factor of DOC was depleted, suggesting that the cryoconite holes experience net respiration.

### 1.43 Carbonate

Carbonates have been found to be present within cryoconite holes across the cryosphere. For example, Langford *et al.* (2010) found significant quantities of dolomite and calcite in 2 samples, of the 12 cryoconite sediment samples collected in Svalbard. Carbonates are particularly likely to be modified by microbial processes (MacDonell and Fitzsimons, 2008). Calcite in particular is more soluble at low temperatures, and requires a high concentration of carbonate ions to precipitate (Doney, 2006). The relative concentrations of carbonate, bicarbonate and carbon dioxide are reflected in the pH, such that an increase in the concentration of $CO_2$ corresponds to more acidic waters. As a result, whether calcite precipitates or dissolves is sensitive to the $CO_2$ concentration in the water, which may be affected by interaction with the headspace as well as primary production/respiration. Indeed, freezing causes carbonate precipitation, as calcium and bicarbonate concentrations increase because of solute rejection, and conversely carbonates dissolve when the cryoconite hole melts (Bagshaw *et al.,* 2007). Primary production may also lead to localised calcite precipitation due to the raised pH, when $CO_2$ is consumed in photosynthesis (Bagshaw *et al.,* 2007). These ideas are supported by Tranter *et al.* (2004), who found waters to be supersaturated with respect to calcite immediately when melting initiates.

### 1.44 Gypsum and Salts

Increase in concentration of calcium and sulphate ions can lead to gypsum saturation. Solute concentrations increase as freezing occurs, so gypsum saturation may occur in cryoconite holes. Bagshaw *et al.* (2007) determined that sulphate concentrations were fairly constant between and within entirely frozen cryoconite holes in the McMurdo Dry Valleys. However, 'wet' lidded cryoconite holes were found to have higher concentrations of sulphate. One possible mechanism for increase in concentration of sulphate would be gypsum dissolution when melting occurs, although sulphide oxidation has also been proposed (Hodson *et al.,* 2010).

Gypsum has been found to be important in the study of supraglacial streams in Taylor Valley. Fortner *et al.* (2005) found the evolution of meltwater, from the snow through to the proglacial stream, to be dominated initially by calcite and gypsum dissolution, with the relative dominance of calcite and gypsum being determined by their presence within the source material, as this was shown to vary across the valley. Continued stream development may lead to salt dissolution and silicate weathering (Fortner *et al.,* 2005). The dissolution of NaCl (halite) is made possible by the high concentrations of salt within soils in the McMurdo Dry Valleys (Porazinska *et al.,* 2004).

## 1.5 Motivation

This study will attempt to delineate and quantify the biogeochemical changes that occur within Antarctic cryoconite holes throughout the freezing process, from a completely-thawed state, to complete freeze-up.

### 1.51 Significance of cryoconite holes

Cryoconite holes provide a habit for active, heterogenous microbial communities within the supraglacial ecosystem. The enzymatic activity of the biota within cryoconite holes is greater than that of microbes within lakes in the McMurdo Dry Valleys, or indeed subglacial outlets at Blood Falls (Foreman *et al.,* 2007). Cryoconite holes provide one of the most significant nutrient reservoirs in the glacial system (MacDonell and Fitzsimons, 2008). As a result, cryoconite holes play an important role in the provision of nutrients further downstream, particularly in warm austral summers, when their sediments, containing bioavailable carbon, nitrogen and phosphorus, are distributed further through the supraglacial drainage network (Bagshaw *et al.,* 2013; Irvine-Fynn *et al.,* 2011). As a result, after a glacial flood in

the warm austral summer of 2001-2, depth-integrated primary production in Lake Fryxell was five times higher than measured during previous samplings, which is due in part to the loading of dissolved inorganic nitrogen and soluble reactive phosphorus, from upstream sources (Foreman *et al.,* 2004). It is clear that biogeochemical processes within cryoconite holes cycle nutrients, enabling significant increases in primary production when their contents are flushed out. This is particularly the case during 'stripping events', in which approximately 50cm of surface ice is removed within the timescale of several days (MacDonell and Fitzsimons, 2008).

Indeed, without cryoconite holes, there would be little meltwater on the surface of Antarctic glaciers, because of their high albedo. Consequently, cryoconite holes are important because they enhance glacial melt, particularly in Antarctica, where frequently, ambient air temperature does not support the melting of ice (Doran *et al.,* 2002). Therefore, despite only covering approximately 4.5% of the glacier surface, contribution to total runoff from Canada Glacier is estimated to be 13-20% (Fountain *et al.,* 2004; Tranter *et al.,* 2005). Cryoconite holes on Wright Lower Glacier are thought to contribute approximately 1/3 of total runoff (MacDonell and Fitzsimons, 2008). If these estimates are representative of the glaciers in the McMurdo Dry Valleys, a substantial proportion of glacial runoff has been subjected to seasonal freeze-thaw cycles in both lidded and open cryoconite holes. Therefore, if indeed lidded cryoconite holes have progressively more extreme chemical conditions over time, this could significantly impact the biogeochemistry of Antarctic glacial runoff as a whole.

Overall, there are several benefits to learning more about cryoconite hole meltwater geochemistry. Firstly, extreme hydrochemical conditions are present within cryoconite holes, so examining the cryoconite hole freeze-up process will enable the quantification of the most extreme conditions the hole exerts on its microbial community. Secondly, the communities within cryoconite holes cycle nutrients, which are liberated upon significant, decadal-timescale melt events. In addition to this, primarily sediment-based provision of nutrients downstream, the solute acquired by the meltwater is also flushed downstream during melt events. This is likely to have significant, measurable impacts on the ecosystems downstream (e.g. Foreman *et al.,* 2004).

### 1.52 Recent methods employed

There are two primary methods by which it is possible to gain a more comprehensive understanding of cryoconite hole meltwater geochemistry: direct, *in situ* measurements, and through geochemical modelling. A number of recent studies have sampled cryoconite hole meltwaters in order to examine geochemical features (Tranter *et al.*, 2004, Bagshaw *et al.*, 2013, Bagshaw *et al*., 2007, Bagshaw *et al*., 2011). Such studies provide accurate data on the concentrations of solutes within the meltwaters, as well as geochemical parameters such as pH. However, whilst it is possible to accurately sample an open cryoconite hole throughout the season, the same is not true for lidded cryoconite holes. In order to sample these features, it is necessary to drill through the thick ice lid, or to break it entirely (e.g. Hodson *et al.,* 2010) which indeed is the component that may cause potentially extreme hydrochemical conditions. In doing so, the conditions under which the cryoconite hole evolves are altered significantly, and thus any later samples from the same cryoconite hole are flawed. As a result, direct measurement of cryoconite hole geochemistry, although accurate, is only possible at a single point in time for each individual hole. The destructive sampling techniques necessary make geochemical modelling a more appropriate method for measuring change in meltwater geochemistry over time.

### 1.53 Research Aims

This study will aim to quantify the impact of seasonal freeze-up of Antarctic cryoconite holes on their geochemistry, with particular focus on pH, DIC, and any saturation, dissolution or precipitation of key species such as calcite, gypsum, or salt (halite). This will be achieved through comparison of open and lidded cryoconite hole meltwaters, with open hole waters to also provide an indication of initial Antarctic hole formation. Furthermore, it will aim to examine the relationship between the headspace and meltwater, to determine whether the presence of a gas headspace impacts upon geochemical conditions in cryoconite meltwaters.

### 1.54 Hypotheses

1. pH will be higher in closed cryoconite hole meltwaters, and will be more stable in open cryoconite hole waters to reflect $pCO_2$.
2. $pCO_2$ will remain constant in open cryoconite hole meltwaters due to contact with the atmosphere, but will rise in closed cryoconite hole meltwaters as solute concentrations increase due to freezing.
3. Calcite will saturate and precipitate as the hole freezes in both open and closed cryoconite hole meltwaters, which may impact upon $pCO_2$ and gypsum saturation state. It may saturate faster in open cryoconite hole waters due to stable $pCO_2$.
4. Gypsum will approach saturation in both open and closed cryoconite hole waters, but will be impeded by calcite precipitation, as calcium will be removed from solution.
5. Halite will not saturate, as the solutions will not become sufficiently concentrated to change the regime from a calcite and gypsum-dominated system to a salt and silicate-dominated system.
6. The presence of a gas headspace will impact on the geochemistry of the meltwater, with ‘freeze-squeeze’ of gas into the headspace, causing high gas pressures to build up.

# 2.0 Data and Methods

This study aims to model the biogeochemical evolution of cryoconite hole meltwaters as freezing occurs. Freezing occurs on a range of temporal scales (Fountain *et al*., 2008), but the primary focus of this investigation is the seasonal freeze-thaw processes that cryoconite holes are subjected to, as this may have implications for the cycling of carbon within the holes (Bagshaw *et al*., 2007). The simulation of freezing was achieved by forward-modelling changes to a range of geochemical parameters, such as pH, $pCO_2$, and the saturation indices of calcite, gypsum and halite. In particular, pH influences the distribution of DIC species, and both $pCO_2$ and $SI_{calcite}$ are controls on the quantity of DIC in solution.

The process of determining the composition and characteristics of an aqueous solution involves the calculation of increasingly complex solution characteristics as ionic strength increases (e.g. Butler *et al*., 2008). As a result, whilst it is possible to manually complete the calculations necessary, this would be time-consuming and labour-intensive. These problems are avoided by using PHREEQC (Version 2.18), a freely-available computer program, accessible from the United States Geological Survey webpage. PHREEQC can perform numerous geochemical calculations concerning low-temperature solutions (Parkhurst and Appelo, 1999). Here, its capacity to determine the chemical composition of an aqueous solution was utilised.

## 2.1 Model Setup

PHREEQC uses initial concentrations conditions specified by the user to iteratively calculate the concentrations and saturation indices of aqueous species. It achieves this by tuning the concentrations of elements in order to reach equilibrium (Parkhurst and Appelo, 1999). The chemical equilibria through which these parameters are calculated are dependent on activity and ion pairing. Ion pairing reduces the free ion activities of the major dissolved species, at least initially (Marcus and Hefter, 2006). PHREEQC, if left unmodified, also uses Debye-Hückel theory to calculate activity coefficients, to account for non-ideality (Parkhurst and Appelo, 1999). This simplified model is appropriate in dilute solutions, but becomes unreliable as ionic strength increases (Harvie and Weare, 1980), particularly at ionic strengths of >1m (Zhang *et al.,* 2005). This is because use of the Debye-Hückel equation assumes indirect proportionality between concentration and activity, as well as deploying inaccurate treatment of the ionic radius in concentrated solutions (Robinson and Stokes, 2002). Empirical activity coefficient calculations have shown that any proportional

relationship quickly breaks down as ionic strength increases. Indeed, empirical activity coefficients of NaCl compiled from Haynes (2014) and Baumgarten (1981) show the distinct nonlinearity of the relationship between activity coefficient and concentration, particularly at high ionic strengths (Fig. 2).

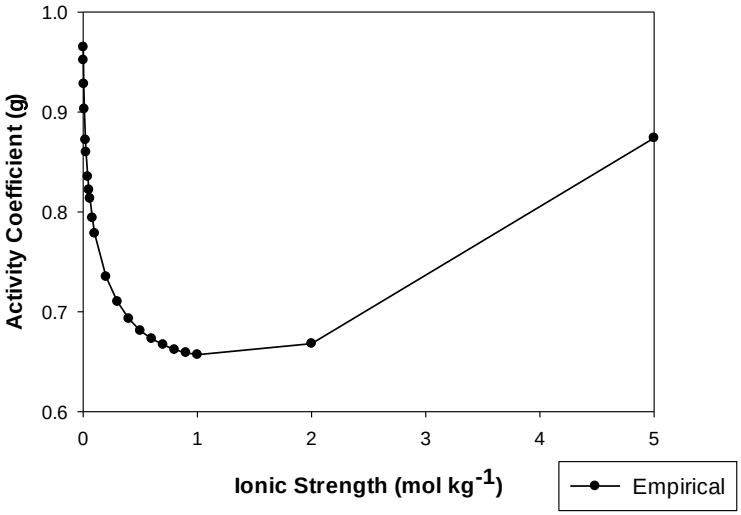


Figure 2 - Empirical values of activity coefficients across a range of Ionic Strengths of NaCl at 298K

Alternative values of these activity coefficients are here calculated through use of the Debye-Hückel equation (Helgeson and Kirkham, 1974), in order to determine the applicability of PHREEQC's default model set up to our problem (Fig. 3).

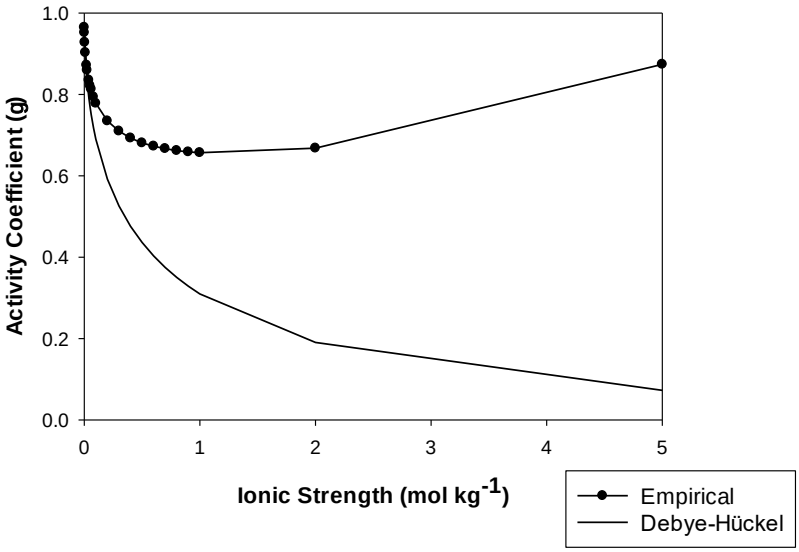


Figure 3 - Empirical and Debye-Hückel activity coefficients of NaCl across a range of ionic strengths at 298K.

The empirical activity coefficients are predicted well by the Debye-Hückel activity coefficients at very low ionic strengths (≤0.05 mol $kg^{-1}$; Fig. 3). Within this range of

ionic strength, in all cases, the Debye-Hückel configuration under predicts the empirical data, but remains to be within 0.05 units of the corresponding observation of γ. The relationship disintegrates at higher ionic strength than this, very dilute, range. Indeed, at the highest calculated ionic strength, of 5 mol $kg^{-1}$, there is an order of magnitude difference between the theoretical and empirical activity coefficients (Fig. 3). It was therefore appropriate to modify the default configuration of PHREEQC to address the aims of this study, since closed cryoconite holes are known to have extreme hydrochemical conditions (Tranter *et al*., 2004), and the full extent of these conditions across the season is not known.

PHREEQC can be extended, using the 'PITZER' datablock to utilise the 'Pitzer specific-ion-interaction aqueous model' (Parkhurst and Appelo, 2013). This is based on the semi-empirical equations proposed by Pitzer (1973), as a substantial extension to the Debye-Hückel equation, and these have been shown to accurately predict activity coefficients even at high ionic strengths (Millero, 1992, Harvie and Weare, 1980). Theoretical activity coefficients calculated through these equations (Baumgarten, 1981) are compared to the empirical and Debye-Hückel activity coefficients in order to determine which method is appropriate for this study (Fig. 4).

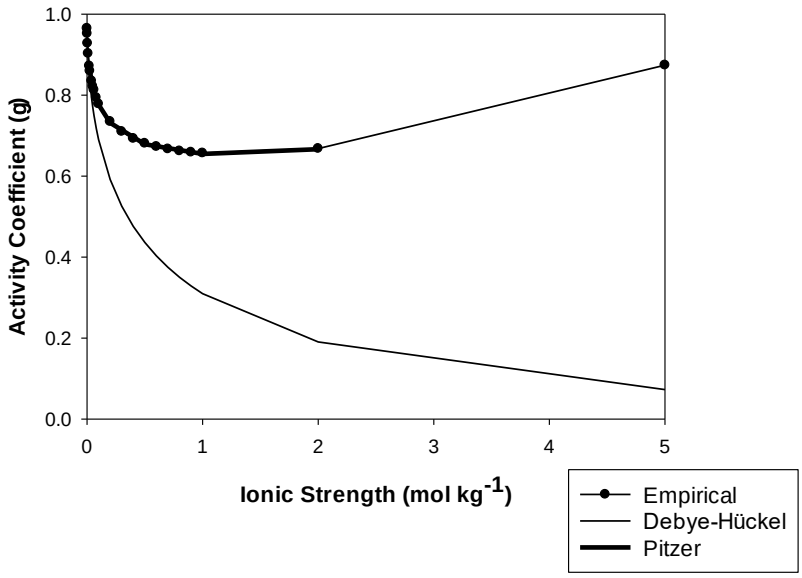


Figure 4 - Empirical, Debye-Hückel and Pitzer activity coefficients for NaCl at 298K

There is substantial agreement between the empirical and Pitzer datasets, with the Pitzer activity coefficients consistently within 0.05 units of the empirical value, across the ionic strengths for which the activity coefficients were available (Fig. 4). It is worth noting that the range of ionic strengths shown is not indicative of a limitation in capability of the Pitzer equations, rather that the study from which the values were

taken did not extend to the range of ionic strengths displayed here. The Pitzer activity coefficients surpass the Debye-Hückel coefficients in terms of accuracy, even at relatively low ionic strengths. As a result, the Pitzer datablock was added to the model configuration within PHREEQC throughout the modelling work involved in this study, in order to retain accuracy in determining the concentration of species regardless of ionic strength. However, the suitability of this decision will be further explored in Section 3.1, through a series of experiments in which the Debye-Hückel and Pitzer models are compared with results from their respective PHREEQC outputs.

One of the most important characteristics of the meltwater to model accurately is pH. pH is a master variable (Garrels and Christ, 1965), as it is a fundamental control on the chemical composition of aqueous solutions, and is a description of carbonate speciation in the solution. Therefore, if pH changes, there will be consequences for $pCO_2$ as well as the saturation indices of carbonate species. Indeed, Tranter *et al*. (2004) found pH in lidded cryoconite holes to have a range of 2.4. Measurements of pH in open cryoconite holes in Svalbard have been as low as 4.7 (Kaštovská *et al*., 2005). With a large range of potential values, and the likelihood that open cryoconite holes experience different pH conditions than lidded holes, it is vital that pH is accurately modelled.

The charge balance configuration within PHREEQC was utilised, to calculate the pH of the solution in order to achieve electroneutrality (Parkhurst and Appelo, 1999). This function sums the negative charges and positive charges in solution. Electroneutrality requires the negative and positive charges to be equal. If the sum of positive charges is greater than that of the negative charges, the pH is increased, thus converting $H_2CO_3$ to $HCO_3^-$, and $HCO_3$ to $CO_3^{2-}$. This is raised iteratively to balance the sums of positive and negative charges (Parkhurst and Appelo, 1999). Conversely, the opposite action is taken if the sum of the negative charges exceeds that of the positive charges.

### 2.2 Initial Conditions

The application of PHREEQC to freezing solutions involves the specification of initial conditions, including solute concentrations, followed by the implementation of logical changes to the concentrations of species in the system that are theoretically appropriate (Charlton and Parkhurst, 2011). To this end, a series of basic parameters, including temperature and major and minor ion concentrations, were

selected as initial conditions, to form the basis of calculations completed by the program.

The systems modelled in this study are based on observational data collected in the McMurdo Dry Valleys, Antarctica. This is an appropriate region of focus, because it is one of only two locations on earth in which lidded cryoconite holes have been observed during the height of the ablation season (Fountain *et al*., 2004). Because these holes are unique in their physical composition, and indeed may be analogous to ice-sealed microcosms on other planets (Tranter *et al*., 2004), it is important to provide a reference by which to compare these lidded cryoconite holes.

Open cryoconite holes were an appropriate choice, for two key reasons. Firstly, as detailed in Section 1,12, open cryoconite holes have been observed on ice masses across the globe, and are generally more accessible than the lidded holes of the McMurdo Dry Valleys, as well as their meltwaters being easily sampled without necessity for destruction. As a result, the biogeochemistry of open cryoconite hole meltwaters is more documented than that of lidded cryoconite holes (Cook *et al*., 2016). This provided an opportunity for some, albeit qualitative, validation of the results obtained in this study, potentially making the modelled biogeochemical processes in lidded cryoconite holes more reliable. Secondly, as detailed in Section 1.22, when lidded cryoconite holes form, the sediment is initially deposited on the glacier surface, so initially the cryoconite holes develop similarly to the open holes found across the cryosphere (Fountain *et al*., 2008). It therefore provides additional benefit to model an open cryoconite hole, as when comparing the results of the two hole types, it is possible to make an assessment of the biogeochemical evolution of a closed cryoconite hole, from the initial formation, to hole maturity.

Bagshaw *et al*. (2007) provide the average major ion concentrations of 34 water-filled lidded cryoconite holes, sampled from Canada Glacier, Taylor Valley, in the 2005-6 austral summer. These initial conditions allow the representation through modelling of an average cryoconite hole, which has been subjected to several freeze-thaw cycles. Concentrations for the initial conditions of an alternative starting water were selected from Fortner et al. (2005), who provide the average major ion concentrations of 81 supraglacial stream water samples on Canada Glacier, Taylor Valley, Antarctica. This is equivalent to ice melt, and so can be modelled to represent open cryoconite hole meltwater, or the meltwater upon initial formation of a closed cryoconite hole. PHREEQC also requires a temperature condition. Cryoconite meltwaters are widely agreed to be of steady temperature, at

approximately 0.1˚C, so this condition was used for all solutions simulated (Säwström *et al*., 2002).

Table 1 contains the initial concentration data adapted from Bagshaw *et al*. (2007) and Fortner *et al.* (2005). The data from Fortner *et al.* (2005) were merely changed into μmol.$l^{-1}$, as their original units, μeq.$l^{-1}$ are not acceptable as an input to PHREEQC. This was also true for the data from Bagshaw *et al.* (2007), but prior to the change in units there was a more substantial alteration necessary. The paper gives solute concentrations having excluded their contributions from sea salt, but assuming that all chloride is from sea salt. It concludes that chloride is likely to be local in source as well as sourced from sea salt, as notably, they achieve a negative concentration of sodium based on these assumptions. As a result, it was necessary to change those values which had been corrected for sea salt.

To do this, the relative concentrations in seawater of the solutes that had been corrected ($SO_4^{2-}$, $Na^+$, $K^+$, $Mg^{2+}$, $Ca^{2+}$ and DIC) were considered, using standard seawater solute concentrations (Drever, 1988). The molar concentration of a given solute in seawater was calculated as a proportion of the molar concentration of chloride in seawater, and multiplied by the chloride concentration measured by Bagshaw *et al.* (2007). This formed an estimate for the concentration of that solute sourced from seawater, which could be added to its concentration provided by Bagshaw *et al.* (2007), which had excluded the contribution of sea salt.

Table 1 - Initial concentrations used, from Fortner et al. (2005) and Bagshaw et al. (2007) in μmol $l^{-1}$. '-' indicates that this data was not available in the source paper.

| | **$Cl^-$** | **$HCO_3^-$** | **$Na^+$** | **$Ca^{2+}$** | **$SO_4^{2-}$** | **$Mg^{2+}$** | **$K^+$** | **$NO_3^-$** | **pH** |
|---|---|---|---|---|---|---|---|---|---|
| **Bagshaw *et al.*, 2007** | 116 | 98.4 | 80.1 | 79.7 | 34 | 17.3 | 11.2 | 1.4 | 7.22 |
| **Fortner *et al.*, 2005** | 39 | 34.3 | 30 | 24.55 | 9.95 | 5.5 | 4 | 0.69 | - |

The concentrations of major ions are substantially higher in the cryoconite hole meltwaters than the supraglacial stream (ice melt) (Table 1). Every solute is more concentrated in the cryoconite hole meltwater, by a factor of approximately 2-3.5. Sulfate is the most enriched in the cryoconite hole meltwater, compared to the ice melt, and nitrate is the least enriched. Cations and anions show similar enrichment between the two waters. The sums of the charges in both initial solutions are very similar, suggesting that there are no substantial omissions of solutes.

It is important to acknowledge that there is a dearth in solute concentration data, particularly for closed cryoconite hole meltwaters, for reasons detailed in Section 1.52. It was therefore appropriate to consider the range of conditions present between different cryoconite holes, particularly of different maturities, and where the physical conditions differ greatly between the cryoconite holes. Indeed, even across Taylor Valley, there have been substantial differences in the physical characteristics of cryoconite holes, and perhaps in the source of the cryoconite material (Fountain *et al*., 2004). It is likely that similarly, there are differences in the biogeochemical conditions found in these holes, a notion supported by substantial ranges found in solute concentrations of lidded cryoconite holes (Tranter *et al*., 2004). As a result, it was appropriate to use each set of initial concentrations to model both a closed and an open cryoconite hole. This may further enable consideration of hole evolution over time, as the supraglacial stream (ice melt) concentrations could be used to represent a 'young' lidded hole.

To this end, six independent hypothetical cryoconite holes were simulated: F-Open, F-Closed, F-Headspace, B-Open, B-Closed and B-Headspace, with 'F' representing initial conditions from Fortner *et al*. (2005), as a proxy for ice melt, and 'B' representing initial conditions from Bagshaw *et al*. (2007). 'Open' indicates that the hole has no ice lid, and remains open to the atmosphere. 'Closed' indicates that the hole is lidded, and is isolated from the atmosphere, but with no headspace accounted for. 'Headspace' indicates that the hole has an ice lid, so is isolated from the atmosphere, but accounts for interaction between the gas headspace and the meltwater. For each simulation, the following variables were noted: pH, Ionic Strength, $pCO_2$, $SI_{calcite}$, $SI_{gypsum}$, $SI_{halite}$, and the concentrations and activity coefficients of all chemical species.

### 2.3 Modelling of Cryoconite Hole Freeze-up

Solute accumulates during the freeze-up of cryoconite holes because solutes are rejected from the freezing lattice (Richardson, 1976). There may be some atmospheric exchange of gaseous and particulate species, through the melt-in of the ice lid, but this process has been deemed negligible as a contributor of solute to cryoconite hole meltwaters (Tranter *et al*., 2004). Meltwaters are subjected to seasonal (and diurnal) freeze-thaw processes. As a result, freezing increases the concentration of all major base cations and acid anions. Assuming that all solute is rejected, when freezing occurs, the volume of liquid water (V) changes, but the mass of solutes (m) remains constant (Eq. 1).

$$m_1 V_1 = m_2 V_2 \qquad \text{Eq. 1}$$

This means that for every 50% of the remaining meltwater that freezes, a doubling of all solute concentrations occurs (Bagshaw *et al.*, 2011). Because the mass of solutes remains constant, due to solute rejection, this information was used conversely in order to forward-model the freezing process (Eq. 2).

$$\% \, Freezing = \frac{V_2}{V_1} \times 100 \qquad \text{Eq. 2}$$

Solute concentrations were therefore doubled, or in certain cases increased by an alternative factor (see Section 2.4), between each simulation. The above conservation of mass equations enabled the calculation of the percentage of the initial meltwater volume that had been subjected to freezing. The results of this calculation were used to create the 'Freezing (%)' variable, which is appropriate to the problem addressed in this study, because it enables the modelling of cryoconite hole systems independently of their size. Since they have been observed to vary substantially in size, this is beneficial, as the results are therefore applicable to all different sizes of hole. Cl concentration was selected as the input for these calculations because it is a conservative species, often used as a proxy for salinity (Bear *et al.*, 1999).

Freeze-up of open cryoconite meltwater was modelled by doubling solute concentrations for each sequential simulation. However, a doubling of all solute concentrations causes $pCO_2$ variation in the simulated meltwater because this exacerbates the differences between positive and negative charges, and so the pH, hence the $pCO_2$, changes to allow for these differences, using the charge balance function (Parkhurst and Appelo, 1999). By contrast, in reality, open cryoconite hole meltwaters are in contact with the atmosphere, so are likely to be relatively constant in terms of $pCO_2$. It is therefore assumed that the $pCO_2$ of the meltwater is at equilibrium with the atmosphere. For this purpose, a value of $pCO_2$=-3.4 log atms was selected, as this is equal to atmospheric $CO_2$ concentration of 400ppm, which was measured at the South Pole Observatory in 2016 (Khan, 2016). It was necessary to alter DIC concentrations, either by removing or adding DIC, in order to maintain this value in the modelled solution.

The freezing of closed cryoconite hole meltwater was modelled by doubling all solute concentrations between simulations. Their meltwaters are isolated from the atmosphere, therefore no assumption was necessary concerning pCO2, hence all

concentrations, including DIC, were increased by the same factor at each Freezing, until saturation of a key species was achieved.

Modelling the freeze-up of closed cryoconite hole meltwater whilst accounting for any interaction with a gas headspace required a series of calculations, which were conducted in Microsoft Excel. These calculations involved the use of the Ideal Gas Law (e.g. Kautz *et al.,* 2005), which contains a volume term; unlike for the 'Open' and 'Closed; scenarios, it was necessary to consider a cryoconite hole of fixed dimensions. The radius selected for the cryoconite hole was 20cm, as an approximate modal value for all cryoconite holes sampled by Bagshaw *et al.* (2013). A total depth of 20cm was used, including both the meltwater and headspace, as this is approximately equal to the wet hole depth, with the ice lid depth excluded, as measured by Bagshaw *et al.* (2007). A 3cm headspace was assumed at the top of the hole, as in Bagshaw *et al.* (2011). These dimensions were used to calculate the volumes of the meltwater and headspace by assuming that the cryoconite hole is a perfect cylinder (Eq. 3). This is an appropriate assumption to make, because close to Earth's poles, the trajectory of the sun through the sky is at its most circular, causing cryoconite holes to be quasi-cylindrical (MacDonell and Fitzsimons, 2008).

$$V = \pi r^2 \mathrm{d} \qquad \text{Eq. 3}$$

Where V=volume, r=radius, d=depth

The same initial meltwater was used as for the 'Open' scenarios, because upon formation of the cryoconite hole, the meltwater is open to the atmosphere before surface refreezing occurs. As a result, the initial headspace is likely to be atmospheric in composition, and any gas bubble contribution from within the ice lid will similarly be atmospheric in origin. Therefore, the initial $pCO_2$ of both the headspace and meltwater were assumed to be atmospheric. The Ideal Gas Law (e.g. Kautz *et al.,* 2005) was used to determine the number of moles of $CO_2$ in the headspace (Eq. 4).

$$pCO_2 V = n_{air} RT \qquad \text{Eq. 4}$$

Where $n_{air}$=number of moles of $CO_2$ in the headspace, R=gas constant, T= temperature in Kelvin.

PHREEQC gives concentrations of DIC species and the activity coefficient of $H^+$, which were used in order to calculate kH, k1 and k2 (Eq. 5) (e,g, Millero, 1995).

$$[CO_2] = k_H pCO_2$$

$$[HCO_3^-] = \frac{k_H k_1 pCO_2}{[H^+]} \quad \text{Eq. 5}$$

$$[CO_3^{2-}] = \frac{k_H k_1 k_2 pCO_2}{[H^+]^2}$$

Eq. 6 was used to find the total number of moles of DIC in solution.

$$n_{water} = V_{water}([CO_2] + [HCO_3^-] + [CO_3^{2-}]) \quad \text{Eq. 6}$$

Each progressive doubling of solute concentrations in the meltwater indicates that 50% of the remaining meltwater in the cryoconite hole has frozen. The meltwater volume at each Freezing was therefore halved, and, assuming that freezing occurs uniformly in the horizontal and vertical, the radius and water depth were multiplied by a linear scale factor of $0.5^{1/3}$. To conserve mass, the mass of the new ice must equal its mass prior to freezing. However, since the densities of water and ice differ, so too must the volumes of the water in its liquid and solid forms (Eq. 7).

$$D_1 V_1 = D_2 V_2 \quad \text{Eq. 7}$$

The density of ice was assumed to be 0.915 g $cm^{-3}$ (Smith *et al.* 2012), and the density of the meltwater was taken from the PHREEQC output to be 0.99985. The new total cryoconite hole volume was calculated by subtracting the volume of new ice ($V_2$) from the previous total cryoconite hole volume. The new headspace volume was then calculated by subtracting the new meltwater volume from the total cryoconite hole volume.

In order to calculate the number of moles in each of the headspace and the meltwater, it is necessary to know the $pCO_2$ value, which should be in equilibrium. However, in Equations 5-6, the new meltwater and headspace after freezing occurs now contain two unknowns: $pCO_2$, and $[H^+]$ for the meltwater. Initially upon freezing, the theoretical headspace $pCO_2$, assuming no exchange of $CO_2$ between the meltwater and headspace, was calculated using Boyle's Law (Eq. 8) (e.g. Bonnar, 1956)

$$P_1 V_1 = P_2 V_2 \quad \text{Eq. 8}$$

Where P = pressure, in this case $pCO_2$, and V = volume.

Eq. 4 was then used in order to verify that the number of moles of $CO_2$ in the headspace remained constant. As a result, the number of moles of DIC in solution must also have remained equal to that prior to freezing. This was used with the new meltwater volume to find the concentration of DIC in meltwater in $\mu mol.l^{-1}$, as an input to the PHREEQC simulation, with all other concentrations doubled. This generated a different $pCO_2$ value to that calculated in the air, meaning that gas transfer between the headspace and meltwater was necessary to attain equilibrium. $pCO_2$ of both air and meltwater, as well as $[H^+]$ were noted. A new $pCO_2$ value for air was then manually selected, with the ideal gas equation used to calculate the number of moles of $CO_2$ now present in the air. It was therefore possible to calculate the concentration of DIC in solution, and then the same parameters were noted. This manual selection and recalculation process was repeated again, in order to ensure that the relationship between the parameters was directly proportional. Finally, using the equation for a straight line, y=mx+c, the y variable being the difference in $pCO_2$ between the headspace and meltwater, and the x variable being $[H^+]$, it was possible to calculate the $pCO_2$ when there was equilibrium between the meltwater and headspace. This process was repeated at each 'Freezing', in order to obtain not only the $pCO_2$, but also the number of moles of $CO_2$ that were required to be transferred between the two phases in order to retain equilibrium.

### 2.4 Saturation

Increase in $Ca^{2+}$ or $CO_3^{2-}$ concentrations may result in calcite saturation. It was necessary to simulate calcite precipitation when $SI_{calcite}$ reached 0, since in reality, when a species reaches saturation in solution, it precipitates into the solid phase. If the solute concentrations were continually doubled, as before saturation occurred, $SI_{calcite}$ would continue to increase, and the solution would be supersaturated with respect to calcite. Therefore, it was necessary for $SI_{calcite}=0$, as well as continuing to hold $pCO_2$ constant at -3.4 log atms for B-Open and F-Open, to ensure all assumptions were met. As a result, each subsequent doubling of other solutes required Ca and DIC to be increased by differing factors both from each other, and from all other solutes, as this could not be achieved through assuming the same rate of increase in both solutes. These factors were obtained by iteration, with changes to both solutes until the assumptions previously mentioned were met.

In all scenarios, calcite saturated first of the species considered. Subsequently, a state of saturation was maintained, by increasing Ca and DIC by a factor differing from exerted upon the other solutes. In both the 'Closed' scenarios, it was possible

to calculate, through iteration, one factor per simulation, by which both Ca and DIC could be increased in order to maintain $SI_{calcite}$=0. Between each simulation, therefore, each solute excluding Ca and DIC is doubled, whilst Ca and DIC are increased by an alternative factor, identical for the two species, but variable between simulations. However, in the 'Headspace' and 'Open' scenarios, no such factor exists by which both species can be altered. As a result, each species was altered independently through iteration, starting from the previous simulation's factor, until both calcite saturation and the pCO2 assumption could be maintained. For all scenarios, the factors of change for Ca and DIC were subsequently used in order to calculate the amount of calcite precipitation they represent, and which was required to fulfil the assumptions.

# 3.0 Results

## 3.1 Evaluation of Model Setup

In Section 3.1, the rationale for choosing the Pitzer specific ion interaction model, rather than the standard Debye-Huckel model was discussed. A series of modelling experiments were conducted in order to determine the impact of this. Figure 4, using data from Baumgarten (1981) and Haynes (2014), showed that the Pitzer model was more accurate than the Debye-Huckel configuration across the range of ionic strengths considered. The Pitzer data, however, did not extend to the full range of ionic strengths, although this model is widely recognised to be more accurate at high ionic strengths (Millero, 1992; Harvie and Weare, 1980; Zhang *et al.,* 2005). The Pitzer model setup was therefore assumed to provide an accurate representation of the real solution. The following experiments examine the impact of instead using the Debye-Huckel setup, using pH as the variable of interest, due to its importance in determining the other conditions in the solution (Garrels and Christ, 1965).

At low ionic strengths, the Debye-Huckel estimated pH values do not deviate from the Pitzer values for both B-Open and B-Closed (Fig. 5). The pH values are in agreement until the solution exceeds approximately 0.05 $mol.kg^{-1}$, which concurs with the observation made in Section 3.1, concerning the data from Baumgarten (1981) and Haynes (2014). The Debye-Huckel gradually begins to differ from the Pitzer model beyond this point, with the Debye-Huckel model underpredicting the pH at every ionic strength value above 0.05 $mol.kg^{-1}$ (Fig. 5). There is substantial disagreement between the two models at high ionic strengths, with the Debye-Huckel model predicting very acidic conditions for both B-Closed and B-Open. Notably, in B-Closed (Fig. 5A), the Debye-Huckel model broke for the final simulation, citing that the mass of water was negative, further indicating its lack of suitability for the problem in question.

Furthermore, DIC concentration in B-Open, for the Debye-Huckel setup, had to be increased by an unprecedented factor in order to maintain atmospheric $pCO_2$ and calcite at saturation at the highest ionic strength (Table 2A). The factor change in DIC following the initial saturation of calcite initially declines, and then gradually rises, but remains within an approximate range of 0.86-1. The final two simulations are outside of this range, and the final increase in concentration by a factor of 71 is highly unrealistic. By contrast, B-Open in the Pitzer configuration is far more uniform

in its decrease, followed by steady increase, in factor change for both DIC and $Ca^{+}$ (Table 2B).

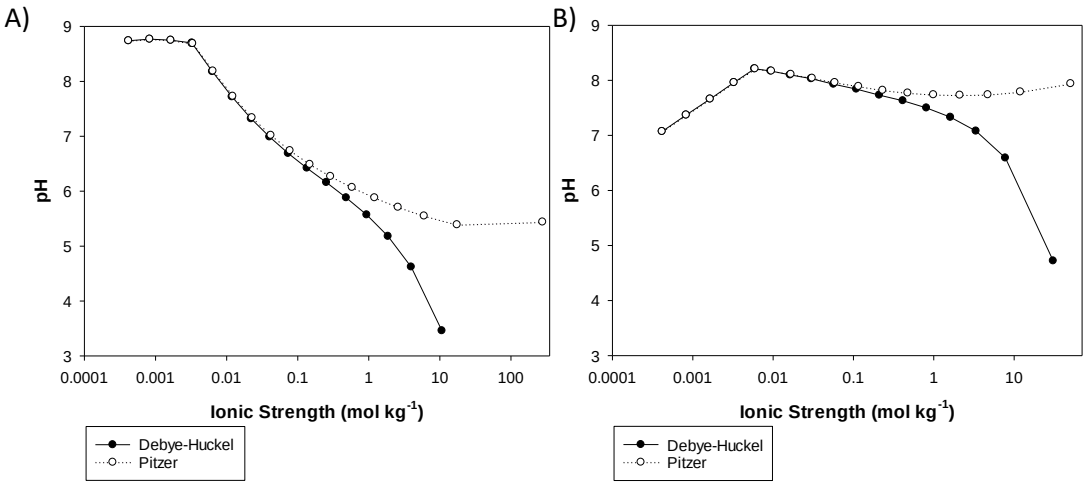


Figure 5 - pH variation over the range of ionic strengths used when freezing up the initial waters. A) B-Closed; B) B-Open

Table 2 – Factors of increase (dimensionless) for $Ca^{+}$ and DIC in B-Open in order to maintain atmospheric $pCO_2$ and simulate calcite precipitation. The point at which calcite initially saturates is in bold. A) Debye-Huckel; B) Pitzer.

A)

| $Ca^{+}$ | DIC |
|---|---|
| 0 | 0 |
| 2 | 1.76 |
| 2 | 1.865 |
| 2 | 1.923 |
| **1.83** | **1.79** |
| 1.3273 | 0.9275 |
| 1.5197 | 0.9045 |
| 1.7031 | 0.8595 |
| 1.8505 | 0.8595 |
| 1.93135 | 0.8685 |
| 1.96917 | 0.8664 |
| 1.98678 | 0.8898 |
| 1.994054 | 0.8807 |
| 1.9974 | 0.8867 |
| 1.999016 | 1.044 |
| 2.0000931 | 2.1384 |
| 2.0416022 | 71.20578 |

B)

| $Ca^{+}$ | DIC |
|---|---|
| 0 | 0 |
| 2 | 1.76 |
| 2 | 1.865 |
| 2 | 1.923 |
| **1.85** | **1.8085** |
| 1.3335 | 0.9375 |
| 1.5225 | 0.917 |
| 1.7056 | 0.8895 |
| 1.847 | 0.8902 |
| 1.92924 | 0.932 |
| 1.96691 | 0.965 |
| 1.98475 | 1.024 |
| 1.9926 | 1.08 |
| 1.99616 | 1.1206 |
| 1.99801 | 1.1842 |
| 1.998828 | 1.17 |
| 1.99952 | 1.204 |

Similarly, the Debye-Huckel model setup accurately predicted the pH until ionic strength reached approximately 0.05 mol.kg$^{-1}$ in both F-Open and F-Closed (Fig. 6). It then tends towards under-prediction in both scenarios, with one key exception. In the Debye-Huckel model of F-Closed, the highest ionic strength is associated with a pH of 14.2, which is outside of the scale usually used to indicate pH. This would suggest that the activity of hydrogen ions in solution would suddenly and abruptly decrease, by approximately nine orders of magnitude. Furthermore, as in B-Closed, the Debye-Huckel configuration in F-Closed breaks during the final simulation.

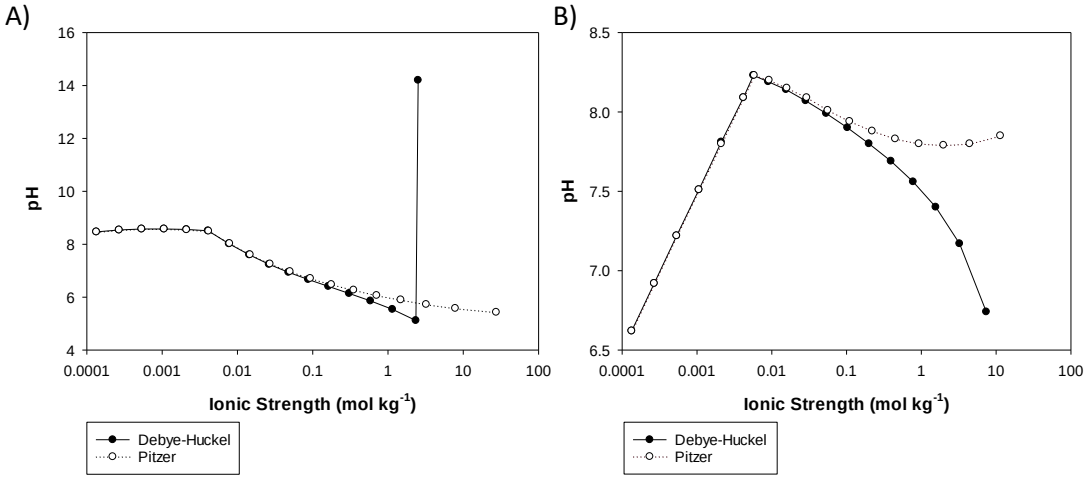


Figure 6 - pH variation over the range of ionic strengths used when freezing up the initial waters. A) F-Closed; B) F-Open

Overall, the Debye-Huckel and Pitzer model setups follow near-identical trajectories at very low ionic strengths, until approximately 0.05 mol.kg$^{-1}$. The Debye-Huckel model is usually considered to be accurate until ionic strengths of 1 mol.l$^{-1}$ (Zhang *et al.,* 2005). There remains to be some correspondence between the two models until this point, although to a lesser degree of accuracy, with differences of approximately 0.3-0.4 pH units (1.s.f) at 1 mol.kg$^{-1}$, which, since pH is a log scale, corresponds to a more significant deviation in $H^+$ activity between the two models. However, beyond this point, there is substantial disagreement between the two models (Figs. 5-6). It was therefore appropriate to determine how this would have affected the results of this study, had it not altered the configuration of the model to include the Pitzer specific ion interaction model.

The 'Freezing (%)' variable is calculated using chloride concentration, as detailed in Section 2.3, and is thus directly proportional to ionic strength. The relationship between these variables is displayed in Figure 7. The most substantial changes in

ionic strength occur at >95% Freezing, which is to be expected since the freezing process is simulated by sequential freeze-up of half the remaining water quantity at each stage. At very high % Freezing ionic strength increases rapidly as the volume of water within which the total initial solute content of the meltwater is held decreases rapidly.

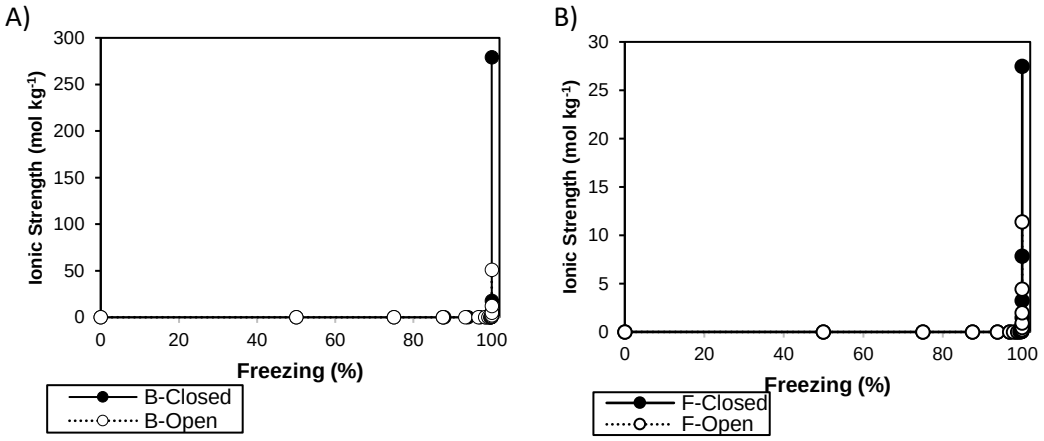


Figure 7 - Relationship between the calculated Freezing parameter and ionic strength for A) B-Closed and B-Open; B) F-Closed and F-Open

As such, Figure 8 provides a different visualisation of similar data to Figures 5 and 6, viewed as a freezing process, on a linear scale, rather than as ionic concentrations, on a logarithmic scale. In all four cryoconite hole scenarios, it is clear from Figure 8 that the substantial deviations of the Debye-Huckel model only affect the results at >99% Freezing. The results of this study are therefore similar to those which would have been achieved through use of the standard Debye-Huckel model setup for the vast majority of the freezing process. However, the extreme, unreliable pH values as the cryoconite hole enters the final stages of freezing, are avoided through use of the Pitzer specific ion interaction model. This is the case for all four cryoconite hole scenarios, with B-Closed, B-Open and F-Open all having estimated pH values lower than that predicted by the Pitzer model, and F-Closed with a spike in pH at high % Freezing, higher than that predicted by the Pitzer model, and indeed higher than pH values commonly found in solutions across the world (Fig. 8C).

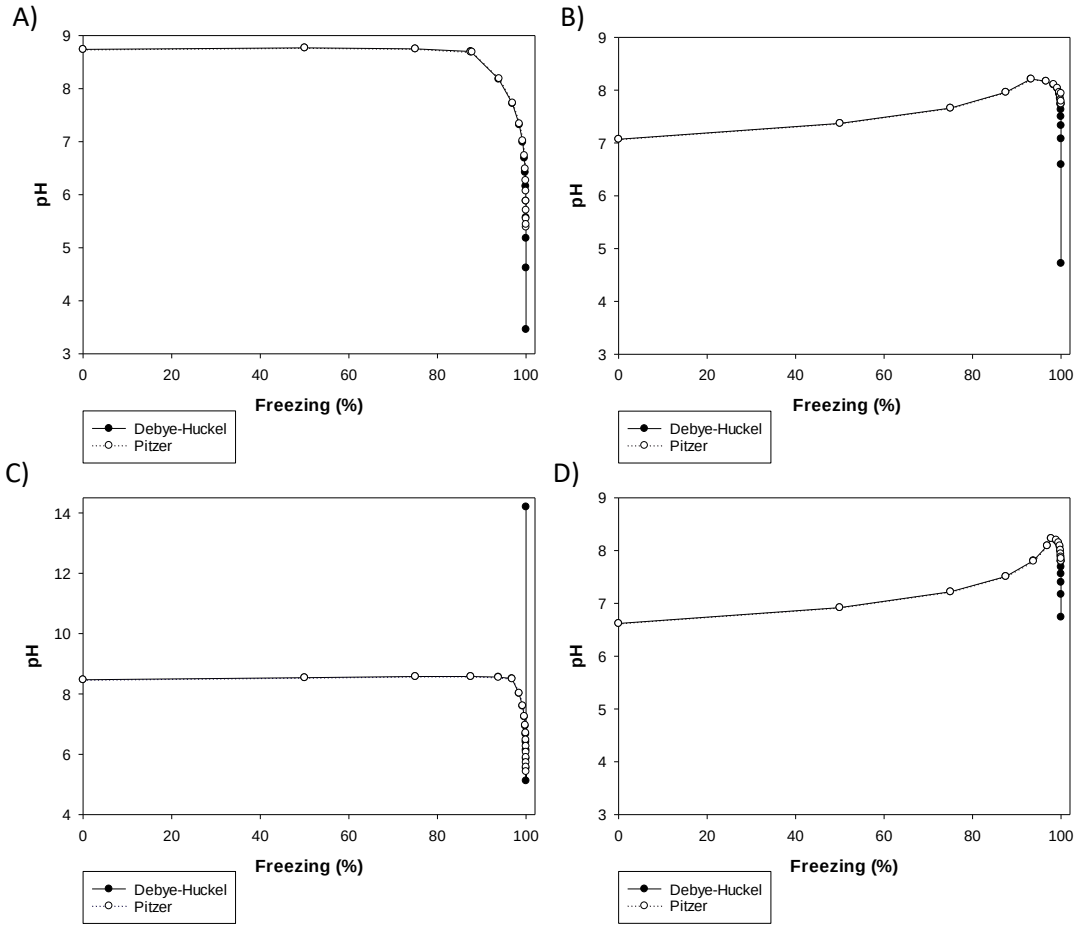


Figure 8 - pH variation as freezing occurs within cryoconite holes. A) B-Closed; B) B-Open; C) F-Closed; D) F-Open

This experiment was not conducted for the 'Headspace' scenarios, because of the highly iterative nature of the simulations involved. However, since all four other scenarios showed the Debye-Huckel model to produce more extreme pH values at high percentage freezing than the Pitzer model (Fig. 8), which is more accurate at high ionic strengths, this omission was not deemed to be of importance, nor to impact on the results of any subsequent experiments.

### 3.2 pH

#### 3.2.1 Open Cryoconite holes

The variation of pH during the freezing process in open cryoconite holes is shown in Figure 9. The pH at 0% Freezing for B-Open and F-Open is similar, with B-Open less than 0.5 units higher than F-Open in terms of pH at this point. B-Open is approximately neutral initially, and F-Open is slightly acidic. Both solutions are forced to be atmospheric in terms of $pCO_2$ throughout the freezing process, so similar pH is to be expected initially and throughout hole freeze-up. The differences

between the two pH values will therefore correspond to a difference between the solutions in terms of their relative concentrations of DIC species. These differences themselves must result from the differing initial solute concentrations in the two solutions, since, at 0% Freezing, the solutions have merely been equilibrated with the atmosphere in terms of $pCO_2$, with no additional changes.

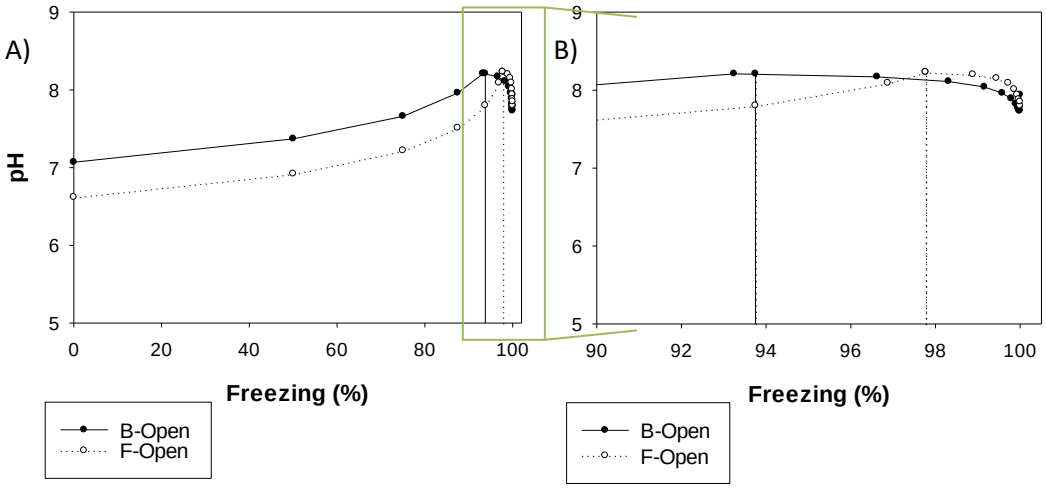


Figure 9 - Impact of hole Freezing on pH in open cryoconite hole scenarios. Vertical lines indicate the first instance of calcite saturation in each hole. A) Entire freezing process; B) A snapshot of 90% Freezing onwards.

In both B-Open and F-Open scenarios, pH rises throughout the freezing process until the point of calcite precipitation (Fig. 9A). This gradual increase takes the form of an approximate translation in the x axis, suggesting that a more dilute cryoconite hole meltwater (F-Open) experiences the same impact of freezing on pH, but this occurs later in the freezing process. It is also important to note that, whilst calcite saturation occurs later in F-Open than in B-Open (Fig. 9B), the peak of pH is approximately equal in the two solutions, with maximum values of 8.21 (B-Open) and 8.23 (F-Open) (2 s.f.). This suggests that open cryoconite holes become more alkaline until calcite saturates, with the most alkaline pH approximately equal between cryoconite holes, regardless of how dilute/concentrated the initial solution is.

Following calcite saturation in open cryoconite holes, pH declines at an increasing rate until the hole completely freezes. B-Open appears to form an approximate stretch of F-Open from the point of saturation until the hole freezes completely, in that, both scenarios saturate with respect to calcite at approximately the same pH, and both decrease to exactly the same pH (7.79). As a result, not only do B-Open and F-Open reach approximately the same pH upon calcite saturation, but also, the

freezing process and calcite precipitation beyond the initial calcite saturation have exactly the same impact on the solutions, despite the initial conditions from Bagshaw *et al.* (2007) being considerably more concentrated from those in Fortner *et al.* (2005).

However, the final two simulations in both B-Open and F-Open exhibit interesting characteristics in terms of pH. In both cases, there is a small increase in pH, which can only be visualised at a higher resolution (Fig. 10). This corresponds to a decrease in the saturation index of gypsum, as well as activity coefficients of calcium, sulphate and carbonate. The reason for this will be explored in Section 4.2.

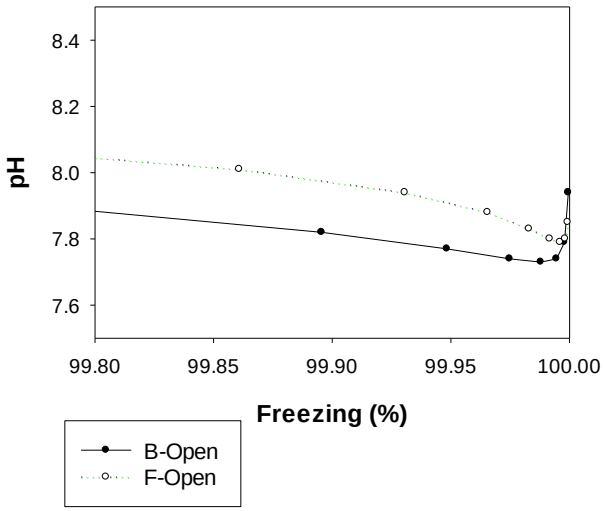


Figure 10 - pH variation at high (≥99.8%) Freezing in open cryoconite holes

### 3.2.2 Closed Cryoconite Holes

pH in closed cryoconite holes, without consideration of a headspace, varies very differently from that in open cryoconite holes (Fig. 11). The initial pH in both solutions is higher than in open cryoconite holes, with B-Closed displaying an initial pH 1.67 units (2 d.p.) higher than B-Open, and F-Closed having an initial pH 1.85 units (2 d.p.) higher than F-Open. Furthermore, the initial pH values of the two closed cryoconite holes are closer to one another than the two open holes were in terms of initial pH, with a difference of 0.27 units (2 d.p.). This suggests that the relative concentrations of DIC species in the initial meltwater are more similar when completely unchanged, as in the closed hole scenarios, than when they have been forced to be equal in terms of $pCO_2$.

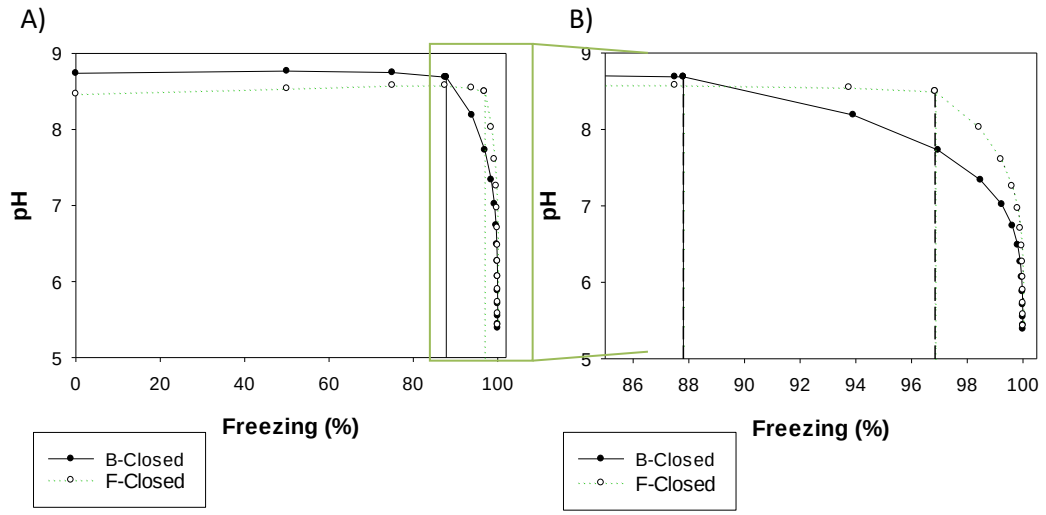


Figure 11 - Impact of Freezing on pH in closed cryoconite hole scenarios. Vertical lines indicate the first instance of calcite saturation in each hole. A) Entire freezing process; B) A snapshot of 85% Freezing onwards.

pH in both holes shows little variation until the point of calcite saturation (Fig. 11A). As in the open cryoconite holes, this occurs firstly in the more concentrated initial solution (B-Closed, Fig. 11B). The subsequent decrease in pH is far more substantial than that experienced by open cryoconite holes. The solution prior to calcite saturation is moderately alkaline, with a decline to a solution that is moderately acidic as the meltwater finally freezes up. This suggests that the subsurface brine ice in completely closed, frozen cryoconite holes may be acidic, so the microbial ecosystem must be tolerant of both alkaline and acidic conditions in order to survive between melt seasons.

Furthermore, as with the open cryoconite hole scenarios, the more dilute meltwater (F-Closed) forms an approximate stretch of the trajectory of the more concentrated solution (B-Closed) in terms of pH, from the point of initial calcite saturation until the meltwater finally freezes entirely (Fig. 11B). The pH at the point of calcite saturation is of very similar magnitude between the two solutions, and the final pH value has a difference of only 0.01 units between B-Closed (5.44) and F-Closed (5.43) (2 d.p.). This again suggests that the initial solute concentration in the cryoconite hole may affect the rate at which changes to pH occur during the freezing process, but the most extreme pH values, at both the upper and lower limits, are unaffected by differences in solute concentrations in the meltwater prior to freezing. This may suggest that the maturity of the cryoconite hole has little impact on the conditions the meltwater assumes, given that holes generated using initial concentrations from Fortner *et al.* (2005) are representative of a newly-formed cryoconite hole.

It must also be noted that, at very high % Freezing, the pH of B-Closed increases slightly, following a sustained decline (Fig. 12). This is similar to the increases observed at high % Freezing in open cryoconite holes (Fig. 10). However, notably, F-Closed does not experience a similar increase. The factors contributing to these increases in pH, and the absence of such an increase in F-Closed, will be explored in Section 4.2.

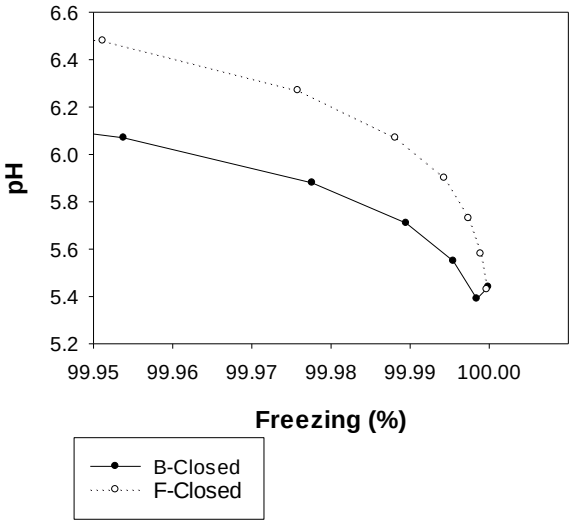


Figure 12 - pH variation at high (≥99.95%) Freezing in closed cryoconite holes

### 3.2.3 Headspace Cryoconite Holes

It is also important to consider the pH in lidded cryoconite holes with a gaseous headspace (Fig. 13). This is more realistic than the closed cryoconite holes examined above, since Antarctic cryoconite holes have been observed to contain headspaces. It is useful therefore to compare the closed cryoconite holes with the headspace scenarios in order to examine the impact on the meltwater chemistry of any interaction with the gas headspace, as well as to determine whether the headspace scenario tends towards the characteristics of a fully open or a fully closed meltwater system.

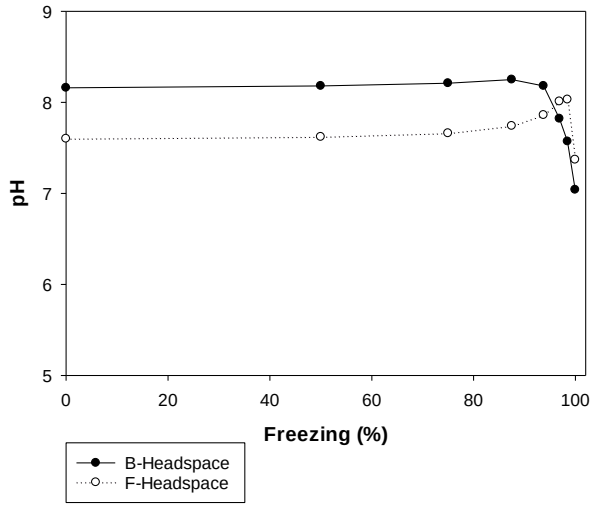


Figure 13 - Impact of hole Freezing on pH in lidded cryoconite hole scenarios with headspace interaction. There is no vertical line to indicate initial calcite saturation in either hole, as in this case, it was not possible to determine the exact moment of calcite saturation, due to the highly iterative method.

The initial pH values of the solutions with headspace are between the values of the open and closed solutions (Figs 9A, 11A and 13). Both headspace solutions are closer in pH to the closed scenario for their respective initial condition dataset, although this is more pronounced in B-Headspace than in F-Headspace. The largest differences in pH in initial solutions exist between the headspace solutions than between either the open or closed solutions (Fig. 13). This is likely to be because the dimensions of the hole, and the $pCO_2$ of the headspace prior to equilibration with the meltwater, were assumed to be equal for B-Headspace and F-Headspace. The two holes required similar increases in DIC concentration in order to achieve an initial equilibrium between the headspace and the meltwater in terms of $pCO_2$. However, F-Headspace is more dilute than B-Headspace, so this increase in concentration has a stronger effect on the chemistry of the meltwater in F-Closed. Therefore, it is likely that the equilibration of $pCO_2$ between the meltwater and the headspace exacerbates the differences in pH between the two solutions, at least initially.

Both meltwaters experience a slight initial increase in pH until they saturate with respect to calcite, which is indicated by a change in direction in each curve (Fig. 13). This increase is more substantial in F-Headspace, whose trajectory in terms of pH prior to calcite saturation is similar to F-Open, though with a lesser magnitude of change (Fig. 9). By contrast, the increase in pH in B-Headspace is much smaller, and is more similar in trajectory to B-Closed, which remains fairly static prior to initial

calcite saturation (Fig. 11). The exact point at which calcite reaches saturation is not known, so this is not indicated with any specificity (Fig. 13). Nevertheless, it is unlikely that this point would significantly deviate from the maximum pH values achieved in Figure 13. Therefore, it is likely that the most alkaline pH experienced in headspace meltwaters are similar to, or lower than those in open cryoconite holes, which in turn are less alkaline at their maxima than completely closed meltwaters.

Calcite precipitation was modelled earlier in the freezing process in B-Headspace than in F-Headspace (Fig. 13), as calcite became saturated earlier in the process, as was true for B-Open and B-Closed, when compared to their more dilute counterparts (Figs. 9B and 11B). As a result, the changes in pH as a result of calcite precipitation are of larger magnitude in B-Headspace, as the solution has experienced the additional forcing for a longer proportion of the freezing process (Fig. 13). pH decreases in both B-Headspace and F-Headspace as calcite is precipitated out of solution. This reduction in pH results in approximately neutral solutions in both meltwaters, with lower pH values than are reached in open cryoconite holes, but substantially higher than those found in completely closed cryoconite hole meltwaters. The complexity of the modelling process for the headspace meltwaters limited the upper extent of the Freezing process that could be modelled, so in the headspace scenarios, complete freeze-up is not represented. Whilst it is therefore likely that the reduction in pH may continue to decrease until the final freeze-up of the cryoconite hole, the modelling of freezing ceased when the volume of meltwater in the headspace holes was 0.01l. As a result, significant reductions in pH during the freeze-up of this small unaccounted volume, are unlikely.

The presence of the headspace, which in every freeze-up simulation required the transmission of $CO_2$ from the meltwater into the headspace, diminishes the impact of calcite precipitation on pH. The completely closed cryoconite hole meltwater simply increases solute concentrations as the hole freezes, but the transfer of $CO_2$ out of solution in the headspace scenarios increases the relative concentrations of bicarbonate and carbonate, potentially offsetting extreme reductions in pH.

### 3.3 $pCO_2$

#### 3.3.1 Open Cryoconite Holes

Open cryoconite holes were modelled by forcing $pCO_2$ to remain constant, in equilibrium with the atmosphere, as it was assumed that any disequilibrium would result in the diffusion of gas into or out of solution. As a result, there were no changes to $pCO_2$ throughout the freezing process (Fig. 14). There were differences between the two solutions in terms of pH, however, which suggests that these differences must correspond entirely with differences in the relative concentrations of carbonate and bicarbonate, as there is no difference between the solutions in terms of $pCO_2$.

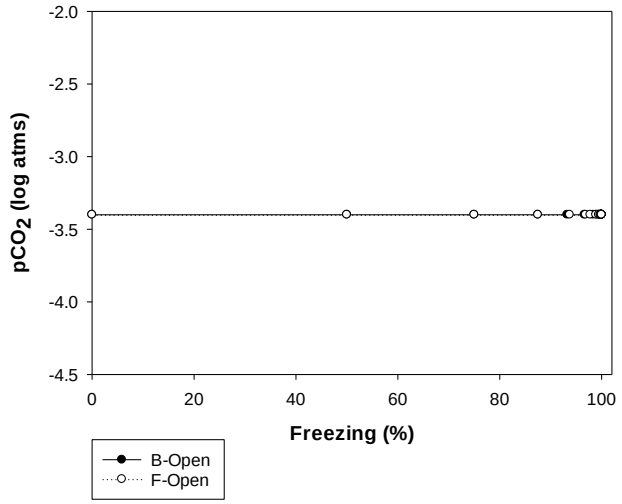


Figure 14 - pCO2 throughout the freezing process in open cryoconite holes.

#### 3.3.2 Closed Cryoconite Holes

The initial $pCO_2$ of the two closed cryoconite hole scenarios are very similar to one another, with the $pCO_2$ of B-Closed slightly higher than that of F-Closed (Fig. 15). This is in line with the similarity in pH values of the two solutions (Fig. 11). The initial $pCO_2$ values of both solutions are undersaturated with respect to atmospheric $CO_2$, as well as the solutions themselves being undersaturated with $CO_2$. The subsequent change in $pCO_2$ resulting from freezing alone, is that of a slight increase in $pCO_2$ until calcite initially saturates. This is likely to result from the increase in concentrations of all major ions during the freezing process, meaning that the concentration of $CO_2$ increases.

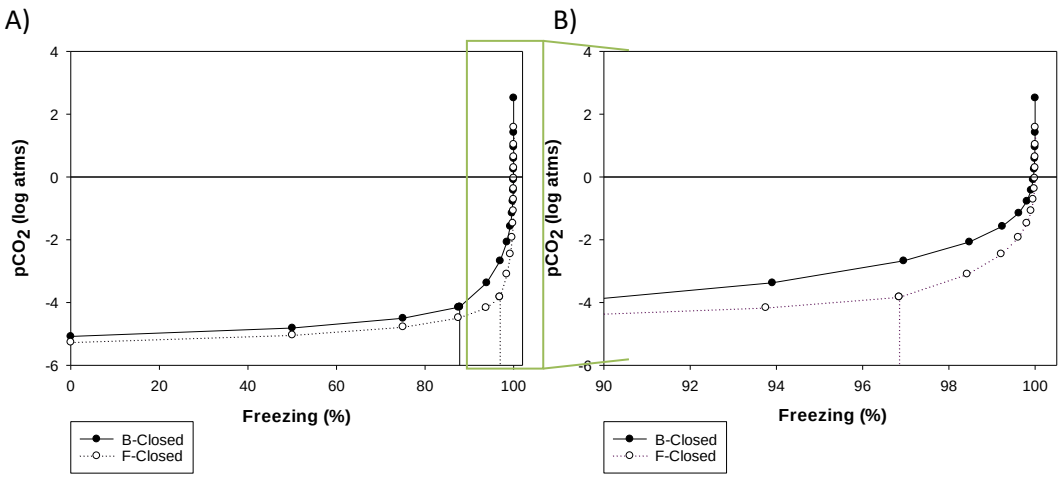


Figure 15- Impact of Freezing on $pCO_2$ in closed cryoconite hole scenarios. Vertical lines indicate the first instance of calcite saturation in each hole. A) Entire freezing process; B) A snapshot of ≥90% Freezing.

The point of initial calcite saturation corresponds to similar $pCO_2$ values in the two solutions (B-Closed=-4.14 log atms; F-Closed = -3.82 log atms, 2 d.p.), despite them differing in the proportion of freezing that has taken place in order to reach that saturation point (Fig. 15A). Following this point, there is a substantial increase in $pCO_2$ in both solutions, with B-Closed and F-Closed both exceeding atmospheric $pCO_2$ in the simulation following the initial calcite saturation (Fig.15B). This increase is at a faster rate than that preceding the initial calcite saturation, and in both scenarios, results in the meltwater solution itself becoming super-saturated with respect to $CO_2$. F-Closed again forms an approximate compression of B-Closed following initial calcite saturation, suggesting that despite initial differences in solute concentrations, closed cryoconite holes may experience similar-magnitude changes in $pCO_2$ throughout the freezing process, with the precipitation of calcite as an important control on this. Indeed, with both the dilute and the concentrated starting water, $CO_2$ becomes super-saturated in solution at high % Freezing.

### 3.3.3 Headspace Meltwaters

The headspace meltwaters are more similar in $pCO_2$ trajectory to closed cryoconite holes than open holes (Fig. 16). They are allowed to vary in $pCO_2$ and are initially undersaturated both with respect to $CO_2$ in solution, as well as with respect to atmospheric $pCO_2$. The initial values of $pCO_2$ are higher than those in the completely closed cryoconite hole meltwaters, and are closer together. This is in direct contrast with the pH results, which found the two headspace meltwaters to have the most substantial deviation in pH compared with the other hole types. However, the initial equilibration between the headspace and meltwater in terms of $pCO_2$ was achieved

by almost exactly the same increase in concentration of DIC in the two meltwaters, with an increase of 3.49µmol.l$^{-1}$ in B-Headspace, and an increase of 3.4 µmol.l$^{-1}$ in F-Headspace. This equates to an almost identical number of moles of $CO_2$ removed from each gas headspace in order to achieve equilibrium. This suggests that B-Headspace is well-buffered in terms of the carbonate system, as an addition of acidic $CO_2$ reduces the pH of the solution by a relatively small amount. By contrast, an addition of the same mass of $CO_2$ has a much larger impact on the pH of F-Headspace, despite both solutions retaining a similar $pCO_2$.

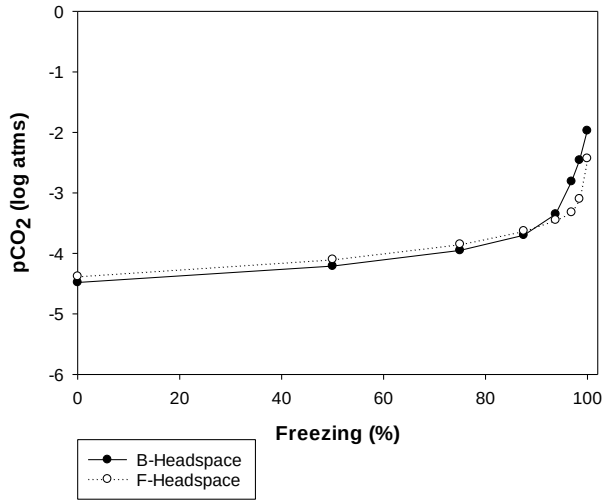


Figure 16 - Impact of Freezing on $pCO_2$ in closed cryoconite holes with gas headspace interactions.

$pCO_2$ increases during the freezing process in both solutions, though at a slower rate than in closed systems (Fig. 16). Calcite precipitation has a noticeable effect on the rate of increase, with an increased gradient following the first instance of calcite saturation. Both solutions exceed atmospheric $pCO_2$ at approximately 90% Freezing, but unlike in the closed hole scenarios, the meltwaters do not exceed saturation with respect to $CO_2$ even at high % Freezing. Therefore, it is possible that the presence of a gas headspace has the effect of moderating the extremities that the solution may experience, particularly at high % Freezing, as was also true for pH.

### 3.3.4 Headspace

$pCO_2$ in B-Headspace and F-Headspace was equilibrated to the $pCO_2$ in their respective gas headspaces. As a result, the $pCO_2$ in the headspace itself is identical to that shown in Figure 16. In order to achieve that equilibrium, transfer of $CO_2$ between the meltwater and headspace was necessary, shown in Figure 17. The removal of DIC from the entire cryoconite hole (including meltwater and headspace)

is concurrent with the precipitation of calcite from solution (Fig. 16). Notably, F-Headspace is considerably more dilute as an entire system, than B-Headspace. However, both cryoconite holes experience transfer of $CO_2$ into the headspace from the meltwater, particularly at high % Freezing. The partitioning changes from the initial amount of $CO_2$ existing almost entirely within the meltwater, to existing almost entirely within the gas headspace at the highest modelled % Freezing. This effect forms almost a direct reflection of the total amount of $CO_2$ in the cryoconite hole, but is not solely driven by calcite precipitation, as it begins in both holes prior to calcite saturation.

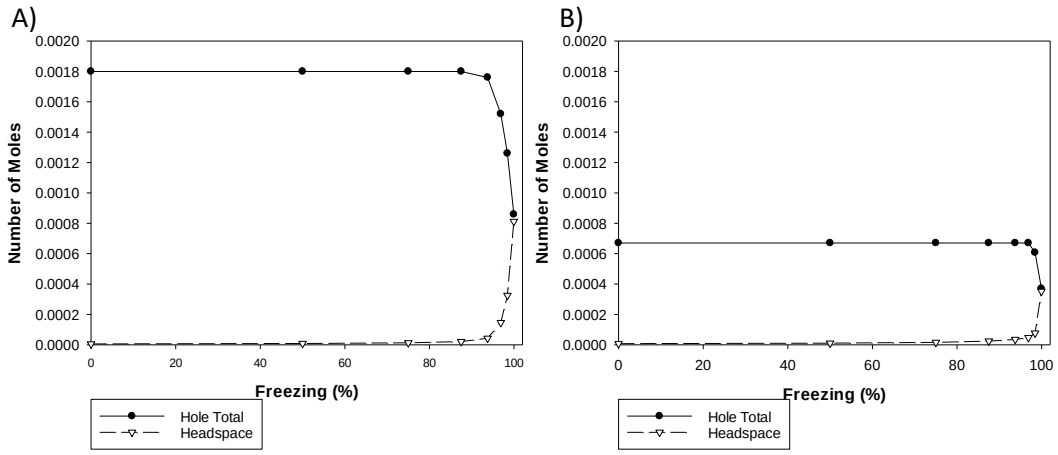


Figure 17 - Amount of DIC in total (meltwater+headspace) and $CO_2$ in the headspace alone in A) B-Headspace and B) F-Headspace

The very high proportion of DIC held as $CO_2$ in the gas headspace at high % Freezing is likely to be related to the freezing process itself. At the maximum modelled Freezing, only 0.01l of meltwater remains, as opposed to 2.14l of gas (Fig 18). Furthermore, the changes in DIC partitioning between the different structural components of the cryoconite hole correspond to the increases in proportion of the hole consisting of headspace, and the concurrent decrease in the proportion of the volume comprising meltwater (Fig. 17; 18). The most substantial changes in DIC partitioning not only coincide with calcite precipitation, but also with the change in dominant structural feature by volume, with the headspace occupying a larger space than the meltwater after approximately 85% of the meltwater freezes (Fig. 18).

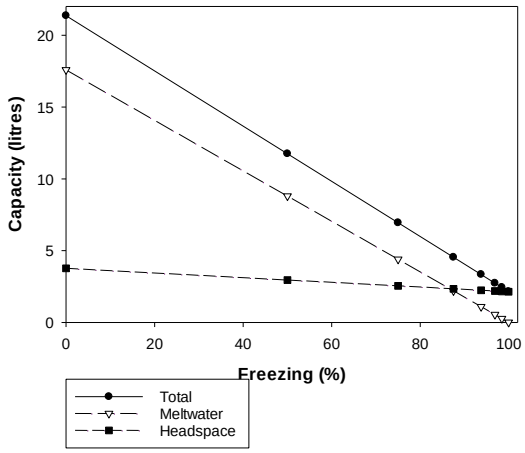


Figure 18 - Composition of the total cryoconite hole (meltwater + headspace) by capacity, as a function of Freezing (%). This is identical for both B-Headspace and F-Headspace.

### 3.4 Simulation of Calcite Saturation

#### 3.4.1 Open Cryoconite Holes

Initially, DIC was increased by an alternative value to all other solutes, which were doubled for each increase in 'Freezing', in order to maintain $pCO_2$ prior to initial calcite saturation (Fig. 19). Calcium was therefore doubled for each progressive freezing until calcite initially saturates. As a result, the changes to DIC concentration prior to initial calcite saturation are solely for the purpose of maintaining $pCO_2$ at atmospheric concentrations. It is consistently necessary in both solutions for DIC to be increased by a smaller factor than calcium, and hence all other solutes, prior to calcite saturation (Fig. 19). This suggests that the solution is required to degas in order to maintain atmospheric equilibrium during freezing, which in turn suggests that during the freeze-up of cryoconite hole meltwaters, they are a net source of $CO_2$ to the atmosphere, when other processes, such as net primary production, are excluded.

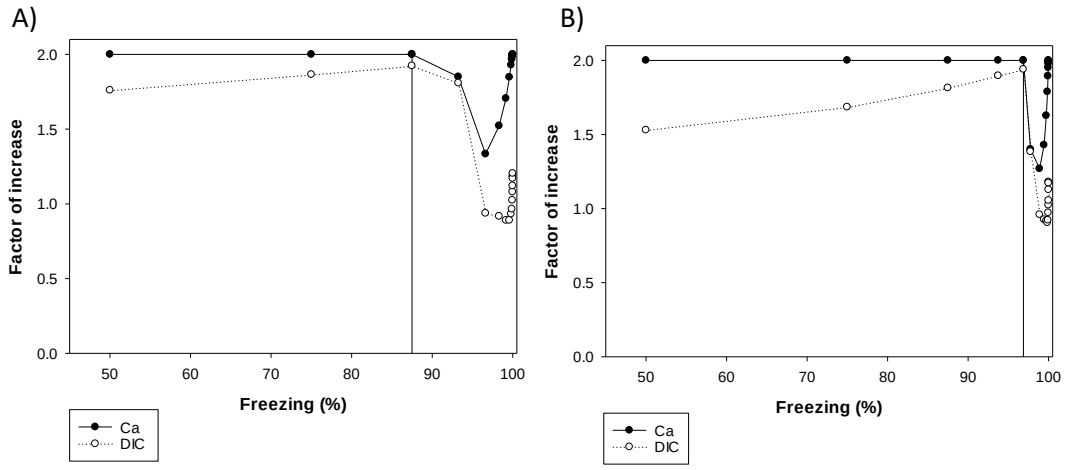


Figure 19 - Factors of increase in terms of calcium and DIC ions that are required in order to maintain atmospheric $pCO_2$ throughout the freezing process, as well as to maintain calcite at saturation following its initial saturation. A) B-Open; B) F-Open

Once calcite begins to precipitate, it is necessary for calcium and DIC to be altered by different factors, both from the other solutes, which still experience a doubling, as well as from each other (Fig. 19). The factors by which they are both altered are non-linear along the freezing gradient, but in both scenarios experience a sharp decrease, followed by a sharp increase, for both calcium and DIC. Again, the changes apparent in F-Open are an approximate compression of those required by B-Open, suggesting that the conditions in cryoconite hole meltwaters close to complete freeze-up may be similar, regardless of how dilute/concentrated the solute concentrations are in the high melt season. Furthermore, DIC is consistently increased by a smaller factor than either the other solute concentrations or calcite concentration. In both cryoconite holes, a number of simulations require a decrease in DIC concentration in order to maintain $pCO_2$ and calcite saturation. This is likely to be because DIC removal contributes to both $pCO_2$ conservation and calcite precipitation, so more DIC must be removed than calcite, in order to maintain both of these factors.

### 3.4.2 Closed Cryoconite Holes

In closed cryoconite holes, without any assumption required concerning $pCO_2$, it was possible to obtain one factor, by which both calcium and DIC could be increased in order to maintain calcite saturation. This required firstly a decrease, then an increase, in the factor of increase, similarly to those required by the open cryoconite holes, though to a lesser degree of magnitude (Fig. 20). Again, there is similarity between B-Closed and F-Closed in the form of an approximate stretch, implying that the changes required in order to maintain calcite at saturation are of similar

magnitude, but later in the freezing process in the more dilute cryoconite hole meltwater. Notably, the factors of increase in the closed cryoconite holes deviate from a doubling much less than those required in the open cryoconite holes (Fig. 19; 20).

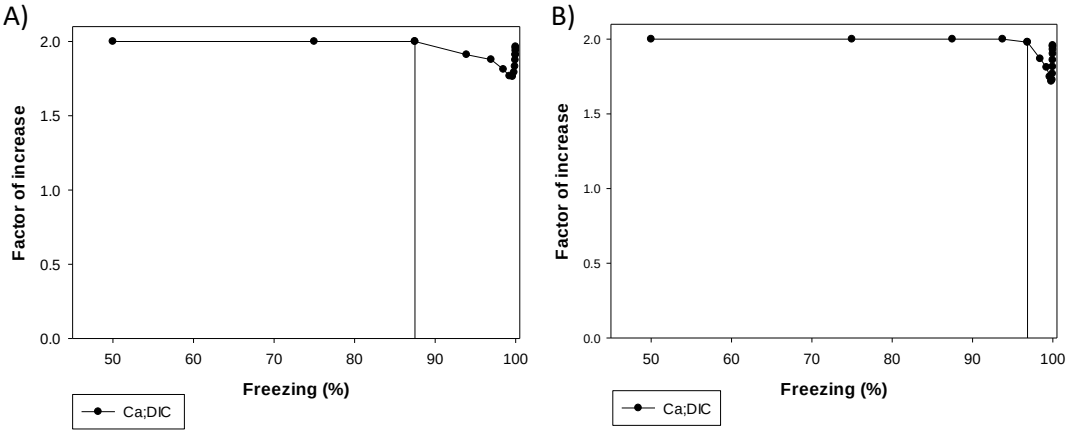


Figure 20 - Factors of increase in terms of calcium and DIC ions that are required in order to maintain calcite at saturation following its initial saturation. A) B-Closed; B) F-Closed

### 3.4.3 Headspace Cryoconite Holes

Calcium concentrations were initially treated identically to other solute concentrations, as they were doubled for each Freezing simulation. Meanwhile, DIC was allowed to vary in order to reach equilibrium in terms of $pCO_2$ with the gas headspace, similarly to the method employed in open cryoconite holes. However, in both B-Headspace and F-Headspace, DIC was increased by a very similar factor between each Freezing simulation to calcium, and all other solutes, prior to calcite saturation (Fig. 21). This contrasts with the changes required in the open cryoconite hole meltwaters, in which changes to DIC concentration differed much more from the changes to other solutes prior to calcite saturation (Fig. 19).

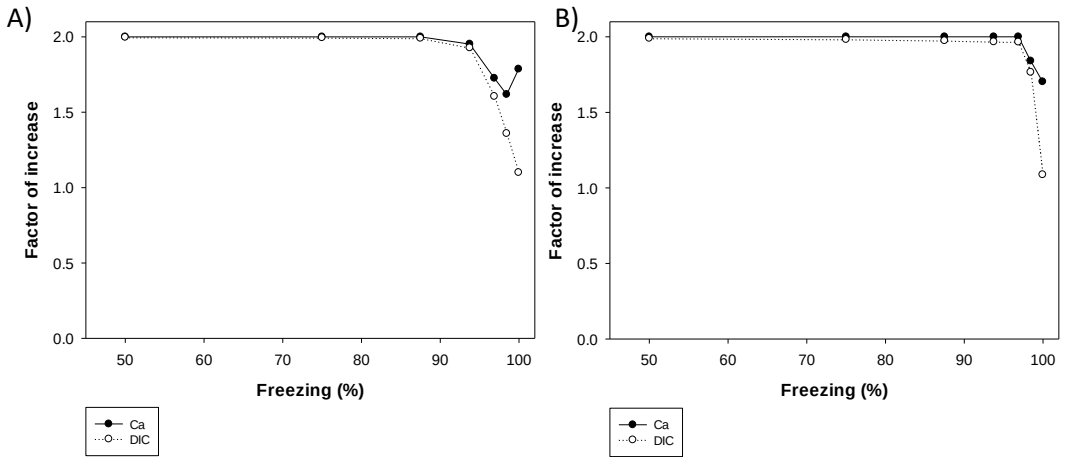


Figure 21 - Factors of increase in terms of calcium and DIC ions that are required in order to maintain calcite at saturation. A) B-Headspace; B) F-Headspace

Following calcite saturation, the changes required to maintain equilibrium with the headspace as well as calcite saturation differ between DIC, calcium, and other solutes, in both solutions (Fig. 21). Calcite appears to require increases of a similar magnitude to those required in closed cryoconite holes, and in B-Headspace there is an increase in factor required at the highest modelled % Freezing (Fig. 21A), which is similar to that found in both open and closed cryoconite holes (Fig. 19;20). A similar increase is not seen in the DIC factor in B-Headspace, or in either factor in F-Headspace (Fig. 21), but the same extent of freezing was not reached by either of these cryoconite holes, so it is likely that in the very final stages of freezing, these factors may also increase.

DIC deviates from calcium in the factor of increase required to maintain the given conditions within the meltwater in both B-Headspace and F-Headspace (Fig. 21). This is by a very similar magnitude for the two holes, with both meltwaters requiring an approximate factor of increase of 1.1, for each doubling of all other solute concentrations, excluding calcium. This remains to correspond to an increase in concentration in DIC, whereas in the open cryoconite holes, DIC is required to decrease in concentration in some instances in order to maintain $pCO_2$ and $SI_{calcite}$ at given values (Fig. 19).

The changes in factors of increase in closed cryoconite holes only reflect the changes required in order to maintain the saturation state of calcite (Fig. 20). The open cryoconite hole meltwaters require more substantial changes to their factors of increase for DIC and Ca than either the headspace or closed meltwaters (Fig. 19-21). This could suggest two things: there may be degassing of $CO_2$ into the atmosphere to maintain $pCO_2$ and $SI_{calcite}$, or, there may be more precipitation of

calcite in the open holes than in the headspace or closed holes in order to maintain these conditions. The combination of these processes will be discussed in Section 4.3.

### 3.5 Saturation Indices

Saturation indices of calcite, gypsum and halite were examined in further detail, as they are potentially important factors in the chemical evolution of cryoconite hole meltwaters (Section 1.4)

#### 3.5.1 Open Cryoconite Holes

All three saturation indices initially display a linear increase, in line with increases in concentration of their component species during the freeze-up process (Fig. 22). Calcite is the first of the examined species to saturate in both B-Open and F-Open, as it had the highest initial saturation index, and the fastest rate of increase (Fig. 22B). This initial saturation occurs earlier in B-Open than in F-Open, and because the two solutions have been subjected to exactly the same changes, this must be a direct result of the solution being initially more concentrated. $SI_{calcite}$ is then kept equal to 0, with any changes made to do so representative of calcite precipitation. The precipitation of calcite results in a faster rate of increase of $SI_{gypsum}$ and $SI_{halite}$. Gypsum saturates within the solution at very high % Freezing in both solutions, whilst Halite increases very quickly to a value slightly below 0 in each case, remaining undersaturated. $SI_{halite}$ increases in rate until it is near-vertical in trajectory, particularly when gypsum saturates.

Gypsum is allowed to supersaturate in these simulations because it was not possible to simulate the precipitation of calcite and gypsum simultaneously, due to the iterative nature of the process. It is unclear as to whether this is entirely representative of changes occurring in the natural environment. Although gypsum is highly soluble (Hodson *et al.,* 2004) and has not been observed within cryoconite holes in the natural environment, cryoconite holes at such high % Freezing have not been sampled, so it is not possible to ascertain the impact any gypsum saturation at very high % Freezing may have. However, it occurs so close to the total freeze-up of the cryoconite hole that the waters may only saturate with respect to gypsum for a very short period of time, so this omission is likely to be insignificant when considering the overall process.

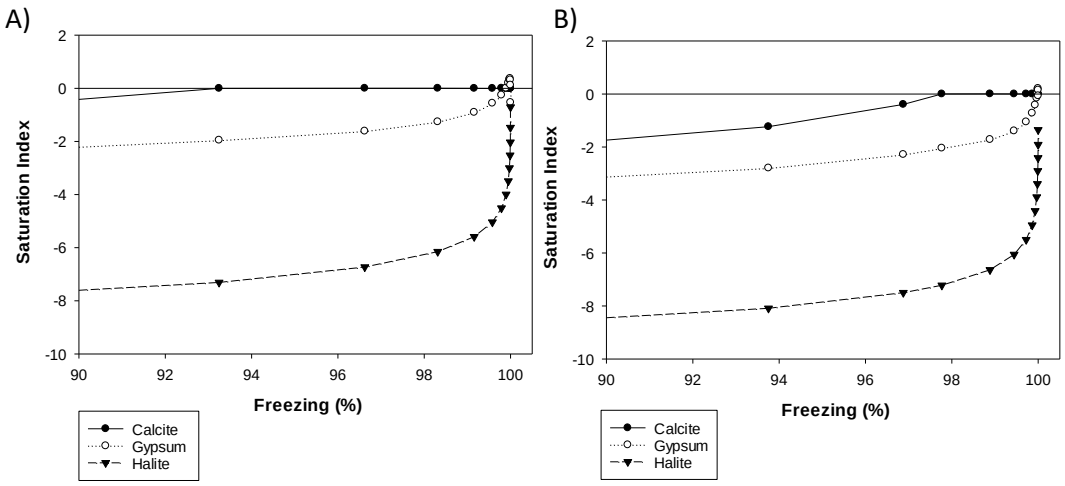


Figure 22 - Saturation indices of calcite, gypsum and halite at ≥90% Freezing. A) B-Open; B) F-Open

Furthermore, in both B-Open and F-Open, $SI_{gypsum}$ decreases (Fig. 23), returning to an undersaturated state in the final simulation of the freezing process. This was mentioned in Section 3.21, as it coincides with a small increase in pH. A possible explanation for this process will be explored in Section 4.4.

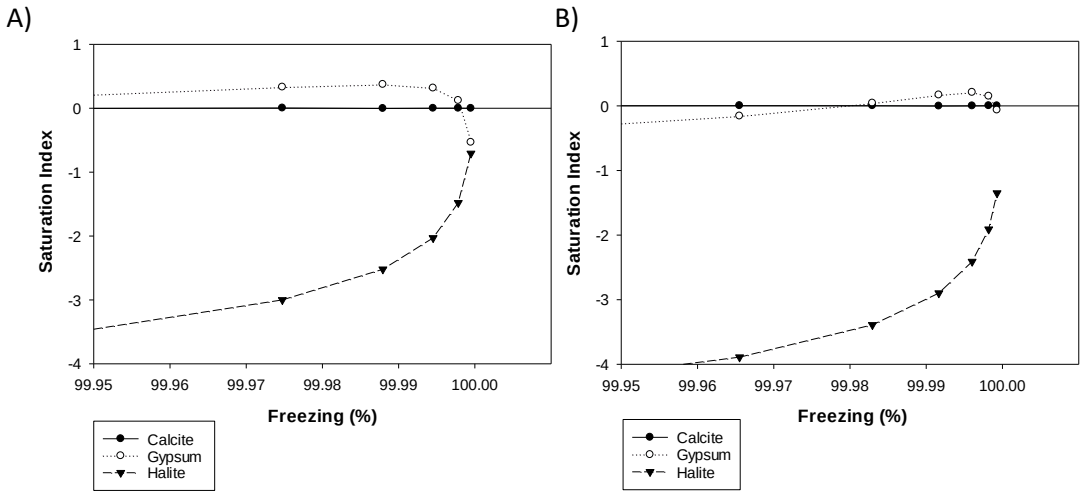


Figure 23 - Saturation indices of calcite, gypsum and halite at ≥99.95% Freezing. A) B-Open; B) F-Open

### 3.5.2 Closed Cryoconite Holes

Calcite saturation occurs earlier in closed cryoconite holes than in open cryoconite holes (Fig. 24; 22). This is only by a very small margin (approximately 1% Freezing) in F-Closed, but in B-Closed, the difference is more substantial (approximately 5% Freezing). The precipitation of calcite escalates the rate of increase for $SI_{gypsum}$ and $SI_{halite}$, similarly to in open cryoconite holes (Fig. 24; Fig. 22). There are few marked differences between the open and closed cryoconite holes in this respect, but it is worth noting that $SI_{halite}$ is less undersaturated in the closed cryoconite holes than in

the open hole meltwaters (Fig. 24; Fig. 22). In fact, $SI_{halite}$ in B-Closed reaches a value of $-3.27 \times 10^{-3}$ (2 d.p.), so does approximately reach saturation (Fig. 24A).

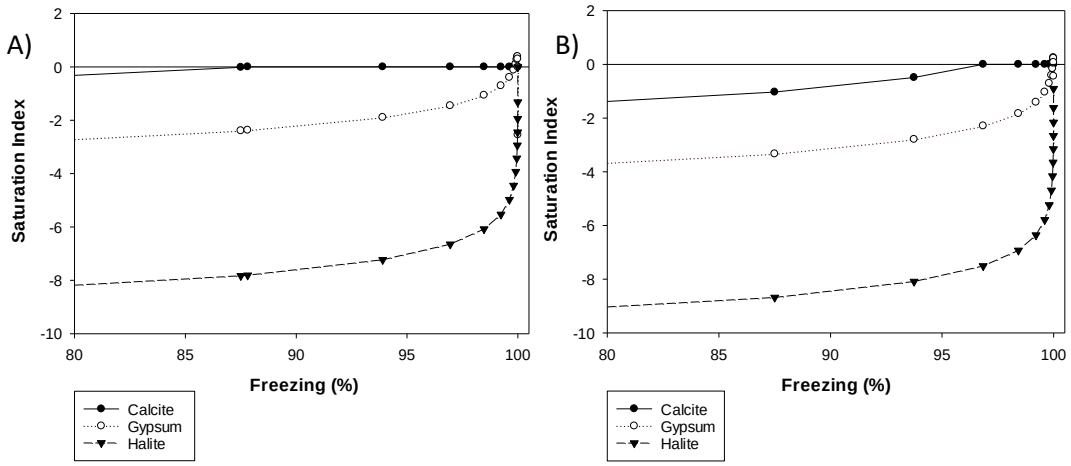


Figure 24 - Saturation indices of calcite, gypsum and halite at ≥80% Freezing. A) B-Closed; B) F-Closed

Similarly to open cryoconite holes, gypsum super-saturates within the hole, as it was not possible to model calcite and gypsum saturation simultaneously (Fig. 25). However, immediately prior to freezing, $SI_{gypsum}$ decreases to below 0, as occurred in open cryoconite holes. This is most substantial in B-Closed, in which it corresponds with the final increase in $SI_{halite}$ to the point of saturation. The decrease in the saturation index of gypsum will be explored in Section 4.4.

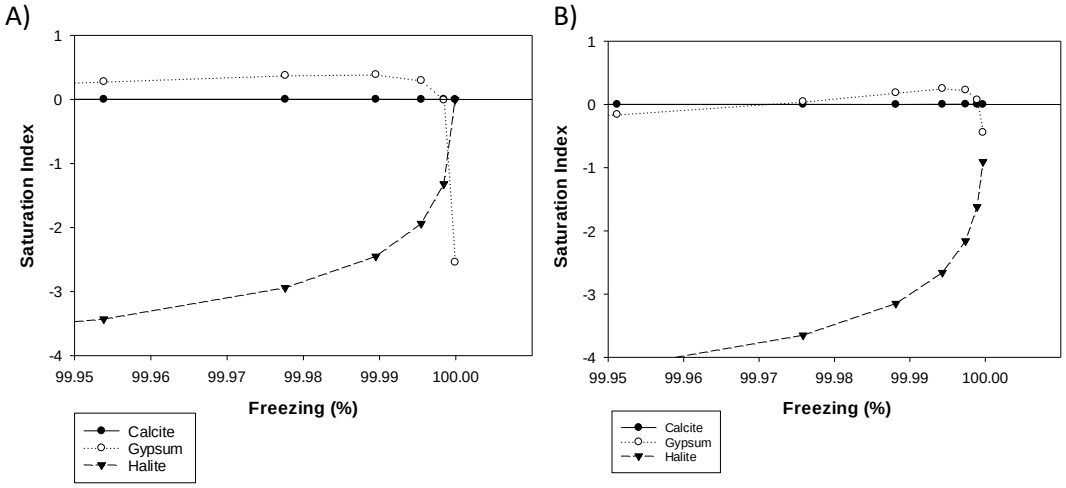


Figure 25 - Saturation indices of calcite, gypsum and halite at ≥99.95% Freezing. A) B-Closed; B) F-Closed

### 3.5.3 Headspace Cryoconite Holes

The initial values of the three saturation indices considered fall between those encountered in their open and closed meltwater counterparts, for both B-Headspace and F-Headspace. Following this point, the saturation indices follow a similar trajectory to all other scenarios modelled, with each species increasing at an approximately linear rate until calcite saturates (Fig. 26). This occurs firstly in B-Headspace than in F-Headspace, in line with both open and closed cryoconite hole scenarios (Fig. 22, 24 and 26). This suggests that a more concentrated initial solution will more rapidly saturate with respect to calcite than a more dilute solution, regardless of cryoconite hole structure.

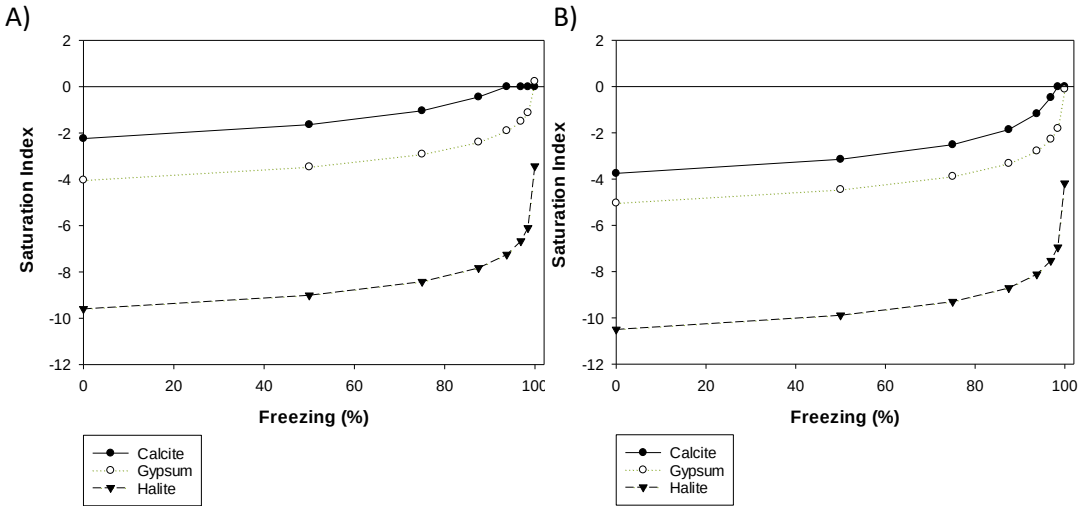


Figure 26 - Saturation indices of calcite, gypsum and halite throughout the freezing process. A) B-Headspace; B) F-Headspace

Following saturation with respect to calcite, there is a rapid increase in the saturation indices of gypsum and halite, which corresponds to similar-magnitude increases in all open and closed scenarios (Fig. 22, 24 and 26). The step-wise leaps seen in this instance, however, are not significant in themselves (Fig. 26). They are a reflection of the modelling process, where a number of freeze-ups were left out, as it was deemed more important to show the overall result than the intricacies of the processes at high % Freezing. As such, the increases in reality would display the same magnitude, but at a smoother rate than reflected in Figure 26. Halite remains to be undersaturated in both solutions, but rapidly increases in saturation index in both B-Headspace and F-Headspace following calcite saturation (Fig. 26). However, given that both open and closed cryoconite holes do not reach halite saturation, it is unlikely that halite saturation is ever achieved in cryoconite holes with gas headspace either.

Gypsum exceeds saturation in B-Headspace, although as with the open and closed scenarios, this could be a methodological flaw rather than a reflection of reality (Fig. 26A). However, it is important to acknowledge that gypsum does reach saturation. The same is not true for F-Headspace (Fig. 26B), as gypsum approaches saturation, reaching a maximum value of -0.10 (2s.f.), but given that the full extent of the freezing process is not quite reached through modelling, it is likely that gypsum does saturate at very high % Freezing in lidded cryoconite holes in reality. This is because in both open and closed cryoconite hole scenarios, this effect has been modelled, and with all other variables examined showing the headspace meltwaters to reflect conditions between those of the open and closed cryoconite holes, an effect found in both open and closed holes is likely to also occur in the lidded hole with a headspace. Similarly, it is not possible to accurately assess whether the effect found in open and closed cryoconite holes of a return to undersaturated conditions with respect to gypsum may occur in lidded cryoconite holes with a gas headspace.

# 4.0 Discussion

## 4.1 Hypotheses

Hereafter, headspace scenarios will be considered as intermediary on a spectrum of conditions between the open and closed cryoconite hole scenarios. The headspace scenarios were the only scenarios in which it was necessary to constrain the dimensions of the cryoconite hole, so whilst these are fixed, open scenarios can be considered to be of any dimensions, but with an infinite headspace, whereas the closed cryoconite hole can be of any dimensions, but with no headspace.

Hypothesis 1 predicted that pH would be higher in closed cryoconite hole meltwaters. This is initially correct, as pH in both closed cryoconite holes is initially higher than in the headspace cryoconite holes, which in turn are higher than the open cryoconite holes (Fig. 11A; 13; 9A). The hypothesis also predicted that the pH in open cryoconite holes would be the most stable because of $pCO_2$ being maintained at equilibrium with the atmosphere. However, initially this is not the case. pH increases steadily in open cryoconite holes prior to calcite saturation (Fig. 9A), whereas it remains approximately equal in closed cryoconite holes (Fig. 11A), with B-Headspace conforming to closed cryoconite holes, and F-Headspace falling between open and closed cryoconite holes in trajectory (Fig. 13). However, as calcite precipitation occurs, closed cryoconite holes experience a dramatic decline in pH (Fig. 11B), whereas open cryoconite holes are buffered in their decline in pH because $pCO_2$ must remain constant (Fig. 9B). Headspace scenarios appear to tend towards the same trend as closed cryoconite holes, although this is unclear due to the limited extent of freezing modelled (Fig. 13). Therefore, although aspects of Hypothesis 1 were correct, the seasonal evolution of cryoconite holes is more complex than predicted, so the hypothesis, in its simplistic form, must be rejected.

Hypothesis 2 predicted that $pCO_2$ would be constant in open cryoconite holes, which can be confirmed, since it was forced to remain at equilibrium with the atmosphere throughout the freezing process (Fig. 14). It also predicted that in lidded cryoconite holes $pCO_2$ would increase, and this was found to be true for both closed and headspace cryoconite hole scenarios (Fig. 15; 16). As a result, the hypothesis can be accepted.

Hypothesis 3 predicted that calcite would precipitate as the cryoconite hole froze in all scenarios, which may impact on $pCO_2$ and gypsum saturation. All cryoconite holes saturated with respect to calcite, and the subsequent precipitation was

modelled (Fig. 19-21). In the headspace and closed cryoconite hole scenarios, the precipitation of calcite appears to inflate the rate of increase for $pCO_2$ (Fig. 15;16), although the same is not true for open cryoconite holes, which were forced to remain at equilibrium with atmospheric $CO_2$ (Fig. 14). It also appears to increase the rate at which gypsum saturates in all cryoconite hole scenarios (Fig. 22; 24; 26), although in both of these cases, the relationship is not sufficiently different from the previous increase that the hypothesis can be fully accepted. Furthermore, calcite was predicted to saturate more quickly in open cryoconite holes, but actually saturated first in closed cryoconite holes, reasons for which will be explored in Section 4.2.

Hypothesis 4 predicted that gypsum would approach saturation in all cryoconite holes, but would decrease in saturation index as calcite precipitates. Gypsum does approach saturation in all cryoconite holes, and indeed supersaturates in all scenarios excluding F-Headspace, in which there is no indication that gypsum would not supersaturate if the full freezing extent were modelled (Fig. 22-26). However, as mentioned previously, $SI_{gypsum}$ appears to saturate at a faster rate as calcite precipitates in all cryoconite holes, indicating that the system is not limited by calcium ion concentrations.

Hypothesis 5 predicted that the meltwaters would not saturate with respect to halite. This was confirmed by the results for all cryoconite holes (Fig. 22; 24; 26), although $SI_{halite}$ increased to very close to saturation in B-Closed, the most concentrated closed cryoconite hole (Fig. 25). However, because the full extent of the freezing process was modelled in this instance, halite did not actually precipitate, and so the primary changes in chemical composition were induced by carbonate and gypsum saturation, and this hypothesis can be accepted.

Finally, hypothesis 6 predicted that the headspace scenarios would be geochemically different to both fully open and fully closed systems, and would cause the build up of gas pressure in the headspace. The results detailed for pH and $pCO_2$ were both different from the open and closed scenarios, falling between the two in trajectories throughout the freezing process (Fig. 13;16). The saturation indices measured were similar to both open and closed cryoconite holes, as all three scenarios were similar in this regard, although the more detailed changes described in both pH and the saturation index of gypsum at very high % Freezing were not modelled in the headspace cryoconite holes because the full extent of the freezing process was not modelled in the headspace scenarios (Fig. 26). $pCO_2$ in the gas headspace increased throughout the freezing process, to above atmospheric values

in both B-Headspace and F-Headspace (Fig. 16). As a result, the final hypothesis can be accepted.

### 4.2 Carbonate Chemistry

The carbonate system in cryoconite hole meltwaters will be here be given a more thorough examination in order to aid explanation of variations in pH, as pH reflects the speciation of carbonates within a solution.

#### 4.2.1 Open Cryoconite Holes

pH in open cryoconite holes was initially lowest, when compared with closed and headspace cryoconite holes, with B-Open having a pH initially higher than F-Open (Fig. 9). $CO_3^{2-}$ is initially very low in relative concentration compared to $CO_2$ and $HCO_3^-$ in both B-Open and F-Open (Fig. 27). B-Open contains a higher proportion of $HCO_3^-$ than F-Open, and, correspondingly, a lower proportion of $CO_2$. This results in a higher pH in B-Open than in F-Open, with the near-equal contributions of $CO_2$ and $HCO_3^-$ in F-Open causing the pH to be slightly acidic.

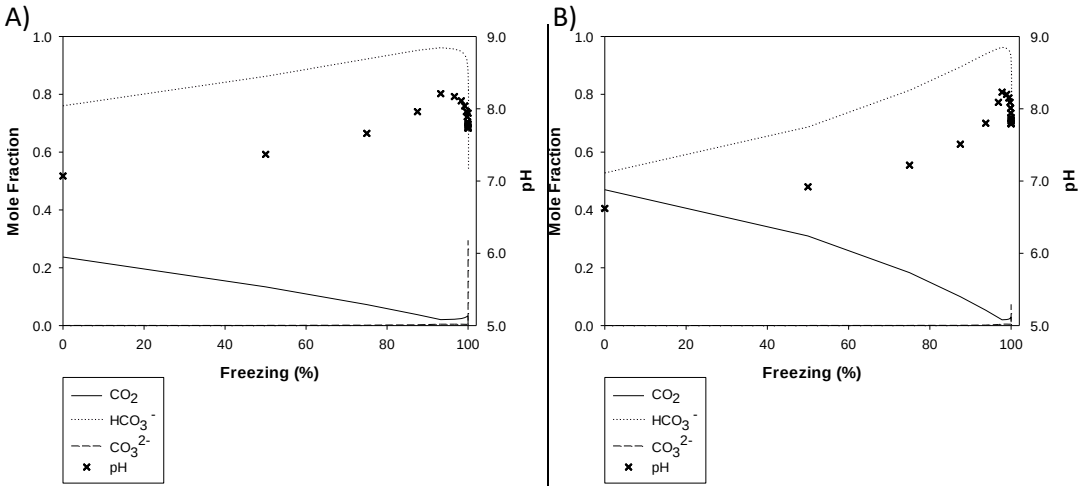


Figure 27 - Relative concentrations of carbonate species, as well as pH, throughout the freezing process in A) B-Open; B) F-Open

This is likely to be because the initial equilibration with atmospheric $pCO_2$ prior to the first simulation required a near-doubling in DIC concentration, from 34.3 to 65.5 $\mu mol.l^{-1}$. By contrast, the increase required in B-Open was smaller, in both absolute and relative terms, from 98.4 to 131 $\mu mol.l^{-1}$. F-Open is more dilute than B-Open, and, as observed in Section 2.2, its charges are approximately in balance. Therefore, an addition of DIC into solution will be primarily speciated as $CO_2$, which is acidic in aqueous form, so drives pH down (Fig. 27B). Similarly, an addition of DIC into B-Open will also predominantly increase $CO_2$ concentrations, but because

the solution itself is more concentrated, particularly in terms of DIC, this increase in $CO_2$ concentration will be less significant relative to the other carbonate species (Fig. 27A).

pH in both B-Open and F-Open is directly described by relative $HCO_3^-$ concentration, as well as being an approximate reflection of relative $CO_2$ concentration (Fig. 27). This suggests that in order to maintain $pCO_2$ at atmospheric levels, as freezing occurs, bicarbonate concentrations increase. Absolute $CO_2$ concentration remains constant for both B-Open and F-Open, but the relative concentration decreases as $HCO_3$ concentrations increase. When calcite precipitation occurs, indicated by a change in direction of the pH, $HCO_3^-$ and $CO_2$ curves, pH, and the relative concentration of bicarbonate decrease. DIC is required to increase by smaller factors than other solutes in order to simulate the precipitation of calcite, as well as maintaining the $pCO_2$ assumption (Fig. 19). Calcite precipitation consumes calcium and (bi)carbonate ions, causing a reduction in pH, as the low concentration of $CO_3^{2-}$ in solution becomes even smaller in relative contribution to DIC.

Notably, in both B-Open and F-Open, the mole fraction of carbonate increases rapidly, at very high % Freezing. This is most clearly visible in Figure 27A, as carbonate, which was previously lower than can be viewed, becomes visible prior to a spike. The same effect is also occurring to a lesser extent in F-Open (Fig. 27B). The point at which carbonate concentration begins to increase corresponds exactly to the point at which the factors of increase for B-Open and F-Open are required to rise in order to maintain calcite saturation, following their initial decline (Fig. 19). The sharp peak in $CO_3^{2-}$ concentration in both B-Open and F-Open also corresponds the points over which gypsum decreases and indeed undersaturates once more. Whether these are causal relationships may be made clear through examination of closed and headspace cryoconite holes. The decline, then rise in factors of increase required clearly exists in all cryoconite holes apart from F-Headspace (Fig. 19-21), so if the same trends in the relative concentration of carbonate are not clear in F-Headspace, the relationship may be causal. In addition, gypsum saturates and then returns to an undersaturated state in closed cryoconite holes, but not in the headspace scenarios. Similarly, it may be possible to determine the presence of a causal link by examining these differences. Crucially, these sharp increases in carbonate concentrations result in the small increase in pH at the maximum extent of freezing, as shown in Figure 10. This was also found to occur in B-Closed, but not in F-Closed, nor in the headspace scenarios. This may contradict the possibility of gypsum providing an explanation. This will be explored further in Section 4.4.

### 4.2.2 Closed Cryoconite Holes

pH and DIC speciation between closed cryoconite holes are initially very similar (Fig. 28). DIC in solution is dominated by $HCO_3^-$ in both B-Closed and F-Closed. The initial differences in pH between the two holes are therefore primarily caused by small differences in the relative concentrations of $CO_2$ and $CO_3^{2-}$. B-Closed has a slightly higher mole fraction of $CO_3^{2-}$ when compared with $CO_2$. The reverse is true for F-Closed, causing B-Closed to be slightly more alkaline.

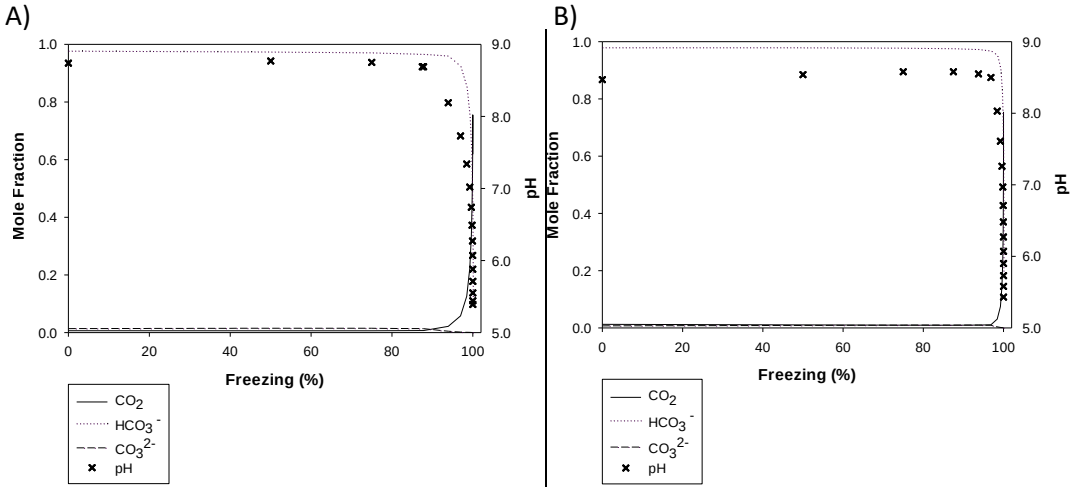


Figure 28 - Relative concentrations of carbonate species, as well as pH, throughout the freezing process in A) B-Closed; B) F-Closed

Throughout the freezing process, B-Closed and F-Closed show very similar trajectories in the partitioning of DIC, as well as pH (Fig. 28). pH also very closely relates to $HCO_3^-$ concentration, and is an approximate reflection of $CO_2$ concentration. pH, and the mole fractions of DIC species, remain fairly static throughout the majority of the freezing process, until the initial instance of calcite saturation, here indicated by a change in direction in the curves of pH, $HCO_3^-$ and $CO_3^{2-}$.

During calcite precipitation, there are significant declines in pH and the relative contribution of $HCO_3^-$ to DIC, which are reflected by the substantial increase in $CO_2$ mole fraction (Fig. 28). Calcite precipitation consumes $HCO_3^-$ ions, which are shown to substantially decrease in their relative contribution to total DIC concentrations. In the closed cryoconite hole scenarios, $CO_2$ is allowed to vary, by contrast to the open cryoconite hole scenarios. This means that the carbonate equilibria shift to a state where $CO_2$ dominates, and particularly because DIC concentrations continue to increase, the resultant solution rapidly decreases in pH to a moderately acidic state, in both B-Closed and F-Closed.

Carbonate ion relative concentration in closed cryoconite holes does not increase when the factor of increase of DIC rises, at very high % Freezing. This may be because $CO_2$ concentrations vary in closed cryoconite hole meltwaters, and with the solution already decreasing in pH at this point, any addition of DIC will remain primarily as $CO_2$, further increasing its dominance at high % Freezing. However, as in open cryoconite holes, the final few freeze-up simulations show increases in carbonate concentration. These increases are on a smaller scale than those found in open cryoconite holes, and indeed are not visible in Figure 28 because of this. The increase in $CO_3^{2-}$ in B-Closed is larger in magnitude than that in F-Closed, particularly in the final freeze-up simulation, in which the relative concentration of $CO_3^{2-}$ increases by an order of magnitude.

It was noted in Section 4.2.1 that open cryoconite holes experienced a sudden increase in the relative concentration of carbonate ions at the final freeze-up simulation which may cause an increase in pH, slightly counter-acting the decreasing trend in pH. The same relationship is seen in B-Closed, although with a smaller increase in pH, but F-Closed has an increase in relative $CO_3^{2-}$ concentration, but not in pH. However, the inextricable relationship between DIC speciation and pH dictates that increases in $CO_3^{2-}$ concentration and pH must be a causal relationship. Open cryoconite holes have fixed $CO_2$ at relatively low concentrations, which become steadily a lesser contributor to DIC as total DIC concentrations increase. Therefore, changes to the relative concentrations of $CO_3^{2-}$ and $HCO_3^-$ will have a more substantial impact on pH. By contrast, $CO_2$ concentrations increase throughout the freezing process in closed cryoconite holes, and indeed increase in relative contribution to DIC. As a result, increases in carbonate ion concentration will have to be more substantial in order to have the same magnitude of impact on pH. Therefore, whilst the mole fraction of carbonate increases by more than an order of magnitude in B-Closed, it is sufficiently low in absolute concentration that this only causes a slight increase in pH. In F-Closed, in which $CO_2$ concentration is also dominant at high % Freezing, the relative contribution of carbonate ion concentration to DIC increases by $10^{-5}$ (1 s.f.). As $CO_2$ concentration is the dominant contributor to DIC at this % Freezing, this increase is insufficient to impact on pH (Fig. 28B).

### 4.2.3 Headspace Cryoconite Holes

Initial pH values in the headspace cryoconite holes are different from one another, and this difference is reflected in the relative concentrations of $HCO_3^-$ and $CO_2$ (Fig.

29). Figure 15 showed that the $pCO_2$ values experienced by the two cryoconite holes were very similar, which means that the absolute concentrations of $CO_2$ in each hole must also be similar. However, total DIC concentrations in F-Headspace are approximately a factor of 3 lower than in B-Headspace initially (Table 1). As a result, although the absolute concentrations of $CO_2$ are similar between the two meltwaters, the relative concentration of $CO_2$ as a proportion of total DIC concentration will be higher in F-Closed (Fig. 29). As a result, F-Headspace experiences a lower pH than B-Headspace initially.

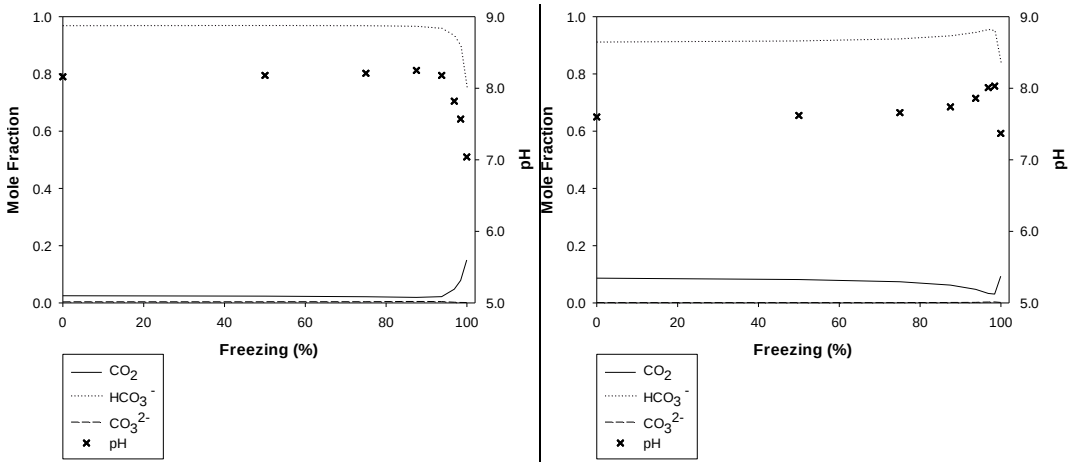


Figure 29 - Relative concentrations of carbonate species, as well as pH, throughout the freezing process in A) B-Headspace; B) F-Headspace

DIC concentrations increase as the cryoconite hole freezes, and the pH and DIC partitioning stay relatively stable throughout the majority of the freezing process, particularly in B-Headspace, while in F-Headspace, $HCO_3^-$ increases in dominance, with a decrease in the relative contribution of $CO_2$ (Fig. 29). This is likely to be because in order to maintain equilibrium with the headspace in terms of $pCO_2$, at every freeze-up simulation, it was necessary for $CO_2$ to be donated from the meltwater into the headspace. These changes were of a similar absolute number of moles, but as F-Headspace is more dilute than B-Headspace, these changes have a more substantial impact on relative $CO_2$ concentration, causing a rise in pH prior to calcite saturation.

pH decreases in both headspace meltwaters when calcite precipitates (Fig. 29). Calcite precipitation uses $HCO_3^-$ ions, so the proportion of DIC held as $HCO_3^-$ decreases, causing $CO_3^-$ to increase in dominance. This change is of a much smaller magnitude than the changes present within open or closed cryoconite holes, but this is because the headspace scenarios were not modelled to the full extent of

freezing. Although only 0.01l of water remained at this stage in the freezing process, the gradients of the pH, $HCO_3^-$ and $CO_2$ curves in the headspace cryoconite holes, in particular in B-Headspace, are similar to those found in closed cryoconite holes, so it is possible that in the very final freeze-up of a cryoconite hole with a gas headspace, pH may decrease to the same extent as in closed cryoconite holes.

### 4.3 Calcite Precipitation and Carbon Degassing

The mass of calcite precipitated in each hole throughout the freezing process, as well as the $CO_2$ removed either into the headspace or into the atmosphere, were calculated, assuming the same dimensions in all holes as are used in the headspace scenarios (Table 3). For each cryoconite hole type, the scenario forced with the data from Bagshaw *et al.* (2007) precipitated substantially more calcite, and released substantially more $CO_2$, than their counterparts with initial data from Fortner *et al.* (2005). Each pair of scenarios received identical treatment to one another, so this will be a direct result of the Fortner *et al.* (2005) scenarios being more dilute, and calcite precipitating later in the freezing process as a result (Fig. 22; 24; 26).

Table 3 - Total precipitation and $CO_2$ removal from solution throughout the freezing process in all cryoconite hole scenarios.

| Cryoconite Hole Scenario | Calcite Precipitated (g) (2 s.f) | $CO_2$ removed from solution (g) (2 s.f) |
|---|---|---|
| B-Open | 0.088 | 0.054 |
| F-Open | 0.030 | 0.032 |
| B-Closed | 0.082 | - |
| F-Closed | 0.028 | - |
| B-Headspace | 0.053 | 0.027 |
| F-Headspace | 0.0094 | 0.010 |

Despite the differences in factors of increase required between open and closed scenarios (Fig. 19-21), there is very little difference in the amount of calcite precipitation modelled, between B-Open and B-Closed, and F-Open and F-Closed (Table 3). However, the headspace scenarios show very different amounts of calcite precipitation, particularly in F-Headspace. This is likely to be because the headspace scenarios were not modelled to the full extent of freezing, and as mentioned previously, interesting changes in meltwater chemistry may occur at the highest % Freezing. F-Headspace was only modelled for two freeze-up simulations during calcite precipitation. The calcite precipitation in other scenarios was built up over a number of freeze-ups, so this reflects the length of time over which calcite has precipitated, rather than the ability of calcite to precipitate. Indeed, since the

headspace scenarios are intermediate between open and closed scenarios in terms of other factors, and the open and closed scenarios are very similar in terms of calcite precipitation, it is likely that at the full extent of freezing, a similar amount of calcite precipitation would have occurred in headspace cryoconite holes.

$CO_2$ removal is likely to be more similar between the open and headspace cryoconite holes, because $CO_2$ is donated to the headspace for the duration of the freezing process, rather than simply being altered following calcite saturation. In the headspace scenarios, however, the differences between the two cryoconite hole types are likely to result from a combination of two factors. Firstly, because the full freezing process is not modelled, the headspace meltwaters will release less $CO_2$ into the gaseous headspace. Secondly, $pCO_2$ does increase in headspace cryoconite holes (Fig. 16), so over the course of the freezing process, there will be less requirement for $CO_2$ outgassing than in open cryoconite holes, which must maintain a constant concentration of $CO_2$. However, it is not possible to disentangle these two factors, and the outgassing of $CO_2$ into the headspace in B-Headspace and F-Headspace must be considered an underestimate, as the final freeze up will likely result in further release of $CO_2$ into the headspace.

It was also possible to consider the calcite precipitation and $CO_2$ degassing throughout the freezing process in each type of cryoconite hole.

### 4.3.1 Open Cryoconite Holes

Initially, calcite is not removed from solution, as it is yet to saturate in solution. $CO_2$ outgassing is of a similar magnitude between both open cryoconite holes initially, and follows a similar trajectory prior to calcite saturation (Fig. 30). The amount of $CO_2$ outgassing decreases over time. This may be because each sequential freeze-up simulation is achieved by a doubling of all solute concentrations from the previous simulation. This previous simulation will have itself been equilibrated with atmospheric $pCO_2$, so the subsequent simulations will require progressively less outgassing, as their predecessors were already at equilibrium with the atmosphere.

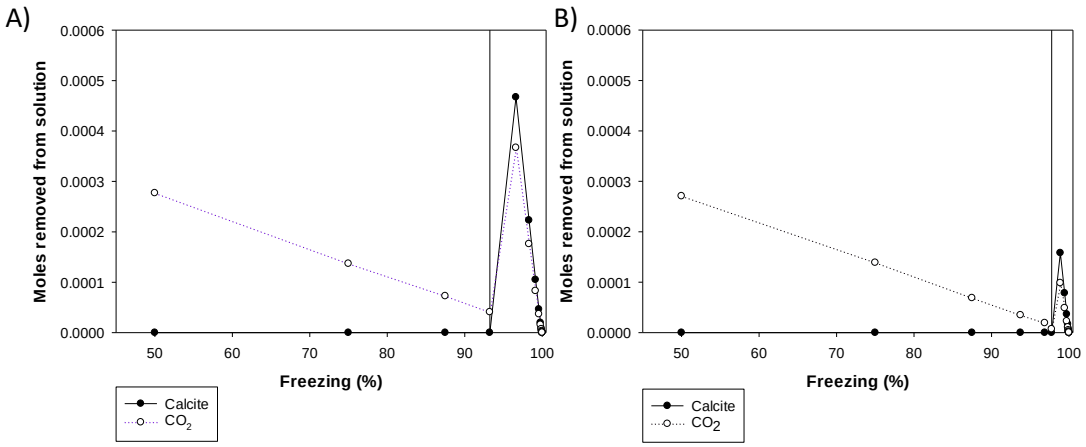


Figure 30 - Number of moles of calcite and DIC removed from solution at each simulation during the freezing process in A) B-Open; B) F-Open. Initial calcite saturation is indicated by a vertical line.

The precipitation of calcite occurs initially very quickly, followed by a decrease in the amount of precipitation occurring until the cryoconite hole freezes completely (Fig. 30). This process is of a greater magnitude in B-Open than in F-Open. This is directly related to the difference in initial concentrations, with B-Open being more concentrated in terms of each solute than F-Open. It is not directly related to the length of time over which calcite precipitation occurs, because the increase in precipitated calcite occurs immediately following initial saturation, in the first subsequent simulation. The pattern of immediate precipitation of a relatively large amount of calcite, followed by sequentially less precipitation may suggest that there is a threshold amount of calcite precipitation that can occur. This is likely to be related to the total concentration of its component parts within solution, based on the magnitudes of the peaks in precipitation amounts (Fig. 30). The initial amount of precipitation is a large proportion of the total potential amount of calcite precipitation (Table 3), so each subsequent freeze-up simulation is limited by the amount of further precipitation which can occur.

Calcite precipitation causes similar-magnitude changes in the amount of $CO_2$ outgassing into the atmosphere which occurs (Fig. 30). Following initial calcite saturation, $CO_2$ outgassing immediately rises to a peak, and then decreases gradually with each subsequent freeze-up simulation. The similarity in trajectory suggests that $CO_2$ and calcite removal from solution must be linked. Calcite precipitation consumes (bi)carbonate ions, so the removal of these other DIC forms from solution would increase the relative concentration of $CO_2$. This only occurs in the form of a stabilisation in the relative contribution of $CO_2$ to DIC in reality (Fig. 27). Removing DIC in the bicarbonate and carbonate forms leads to a reduction in pH, which means that a further increase in DIC, such as that caused by the next

sequential freezing, tends to speciate predominantly as $CO_2$. To maintain $pCO_2$ at equilibrium with the atmosphere, outgassing must occur. Calcite precipitation is then limited at each subsequent freezing, so this rejuvenated outgassing quickly decreases in magnitude until the meltwater completely freezes.

### 4.3.2 Closed Cryoconite Holes

By definition, closed cryoconite holes do not exchange gas with the atmosphere, so in these scenarios calcite saturation alone was modelled. The precipitation of calcite increases after initial saturation, and then decreases at high % Freezing, but differently to open cryoconite holes, the increase in amount precipitated is more gradual (Fig. 31). Furthermore, the peak in precipitation is lower than in open holes for each pair of scenarios, but the total amount precipitated is very similar, partly because saturation occurs earlier in the freezing process, and also because the precipitation is more enduring.

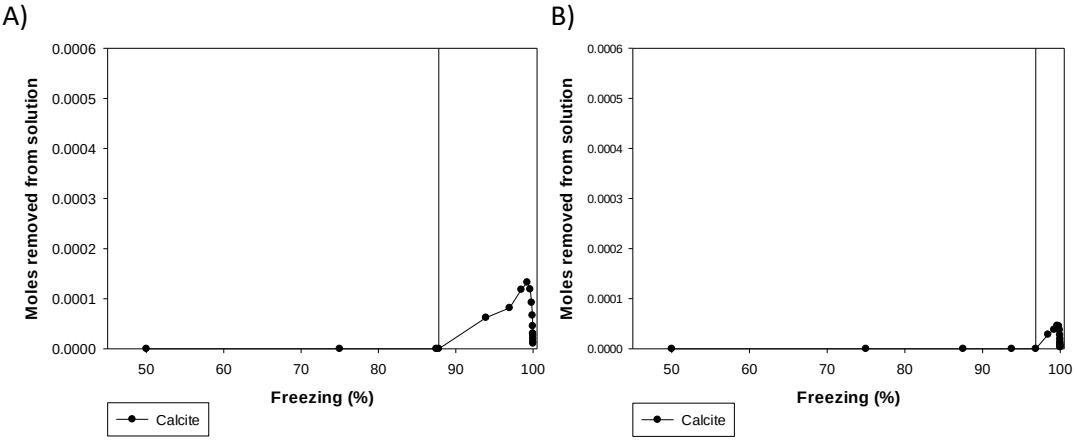


Figure 31 - Number of moles of calcite precipitated at each simulation during the freezing process in A) B-Closed; B) F-Closed. Initial calcite saturation is indicated by a vertical line.

The more gradual increase in amount of calcite precipitation, followed by a decline, suggests that, as in open cryoconite holes, there is a limit to the amount of precipitation which can occur. However, this limit takes longer to reach. This may suggest that the limit of total precipitation is primarily dictated by DIC concentration, which, in the closed cryoconite holes continues to increase with each sequential freezing, but in the open cryoconite holes actually decreases during some freeze-up simulations due to the requirement for DIC by both calcite and $CO_2$ removal.

### 4.3.3 Headspace Cryoconite Hole Meltwaters

The headspace scenarios show some similarities to both open and closed scenarios (Fig. 30-32). Calcite again does not precipitate until the initial instance of saturation,

here indicated by the initial increase in calcite precipitation (Fig. 32). Although $CO_2$ concentration is allowed to vary until this point, little outgassing is required in order to maintain equilibrium with the headspace, so the initial trajectory is similar to that of the closed cryoconite hole scenarios.

When calcite precipitation increases, so too does $CO_2$ outgassing (Fig. 32). Both B-Headspace and F-Headspace show a continued increase in $CO_2$ outgassing until the maximum modelled % Freezing. This is because the removal of bicarbonate and carbonate from solution decrease the pH of the meltwater, which causes additional DIC concentration increases, such as that which occurs during the freezing process, to tend to speciate towards $CO_2$. This increases $pCO_2$ in a meltwater which is steadily freezing, which in itself causes $pCO_2$ to rise, as it increases in concentration due to freezing. Furthermore, at this stage of freezing, the meltwater volume is smaller than the volume of the gaseous headspace, and as it freezes, it decreases in volume at a faster rate than the headspace (Fig. 18). Consequently, the $pCO_2$ of the meltwater rises at a faster rate than $pCO_2$ in the headspace, so it is necessary for degassing to occur at a faster rate than previously (Fig. 32).

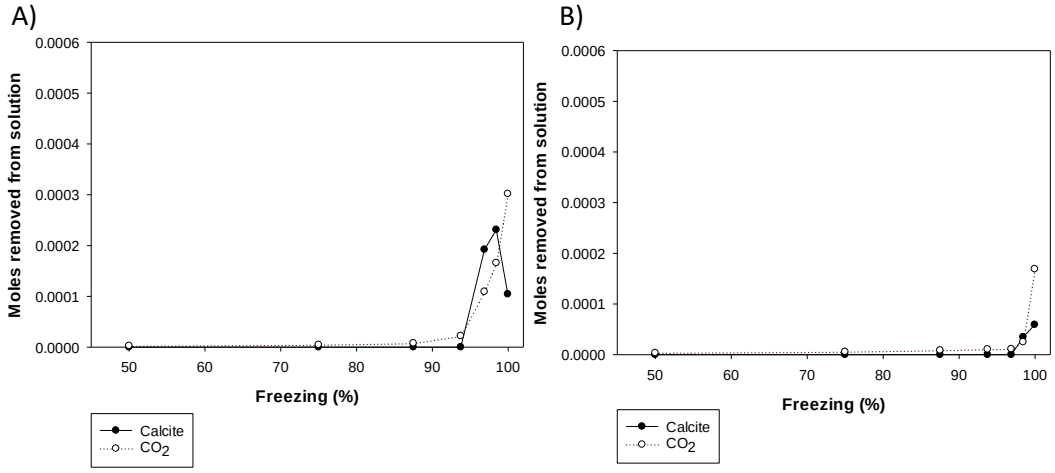


Figure 32 - Number of moles of calcite and DIC precipitated at each simulation during the freezing process in A) B-Headspace; B) F-Headspace. Initial calcite saturation is not indicated, because the exact point at which it occurs is not known.

It is unclear in F-Headspace whether there is a limit to the amount of calcite precipitation, or indeed $CO_2$ degassing, which can occur. This is because there are not sufficient simulations following initial calcite saturation for calcite precipitation to decrease, although it can be assumed that this would happen during the full extent of freezing, since it has been modelled in every other scenario (Fig. 30-32). However, in both B-Headspace and F-Headspace, the $CO_2$ outgassing does not decrease at high % Freezing, the reason for which is likely related to the ratio of

meltwater to headspace volume decrease with freezing (Fig. 32; 18). However, B-Headspace still shows a decrease in calcite precipitation (Fig. 32). This indicates that the decrease in calcite precipitation is not caused by changes in $CO_2$ outgassing, but may indeed result from a limitation by DIC concentration, as the outgassing of $CO_2$ into the headspace causes a decrease in DIC concentration in the meltwater, limiting the available bicarbonate and carbonate for calcite precipitation to occur.

### 4.4 Behaviour of Gypsum at High % Freezing

In Section 3.5, it was noted that gypsum, at very high % Freezing, supersaturates, and then returns to an undersaturated state. This effect only occurred in the open and closed cryoconite hole scenarios, and it is suggested that the effect's absence in headspace cryoconite holes is likely due to the omission of the final freeze-up from the modelling procedure. This means that, providing the same cryoconite hole dimensions are assumed, this effect would only occur in the last few millilitres of meltwater within the cryoconite hole. However, in a particularly large cryoconite hole, the meltwater volume at this % Freezing would be substantially more. Furthermore, since it is perhaps linked to a change in direction of pH change (Section 3.2), the mechanics of the change in gypsum saturation state is potentially important in understanding the chemical transformations in the final freeze-up of meltwater.

'Salting out' is the suggested mechanism for the reduction in saturation index of gypsum at high % Freezing. At low ionic strengths, increase in solute concentrations, for example by freezing, causes an increase in the solubility of a particular solute, but at high ionic strengths, the continued increase in solute concentrations can cause a decrease in the solubility of that same solute (e.g. Gross, 1933). There are several theories behind this effect (Long and Devit, 1952), but it is largely thought to be because at high ionic strengths, water molecules are preferentially attracted to the salt ions, which limits the availability of water to the solute in question (e.g. Bockris and Egan, 1948). The tangible impact of this effect is usually indicated by a high activity coefficient relative to the concentration of the species (Long and Devit, 1952).

However, the activity coefficients and concentrations of the species of importance in this study, gypsum, are identical even at high ionic strengths (Fig. 33). Nevertheless, it was noted in Section 3.2 that the changes in pH and gypsum saturation state coincided with changes in the activity coefficients of $Ca^{2+}$ and $SO_4^{2-}$

, the ions from which gypsum is composed. Furthermore, each sequential freezing was modelled by increasing concentrations of both $Ca^{2+}$ and $SO_4^{2-}$, but the concentration and activity coefficients of $CaSO_4$ decrease at very high % Freezing. As a result, the concentrations and activity coefficients of $Ca^{2+}$, $SO_4^{2-}$ and $CaSO_4$ have been examined in more detail at high % Freezing (Fig. 33).

In all open and closed cryoconite hole scenarios, concentrations of calcium and sulphate ions are higher than their respective activity coefficients, and increase immediately prior to total freeze-up (Fig. 33). By contrast, the activity coefficients, as well as the concentration and activity of $CaSO_4$ diverge, and decrease prior to freezing. This is exactly the opposite effect, in terms of the calcium and sulphate ions, than would be expected in gypsum during salting out. This suggests that gypsum solubility does decrease at high % Freezing, as its concentrations and activity coefficients decline simultaneously with the decrease in saturation index (Fig. 33; 23; 25). However, since the meltwater is unable to hole as much gypsum in the dissolved form, it dissociates back into its component ions. This is supported by the factors of increase of calcium required by the model, in which the factor of increase rises at high ionic strengths (Fig. 19; 20). Indeed, during the final freeze-up simulation in F-Open, calcium is required to increase in concentration in order to maintain the conditions of the modelling procedure (Appendix 1), which is only made possible by a further source of calcium. This suggests that there may be some degree of interdependence between calcite and gypsum saturation states.

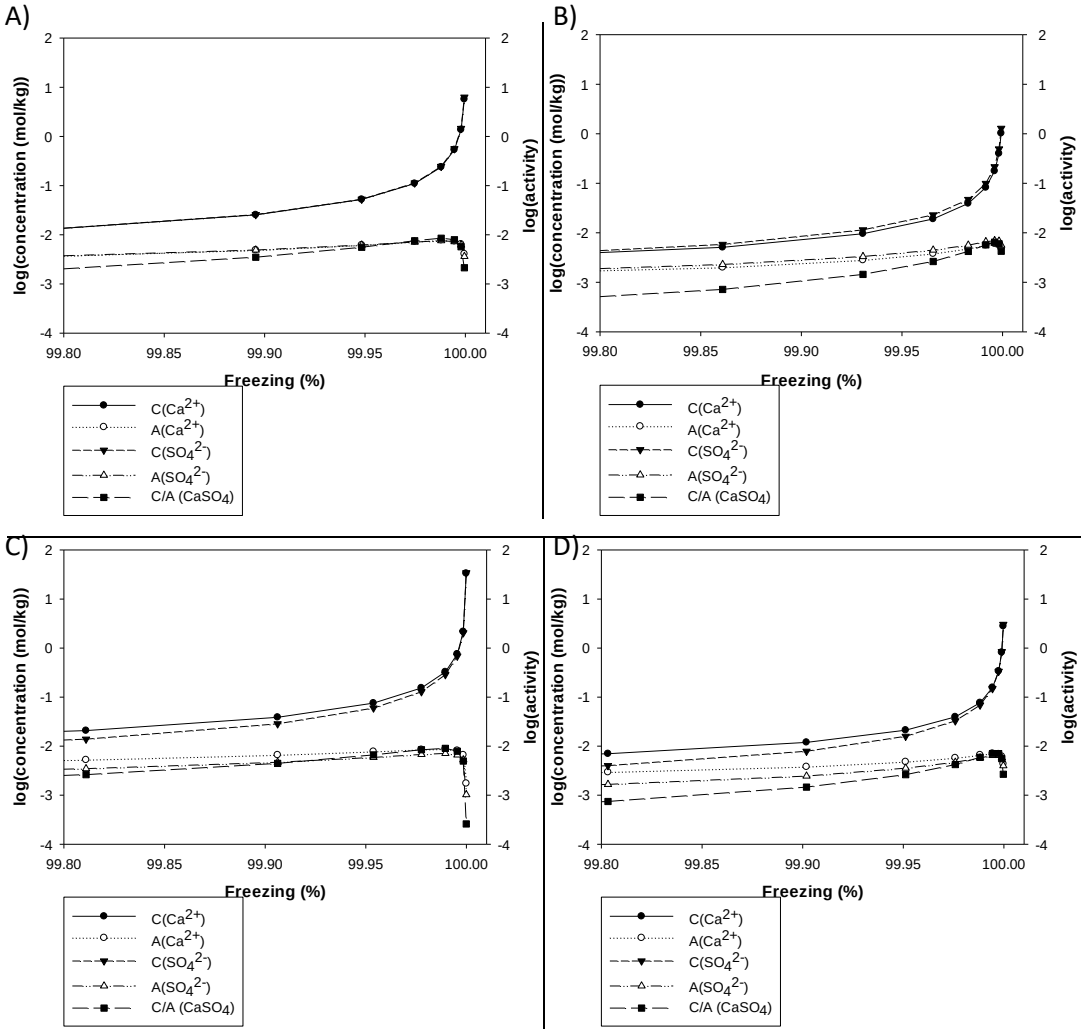


Figure 33 - Logged concentrations and activity coefficients of $Ca^{2+}$, $SO_4^{2-}$ and $CaSO_4$ at ≥99.8% Freezing for A) B-Open; B) F-Open; C) B-Closed; D) F-Closed. $CaSO_4$ is plotted as a single line, as the concentrations and activity coefficients are the same. In the legend, 'C' denotes concentration and 'A' denotes activity coefficient.

Notably, the divergence in activity coefficients and concentrations of $Ca^{2+}$ and $SO_4^{2-}$ is linked to the extent to which $SI_{gypsum}$ decreases, further supporting a causal relationship. In the open cryoconite hole scenarios, B-Open experiences a greater-magnitude decrease in $SI_{gypsum}$ than F-Open (Fig. 23) and this is reflected in the divergence of the activity coefficient and concentration in Figure 33 (A-B). The same is true for B-Closed, with respect to F-Closed (Fig. 25; Fig. 33. C-D). B-Closed experiences the largest change in $SI_{gypsum}$ of all open and closed scenarios (Fig. 23; 25) and again this is reflected in the divergence shown in Fig. 33.

The headspace scenarios did not return to an undersaturated state with respect to gypsum, with F-Headspace not actually reaching a supersaturated state (Fig. 26). If the above proposed mechanism for $SI_{gypsum}$ decrease at high % Freezing is

correct, the same divergence in activity coefficients and concentrations will not be seen.

Figure 34 shows the same activity coefficients and concentrations for the two headspace scenarios, and in both cases, the activity coefficients and concentrations of $Ca^{2+}$ and $SO_4^{2-}$ are equal at the highest modelled % Freezing. There is also no divergence between the activity coefficients and concentrations as ionic strength increases. This further supports the suggestion that the salting out of gypsum and subsequent dissociation occurs at very high % Freezing, as gypsum is not found to supersaturate and then return to an undersaturated state in headspace cryoconite holes.

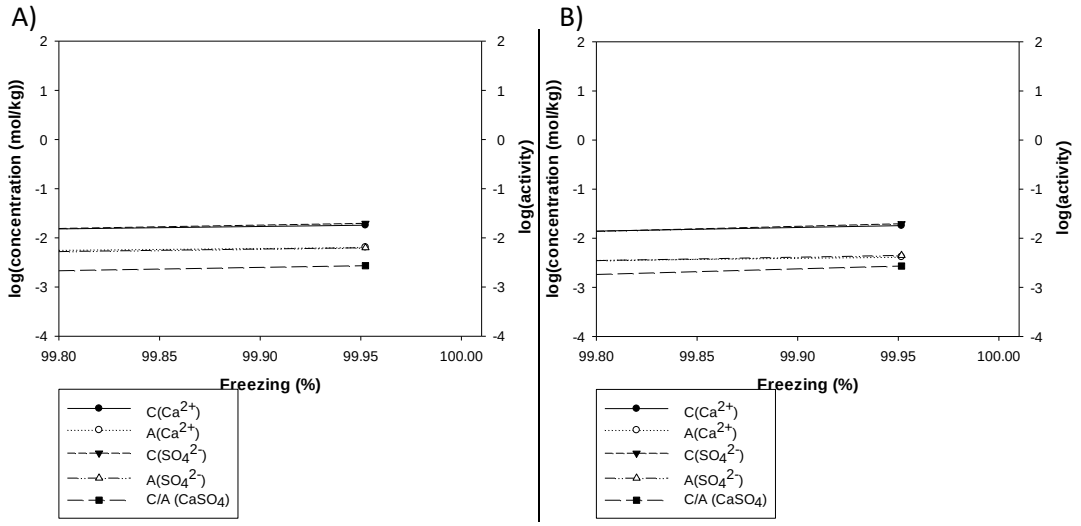


Figure 34 - Logged concentrations and activity coefficients of $Ca^{2+}$, $SO_4^{2-}$ and $CaSO_4$ at ≥99.8% Freezing for A) B-Headspace; B) F-Headspace. $CaSO_4$ is plotted as a single line, as the concentrations and activity coefficients are the same.

In Section 4.2, it was suggested that changes in pH, at the same point in the freezing process at which the meltwater returns to an undersaturated state with respect to gypsum, may be coincidental. The mechanism here proposed of the salting out and dissociation of gypsum into calcium and sulphate ions is not directly linked to pH, and so this notion is likely to be true.

### 4.5 Points of Interest With Previous Work

There are a limited number of other studies with which the results of this study are directly comparable, due to the difficulty of sampling cryoconite holes in Antarctica continuously, as discussed in Section 1.52. The comparisons that were possible are detailed in this section.

Bagshaw *et al.* (2007) was the source material for one set of initial solute concentration conditions. Their study measured major solute concentrations and chemical features of samples taken from glacier ice, 'frozen' cryoconite holes, and 'wet' cryoconite holes. The difference between the latter two environments was that at the time of sampling, the 'frozen' holes contained no meltwater, whilst the 'wet' cryoconite holes contained meltwater, separated from the atmosphere by an ice lid. The samples were melted prior to chemical analyses, so differences in solute concentrations between the frozen and wet holes may result from biotic processes during the summer melt. Such processes were not modelled in this study, so it is not possible to directly compare solute concentrations, except to say that every eventual solute concentrations in all six modelled cryoconite hole scenarios were substantially higher than the mean, plus standard deviation, of both wet and frozen holes measured by Bagshaw *et al.* (2007). Similarly, the solute concentrations at high % Freezing are far higher than the upper limit of the range measured by Tranter *et al.* (2004). The solute concentrations immediately prior to total freeze-up in both open and closed cryoconite hole are actually approximately an order of magnitude greater than average seawater solute concentrations (Drever, 1988), except for in open cryoconite holes, DIC concentrations are slightly lower than in seawater, having precipitated calcite.

Bagshaw *et al.* (2007) give a pH value of 7.22 for the 'wet' holes, corresponding to $pCO_2$=-3.68. This should theoretically correspond to the initial values of the closed cryoconite holes, but it is closest in value to B-Open. This is likely to be because the ice lid of the cryoconite hole sampled was broken in order to collect the meltwater, which allowed some equilibration with the atmosphere prior to analysis, leading to pH and $pCO_2$ values between those modelled in open and closed cryoconite holes, but closer to the open hole scenarios. However, there is a substantial difference in measured pH between Bagshaw *et al.* (2007) and Tranter *et al.* (2004), who measured a mean pH value of 9.6. These measurements were both taken on Canada Glacier, though in different field seasons. No pH value in this study exceeded pH=9, and initial closed cryoconite hole modelled pH values only just fall within the lower limits of the range measured in the field. It is possible that the differing conditions between the two sampling years caused significant differences in net primary production, which itself causes pH to increase (Tranter *et al.,* 2004). This is supported by the hole dimensions measured by Tranter *et al.* (2004), which were substantially larger than those made by Bagshaw *et al.* (2004), suggesting that

a warmer melt season may result in higher pH values in meltwater due to elevated rates of community production.

The open cryoconite holes in this study can also be qualitatively compared to those found elsewhere in the world. There are few studies detailing solute concentrations in other regions, but those that do exist suggest that the solute content of an Arctic cryoconite hole is more dilute than either an Antarctic cryoconite hole or indeed Antarctic ice melt/supraglacial stream water (De Smet and Van Rompu, 1994; Bagshaw *et al.,* 2007; Fortner *et al.,* 2005). Although sample sizes are generally small, Arctic cryoconite holes have consistently been found to be lower in pH than those in Antarctica (Mueller and Pollard, 2004; De Smet and Van Rompu, 1994; Lutz *et al.,* 2014), and this was reflected in the open cryoconite holes, which were initially lower in pH than closed cryoconite holes. Cryoconite holes in the Arctic are less variable in pH (Mueller and Pollard, 2004), but experience acidic pH values. The values achieved in open cryoconite holes in this study were not sufficiently acidic initially, to match this. Cryoconite holes in the Arctic are less concentrated, so likely contain less DIC, but as they are in contact with the atmosphere, their $pCO_2$ must remain constant, so a greater proportion of that DIC must be held in the $CO_2$ form, making the cryoconite holes more acidic.

A number of studies suggest that differences in the source material of cryoconite debris can hold a strong influence over the chemistry of cryoconite holes (e.g. Bagshaw *et al.,* 2007; Langford *et al.,* 2011). This study used two sets of initial concentration conditions that were substantially different from one another, and could in this instance be viewed as having different solute sources. The simulations for each type of cryoconite hole initially generated very different pH and $pCO_2$ values for each set of initial conditions, but as the freezing process occurred, the two variants of each cryoconite hole type became more similar to one another. This is also the case as calcite precipitates, as although different amounts of calcite are removed from solution in each case, the resultant solution becomes more similar at very high % Freezing.

It must also be noted that Tranter *et al.* (2004) suggest that as pH rises, $pCO_2$ decreases to very low values (-7.6 log atms), and this causes the drawdown of a large proportion of the $CO_2$ from the headspace into the meltwater. In this study, $pCO_2$ increases as freezing occurs in lidded cryoconite holes, both with and without headspace (Fig. 15; 16), and with pH remaining fairly static until calcite saturates, with the exception of F-Headspace, which does increase in pH (Fig. 11; 13). There

is transfer of $CO_2$ from the meltwater to the headspace throughout the freezing process, which is enhanced as calcite precipitates (Fig. 17), although calcite precipitation does correspond to a decrease in pH. This suggests that as calcite precipitation occurs, there may be agreement with the findings of Tranter *et al.* (2004) in this regard, but prior to calcite saturation there is perhaps an insufficient increase in pH during the freezing process for $pCO_2$ to decrease.

### 4.5.1 Application of Results to Thawing Process

This study has examined the freezing process in detail. Thawing is the reverse phase change to freezing; theoretically the modelled changes achieved in this study are the reverse of those which occur during the seasonal melt of cryoconite holes. The findings of Telling *et al.* (2014) will assist in the appraisal of the applicability of the results of this study to the thawing process.

Telling *et al.* (2014) examined the first 10 days of the thawing process and observed an 'ionic pulse', whereby as the cryoconite hole initially begins to melt, solute concentrations increase very rapidly. For example, $Cl^-$ concentration increases by a factor of 9.3 during 3 days of melting. The results of this study follow the meltwater until the final moments prior to total freezing, when it experiences very high ionic strength (Fig. 7). This suggests that the moment after thawing, the water would similarly be highly concentrated, and would become gradually more dilute as the volume of meltwater increased.

The results do not show a decrease in ionic strength as the cryoconite hole finally freezes because the strategy employed for the modelling of the freezing process requires continuous increase in ionic strength, which would, if continued indefinitely, lead to an infinitely small, highly concentrated volume of water. Telling *et al.* (2014) melted an entire frozen cryoconite hole core to produce their fully-frozen solute concentrations. Therefore, the same solute content as found in this study may indeed have been present, but measured within a volume equivalent to the entire cryoconite hole. This results in low initial solute concentrations prior to thawing. Consequently, the results found in this study are indeed comparable to those found by Telling *et al.* (2014), as it is likely that both studies measured equivalent total solute masses. The difference between the studies is that Telling *et al.* (2014) measured the total volume of a frozen cryoconite hole, the modelling procedure in this study calculates concentrations for a very small volume of meltwater containing the same total mass of solute.

Telling *et al.* (2014) found that DIC was depleted, with an enrichment factor of 0.5, over the same 3 days of melting that the ionic pulse occurred. They suggested that this may relate to mineral precipitation reactions. This study found calcite precipitation to occur during the latter stages of cryoconite hole freezing. If it is indeed applicable to the thawing process, this would suggest that in the early stages of melting, calcite would dissolve into solution. This would occur slowly to begin with (Fig. 30-31). This suggests that much of the DIC is held as calcite in the solid form initially when melting occurs, causing low DIC concentrations in the meltwater, but is not a reason for a decrease in DIC concentration. Telling *et al.* (2014) found evidence of a small burst of photosynthesis during the first 3 days of thawing, which leads to localised elevation of pH and promotes carbonate precipitation. Therefore, it is possible that the results of this study are not contradictory, but that if biological processes were included in the modelling procedure it may confirm that the dissolution of calcite into solution is delayed by the onset of photosynthesis.

It is therefore likely that the results found in this study can be viewed as both the freezing process, and in reverse, as the thawing process. However, at the beginning of the thawing process, the precise nature of carbonate chemistry transformations may not entirely represent reality, given that the effects of biology were not incorporated in the modelling process. Graphs were produced for the freezing process and not the whole melt season however, because to represent the whole melt season on a single graph would by implication ignore the effect of solute accumulation between freeze cycles.

### 4.6 Other Processes

This study modelled the freezing process itself, as well as calcite precipitation at the appropriate moment. However, two key processes were not included in the modelling procedure.

Firstly, dissolution of minerals from the sediment into the meltwater was not included. Dissolution of silicates, which is thought to dominate mineral dissolution within cryoconite holes, occurs at a faster rate in higher-pH waters (Tranter *et al.,* 2004; Gratz and Bird, 1993). This suggests that the lower the headspace volume as a proportion of total cryoconite hole volume, the more silicate dissolution may occur, as the highest initial pH was modelled in closed cryoconite holes, though perhaps not as much as may be found in warmer conditions, as the pH of cryoconite holes can be much higher than those modelled in this study (Tranter *et al.,* 2004). However, it is difficult to suggest what impact the inclusion of this process would

have on the chemistry of the meltwater, as the dissolution of silicates can influence a range of solute concentrations, and it will be the relative impact on these concentrations that instigates changes in meltwater chemistry (Lyons *et al.,* 2003). However, since cryoconite sediment composition varies, and sample sizes tend to be small, the dissolution of debris could have a range of impacts, so it was not possible, nor appropriate, to model 'average' silicate dissolution (Langford *et al.,* 2011).

Secondly, primary production and respiration were not included in the modelling process. The balance between these is likely to be fairly evenly matched over the whole season (Bagshaw *et al.,* 2011), but during the freeze-up, net respiration is thought to dominate (Bagshaw *et al.,* 2007; Tranter *et al.,* 2004). This would, in reality, act to decrease pH in lidded cryoconite holes, as $CO_2$ is released during respiration, which causes the waters to become more acidic (e.g. Tranter *et al.,* 2004). This suggests that the minimum pH experienced when the cryoconite hole completely freezes, should be viewed as a higher-end estimate for the pH at that % Freezing. In reality, the pH in Antarctic cryoconite holes at very high % Freezing will be lower, because net respiration will drive pH downwards. The interaction with the headspace would lead to further donation of $CO_2$ into the headspace, so in holes with a larger headspace volume, the reduction in pH due to respiration would be smaller in magnitude. An open hole is likely to experience a much smaller change than a lidded hole, because the concentration of $CO_2$ is fixed due to the equilibrium with the atmosphere in terms of $pCO_2$, so an excess of $CO_2$ would either degas, or would dissociate into the bicarbonate form.

# 5.0 Limitations

As previously mentioned, the study modelled the freezing process itself, as well as the precipitation of secondary carbonates, but did not account for the effects of dissolution of cryoconite sediment, or net primary production/respiration. These would have been troublesome to include in the present model setup, because both processes are variable between cryoconite holes, and depend on the specific conditions the melt season in question dictates. Furthermore, respiration is expected to be dominant when cryoconite hole freezing occurs, but this will likely be limited by the physical and hydrochemical conditions at high % Freezing (Tranter *et al.,* 2004), but this process is as yet unquantified. Therefore, both processes would require further laboratory-based work in order to quantify: the proportion of the freezing process over which they are viable; the rate at which their action decays with respect to freezing; in the case of sediment dissolution, the solute concentrations which would be impacted upon. This study simulated cryoconite holes of three structures: two extremes and an intermediate system, as well as using a likely extreme and average set of initial solute conditions.

Each of the excluded processes would be best suited to at least three scenarios, in order to explore the range of conditions that may result from their variability over time and space. Not only would each of these scenarios need to be more dynamic than the present model setup would allow, but it would also require a minimum of 54 cryoconite hole scenarios, which would be very difficult to analyse in any detail, as to the impact of each process on cryoconite hole chemistry. However, the exclusion of net primary production and dissolution of sediment in this study was not entirely detrimental, as it enable the probable least-extreme estimates to be modelled of chemical conditions within cryoconite holes in Antarctica.

The other main limitation of the modelling process is that it made use of equilibrium thermodynamics to calculate the chemical conditions at each progressive freeze-up of the meltwater. This is one of the key reasons that seasonal, rather than diurnal, freezing of cryoconite hole meltwaters was selected as the focus of the study, as on the timescales involved in diurnal freezing, equilibrium in the meltwater may not be reached, to say nothing of equilibrium in $pCO_2$ between the meltwater and headspace, or atmosphere. However, even in terms of the seasonal freeze-up of cryoconite holes, the approximate length of summer is detailed each year, but the uniformity of the freezing process is not known. This study has treated the 'Freezing (%)' parameter as a form of time series, but whether this time series unfolds at a

steady rate requires further research into the physical mechanisms of cryoconite hole evolution. The assumption of chemical equilibrium within the meltwater would be deemed appropriate or inappropriate according to this further research, as particularly at very high % Freezing, the length of time between freeze-ups modelled could be very short. However, given that this is a new, and developing field of research, the insight that this study gives into the potential changes that may occur in terms of chemical conditions in cryoconite holes is a valuable addition to current knowledge.

Field data also presents limitations to this study. Few studies have measured the composition of cryoconite hole meltwaters in the field, and none have achieved this at very high % Freezing, so validation of the results is not possible. Furthermore, the studies which have been conducted into cryoconite hole meltwater chemistry have shown large variations in chemical conditions, including pH (Tranter *et al.,* 2004; Bagshaw *et al.,* 2007). Therefore, selecting a single set of solute concentrations for a mature cryoconite hole, and a single set for ice melt, may exclude some of these variations. However, the ice melt concentrations and cryoconite hole concentrations, when modelled to represent each cryoconite hole structure, produced initially differing conditions, which were discussed in this study, but became more similar at very high % Freezing, which was also when the most substantial changes in cryoconite hole meltwater chemistry occurred. This was reflected in holes modelled using each of the sets of initial conditions, suggesting that regardless of how dilute or concentrated the initial solution is, the conditions during the total freeze-up of the cryoconite hole will be similar.

The assumption of complete melting was ingrained into the model setup. The modelling procedure assumes that the initial concentration conditions were measured in the field at 0% Freezing. This is appropriate for the supraglacial stream data (Fortner *et al.,* 2005), because the stream water was entirely melted at the time of sampling. However, the cryoconite holes sampled by Bagshaw *et al.* (2007) may not have been entirely melted. Indeed, the sampling occurred between October and February, and a number of 'frozen' cryoconite holes were also sampled, so it is possible that a proportion of the 'wet' holes were not at 0% Freezing when sampled (Bagshaw *et al.,* 2007). The samples were fully melted prior to solute analysis, and were not distinguishable from the frozen holes in meltwater chemistry, so at the time of analysis for solute concentrations, the 0% Freezing assumption is appropriate. Even if the assumption were not appropriate however, this would only impact on the results for B-Headspace, since the dimensions of the cryoconite hole were fixed. B-

Open and B-Closed represent cryoconite holes of any initial dimensions. Even if 0% Freezing in this study does not correspond to an entirely melted cryoconite hole chemistry, it will correspond to a point during the freeze-up of the cryoconite hole, so the eventual conditions would be unchanged.

Finally, it is possible that there are other solutes present in the meltwater which were not measured in the studies from which the data was sourced. This would provide a further possible explanation for the difference in measured and modelled pH values (Section 4.5), as the pH values modelled in this study were achieved through charge balance. Other, unmeasured solutes would impact on the balance of charges in the meltwater solution, so may affect the resultant pH in solution. All major ion concentrations were provided by Bagshaw *et al.* (2007) and Fortner *et al.* (2005), so it is unlikely that any omissions would have a significant impact on the validity of this study.

# 6.0 Future Research

The field of research into cryoconite hole meltwater chemistry is developing, and this study begins to widen understanding into the processes occurring within cryoconite holes throughout their seasonal freeze-up. This understanding is in its infancy, and would be greatly improved by the development of a more dynamic model, in which the physical, chemical and biological processes in cryoconite holes during freezing could be fully explored.

A number of processes and characteristics in cryoconite holes in Antarctica have been quantified, but sample sizes are small. A continued field-based effort into determining the chemical conditions in cryoconite hole meltwaters is necessary to better constrain the reasons for differences in initial solute chemistries, which in turn may be used as inputs to a more dynamic biogeochemical modelling process.

The impact of biology was not included in this study, due to time constraints as well as a lack of data about the timescale over which freezing occurs, and net primary production time series across the season. Inclusion of microbiological processes would involve the addition/removal of DIC from solution depending on whether the solution was net autotrophic or net heterotrophic. This is because photosynthesis can crudely be denoted as in Equation 9 (E.g. Bagshaw *et al.,* 2013).

$$HCO_3^- \leftrightarrow OH^- + C_{org} + O_2 \qquad \text{Eq. 9}$$

It is likely that cryoconite holes are generally net heterotrophic during the freezing process (Bagshaw *et al.,* 2007). DIC must therefore be added to the solution to simulate a state of net respiration (Eq. 9). PHREEQC requires a total concentration of DIC to be set as an initial condition to the model, so determining the amount of DIC addition to simulate respiration is crucial to the modelling process. Bagshaw *et al.* (2011) observed respiration and photosynthesis of cryoconite sediment placed in an ice melt solution, with net respiration of 0.8 $\mu g.C.g^{-1}.day^{-1}$. It must be acknowledged that this value reflects ice melt as the solution, so use of these values would not take account of solute accumulation in cryoconite holes, and the conditions this exerts on the microbial community. As a result, it must be viewed as a crude estimate of net respiration.

PHREEQC requires the DIC addition in the form of a concentration, so in addition to the estimated net respiration, units of time, volume, and mass are required. Liquid water is thought to be present in cryoconite holes for 1-3 months in the austral

summer (Foreman *et al.,* 2007). An approximate median value of 2 months, or 60 days, is selected. A cryoconite hole exists in three main states during this time: thawing, fully melted, and freezing. The 60 day season can be crudely separated into three to account for this. Therefore, the hypothetical freeze-up occurs over 20 days. There is no data at present to indicate whether the freezing itself occurs at a steady rate, but this will have to be assumed to be the case. At each sequential freezing, the length of time it corresponds to can be simply calculated as a percentage (% Freezing) of the 20 day period. The mean density of cryoconite material within a cryoconite hole is 1.3 $g.ml^{-1}$. The meltwater volume calculated for the headspace scenario will enable calculation of the initial mass of cryoconite material.

This combination of data would facilitate the crude estimation of DIC addition required in order to simulate net respiration within a cryoconite hole of fixed dimensions. This estimate would vary between simulations, because the length of time over which biological processes were being simulated would become progressively shorter as the simulations become closer together. However, in addition to the assumptions stated previously, a key consideration with completing this modelling work is that this would assume that net respiration would continue to occur at the same rate over time, which is not the case in reality (Telling *et al.,* 2014). This assumes not only that respiration and photosynthesis are unaffected by substantial changes in meltwater chemistry, but also that the organisms present within the sediment remain equally efficient in all physical conditions during cryoconite hole freeze-up.

The extreme chemical conditions found in this study in closed cryoconite holes could be used in a laboratory environment to study the impact on cryoconite microbial communities of not only the stress due to temperature and dwindling liquid water supplies, but also the extreme chemical characteristics of the remaining meltwater. It may be possible to reproduce the conditions present in a lidded cryoconite hole at each sequential freeze-up, in terms of temperature, solute concentrations, volume of water and volume of headspace. The addition of sediment into these replicas, both containing biotic material, and with organic matter removed, may provide further insights into the rates at which processes such as photosynthesis, respiration and sediment dissolution occur throughout the freezing process and the subsequent impact on meltwater chemistry.

Finally, the fate of cryoconite holes in Antarctica in the future, as changes to the present climate occur, are as yet uncertain. Increases in ambient air temperature may increase annual snowfall in Antarctica (Davis *et al.,* 2005), which may impact on sediment loading from aerosols. Sensitivity of the ice lid to long-term temperature fluctuations, as well as the impact on cryoconite hole water chemistry in the future could be further explored in a more dynamic modelling process.

# 7.0 Conclusions

Cryoconite holes in Antarctica experience a range of chemical conditions throughout the freezing process, which critically depend upon their structure. In this study, changes in cryoconite hole chemistry were determined throughout the seasonal freeze-up. This provides a completely novel insight into the conditions present in cryoconite holes throughout this process, particularly very close to complete freeze-up of the meltwaters. Cryoconite holes vary in dimensions, and so it was not possible to examine all possible combinations of meltwater volume and gas headspace volumes, so a set of dimensions was selected for the simulation of 'headspace' cryoconite holes. It was therefore important to examine the conditions present in fully open and fully closed cryoconite holes, which could be achieved without prescribing dimension conditions. Cryoconite hole meltwaters of each structural form were modelled using a set of dilute, and a set of more concentrated, initial solute concentration conditions, in order to determine whether this would be a control on the eventual conditions present in the hole when freezing occurs.

pH was initially higher in the closed cryoconite holes than the open holes, with headspace holes between the two. In every hole type, the precipitation of calcite, which occurs at approximately 90% Freezing in all scenarios, led to a reduction in pH. In open cryoconite holes, this was relatively small in magnitude, and was buffered by the equilibrium between the meltwater and atmosphere in terms of $pCO_2$. By contrast, the closed cryoconite holes decreased rapidly in terms of pH to moderately acidic levels. It was not possible to model the very final freeze-up in headspace scenarios, but the reduction in pH that was modelled would suggest that a cryoconite hole with a headspace will experience similar acidification very close to total freezing (<10ml meltwater remaining).

$pCO_2$ remained at equilibrium with the atmosphere in open cryoconite holes, but in closed and headspace scenarios, there was an increase throughout the freezing process. This was quite substantial in closed scenarios, with initial $pCO_2$ undersaturated with respect to atmospheric levels, but the $pCO_2$ at the eventual freeze-up was saturated within the meltwater. The presence of a gaseous headspace considerably decreased the magnitude of these deviations, both and the lower and upper limits, but still reached $pCO_2$ values higher than atmospheric $pCO_2$. This is a possible mechanism for high gas pressures observed in lidded cryoconite holes (Fountain *et al.,* 2004).

Calcite was precipitated from solution in all cryoconite hole scenarios, causing decreases in pH, and possibly increases in $pCO_2$, $SI_{gypsum}$ and $SI_{halite}$. The precipitation of calcite from solution was the primary cause of the most substantial changes in pH throughout the freezing process in every cryoconite hole measured, and so is likely to be the cause of extreme chemical conditions close to the complete freeze-up of cryoconite holes in Antarctica.

Gypsum was found to supersaturate in cryoconite holes, and then return to an undersaturated state at the very highest modelled freezing simulations. It is suggested that this is because it is 'salted out', whereby the solubility of gypsum decreases at high ionic strengths. pH also is found to slightly increase at the highest % Freezing, despite the prior decreasing trend, which was found to be due to a small increase in $CO_3^{2-}$ concentration immediately prior to total freeze-up, but this was not deemed to be directly related to the change in gypsum saturation state.

The findings of this study enable consideration of the extremities of the hydrochemical environment in which the microbial community hosted by an Antarctic cryoconite hole must reside. Active microbial communities have been found to exist between melt seasons (e.g. Christner *et al.,* 2003), so the organisms must be able to survive the conditions throughout the freezing process. The moderately acidic meltwaters at high % Freezing in closed cryoconite holes are here suggested to be an upper-bound estimate of the pH existing in reality, due to the exclusion of respiration from the modelling process. Moderately acidic pH values contrast strongly with the alkaline meltwaters measured in the high melt season in previous studies (e.g. Tranter *et al.,* 2004). The microorganisms present in Antarctic cryoconite holes are thought to be psychrotolerant, rather than psychrophilic (Cook *et al.,* 2016). This study postulates that these organisms must also be able to withstand a large range of pH values, from moderately alkaline to moderately acidic, as well as a range of $pCO_2$ values. The ability of the inhabitants of cryoconite holes to tolerate such extreme hydrochemical conditions, in addition to their tolerance of the temperature characteristics themselves, may further support the notion that the study of life in cryoconite holes can be viewed as a precursor to the study of life in extraterrestrial cold environments (Tranter *et al.,* 2004).

# Reference List


Anesio, A.M., Hodson, A.J., Fritz, A., Psenner, R. and Sattler, B., 2009. High microbial activity on glaciers: importance to the global carbon cycle. *Global Change Biology*, *15*(4), pp.955-960.

Anesio, A.M. and Laybourn-Parry, J., 2012. Glaciers and ice sheets as a biome. *Trends in Ecology & Evolution*, *27*(4), pp.219-225.

Anesio, A.M., Mindl, B., Laybourn-Parry, J., Hodson, A.J. and Sattler, B., 2007. Viral dynamics in cryoconite holes on a high Arctic glacier (Svalbard). *Journal of Geophysical Research: Biogeosciences*, *112*(G4).

Bagshaw, E.A., Tranter, M., Fountain, A.G., Welch, K.A., Basagic, H. and Lyons, W.B., 2007. Biogeochemical evolution of cryoconite holes on Canada glacier, Taylor Valley, Antarctica. *Journal of Geophysical Research: Biogeosciences*, *112*(G4).

Bagshaw, E.A., Tranter, M., Fountain, A.G., Welch, K., Basagic, H.J. and Lyons, W.B., 2013. Do cryoconite holes have the potential to be significant sources of C, N, and P to downstream depauperate ecosystems of Taylor Valley, Antarctica?. *Arctic, antarctic, and alpine research*, *45*(4), pp.440-454.

Bagshaw, E.A., Tranter, M., Wadham, J.L., Fountain, A.G. and Mowlem, M., 2011. High-resolution monitoring reveals dissolved oxygen dynamics in an Antarctic cryoconite hole. *Hydrological Processes*, *25*(18), pp.2868-2877.

Bagshaw, E.A., Wadham, J.L., Tranter, M., Perkins, R., Morgan, A., Williamson, C.J., Fountain, A.G., Fitzsimons, S. and Dubnick, A., 2016. Response of Antarctic cryoconite microbial communities to light. *FEMS microbiology ecology*, *92*(6).

Baumgarten, C.M., 1981. A program for calculation of activity coefficients at selected concentrations and temperatures. *Computers in biology and medicine*, *11*(4), pp.189-196.

Bear, J., Cheng, A.H.D., Sorek, S., Ouazar, D. and Herrera, I. eds., 1999. *Seawater intrusion in coastal aquifers: concepts, methods and practices* (Vol. 14). Springer Science & Business Media.

Bockris, J.M. and Egan, H., 1948. The salting-out effect and dielectric constant. *Transactions of the Faraday Society*, *44*, pp.151-159.

Bøggild, C.E., Brandt, R.E., Brown, K.J. and Warren, S.G., 2010. The ablation zone in northeast Greenland: ice types, albedos and impurities. *Journal of Glaciology*, *56*(195), pp.101-113.

Bonnar, W.B., 1956. Boyle's Law and gravitational instability. *Monthly Notices of the Royal Astronomical Society*, *116*(3), pp.351-359.

Butler, B.A., Ranville, J.F. and Ross, P.E., 2008. Observed and modeled seasonal trends in dissolved and particulate Cu, Fe, Mn, and Zn in a mining-impacted stream. *Water research*, *42*(12), pp.3135-3145.

Charlton, S.R. and Parkhurst, D.L., 2011. Modules based on the geochemical model PHREEQC for use in scripting and programming languages. *Computers & Geosciences*, *37*(10), pp.1653-1663.

Christner, B.C., Kvitko, B.H. and Reeve, J.N., 2003. Molecular identification of bacteria and eukarya inhabiting an Antarctic cryoconite hole. *Extremophiles*, *7*(3), pp.177-183.

Cook, J., Edwards, A., Takeuchi, N. and Irvine-Fynn, T., 2016. Cryoconite: the dark biological secret of the cryosphere. *Progress in Physical Geography*, *40*(1), pp.66-111.

Davis, C.H., Li, Y., McConnell, J.R., Frey, M.M. and Hanna, E., 2005. Snowfall-driven growth in East Antarctic ice sheet mitigates recent sea-level rise. *Science*, *308*(5730), pp.1898-1901.

De Smet, W.H. and Van Rompu, E.A., 1994. Rotifera and Tardigrada from some cryoconite holes on a Spitsbergen (Svalbard) glacier. *Belgian Journal of Zoology*, *124*, pp.27-27.

Doney, S.C., 2006. The dangers of ocean acidification. *Scientific American*, *294*(3), pp.58-65.

Dong, Z., Kang, S., Qin, D., Li, Y., Wang, X., Ren, J., Li, X., Yang, J. and Qin, X., 2016. Provenance of cryoconite deposited on the glaciers of the Tibetan Plateau: New insights from Nd-Sr isotopic composition and size distribution. *Journal of Geophysical Research: Atmospheres*, *121*(12), pp.7371-7382.

Doran, P.T., Priscu, J.C., Lyons, W.B., Walsh, J.E., Fountain, A.G., McKnight, D.M., Moorhead, D.L., Virginia, R.A., Wall, D.H., Clow, G.D. and Fritsen, C.H., 2002. Antarctic climate cooling and terrestrial ecosystem response. *Nature*, *415*(6871), p.517.

Drever, J.I., 1988. *The geochemistry of natural waters* (Vol. 437). Englewood Cliffs: Prentice Hall.

Edwards, A., Anesio, A.M., Rassner, S.M., Sattler, B., Hubbard, B., Perkins, W.T., Young, M. and Griffith, G.W., 2011. Possible interactions between bacterial diversity, microbial activity and supraglacial hydrology of cryoconite holes in Svalbard. *The ISME journal*, *5*(1), p.150.

Foreman, C.M., Sattler, B., Mikucki, J.A., Porazinska, D.L. and Priscu, J.C., 2007. Metabolic activity and diversity of cryoconites in the Taylor Valley, Antarctica. *Journal of Geophysical Research: Biogeosciences*, *112*(G4).

Fortner, S.K., Tranter, M., Fountain, A., Lyons, W.B. and Welch, K.A., 2005. The geochemistry of supraglacial streams of Canada Glacier, Taylor Valley

(Antarctica), and their evolution into proglacial waters. *Aquatic Geochemistry*, *11*(4), pp.391-412.

Fountain, A.G., Nylen, T.H., Tranter, M. and Bagshaw, E., 2008. Temporal variations in physical and chemical features of cryoconite holes on Canada Glacier, McMurdo Dry Valleys, Antarctica. *Journal of Geophysical Research: Biogeosciences*, *113*(G1).

Fountain, A.G., Tranter, M., Nylen, T.H., Lewis, K.J. and Mueller, D.R., 2004. Evolution of cryoconite holes and their contribution to meltwater runoff from glaciers in the McMurdo Dry Valleys, Antarctica. *Journal of Glaciology*, *50*(168), pp.35-45.

Garrels, R.M. and Christ, C.L., 1965. Minerals, solutions, and equilibria.

Gerdel, R.W. and Drouet, F., 1960. The cryoconite of the Thule area, Greenland. *Transactions of the American Microscopical Society*, *79*(3), pp.256-272.

Gratz, A.J. and Bird, P., 1993. Quartz dissolution: Negative crystal experiments and a rate law. *Geochimica et cosmochimica acta*, *57*(5), pp.965-976.

Gribbon, P.W.F., 1979. Cryoconite holes on Sermikavsak, west Greenland. *Journal of Glaciology*, *22*(86), pp.177-181.

Gross, P.M., 1933. The" Salting out" of Non-electrolytes from Aqueous Solutions. *Chemical Reviews*, *13*(1), pp.91-101.

Harvie, C.E. and Weare, J.H., 1980. The prediction of mineral solubilities in natural waters: the Na□ K□ Mg□ Ca□ Cl□ SO4□ H2O system from zero to high concentration at 25° C. *Geochimica et Cosmochimica Acta*, *44*(7), pp.981-997.

Hatzianastassiou, N., Matsoukas, C., Fotiadi, A., Pavlakis, K.G., Drakakis, E., Hatzidimitriou, D. and Vardavas, I., 2005. Global distribution of Earth's surface shortwave radiation budget. *Atmospheric Chemistry and Physics*, *5*(10), pp.2847-2867.

Haynes, W.M., 2014. *CRC handbook of chemistry and physics*. CRC press.

Hedges, J.I., 1992. Global biogeochemical cycles: progress and problems. *Marine chemistry*, *39*(1-3), pp.67-93.

Hodson, A., Anesio, A.M., Tranter, M., Fountain, A., Osborn, M., Priscu, J., Laybourn-Parry, J. and Sattler, B., 2008. Glacial ecosystems. *Ecological monographs*, *78*(1), pp.41-67.

Hodson, A., Bøggild, C., Hanna, E., Huybrechts, P., Langford, H., Cameron, K. and Houldsworth, A., 2010. The cryoconite ecosystem on the Greenland ice sheet. *Annals of Glaciology*, *51*(56), pp.123-129.

Hodson, A., Cameron, K., Bøggild, C., Irvine-Fynn, T., Langford, H., Pearce, D. and Banwart, S., 2010. The structure, biological activity and biogeochemistry of

cryoconite aggregates upon an Arctic valley glacier: Longyearbreen, Svalbard. *Journal of Glaciology*, *56*(196), pp.349-362.

Irvine-Fynn, T.D., Bridge, J.W. and Hodson, A.J., 2011. In situ quantification of supraglacial cryoconite morphodynamics using time-lapse imaging: an example from Svalbard. *Journal of Glaciology*, *57*(204), pp.651-657.

Kaštovská, K., Elster, J., Stibal, M. and Šantrůčková, H., 2005. Microbial assemblages in soil microbial succession after glacial retreat in Svalbard (High Arctic). *Microbial ecology*, *50*(3), p.396.

Kautz, C.H., Heron, P.R., Loverude, M.E. and McDermott, L.C., 2005. Student understanding of the ideal gas law, Part I: A macroscopic perspective. *American Journal of Physics*, *73*(11), pp.1055-1063.

Khan, B., 2016. 'Antarctic CO2 Hit 400 PPM For First Time in 4 Million Years'. *Climate Central*. 15th June 2016. [Online] Available at: http://www.climatecentral.org/news/antarctica-co2-400-ppm-million-years-20451 (Accessed on 21st August 2018).

Langford, H., Hodson, A., Banwart, S. and Bøggild, C., 2010. The microstructure and biogeochemistry of Arctic cryoconite granules. *Annals of Glaciology*, *51*(56), pp.87-94.

Leslie, A., 1879. *The Arctic Voyages of Adolf Erik Nordenskiöld: 1858-1879...* London: Macmillan.

Long, F.A. and McDevit, W.F., 1952. Activity coefficients of nonelectrolyte solutes in aqueous salt solutions. *Chemical reviews*, *51*(1), pp.119-169.

Lutz, S., Anesio, A.M., Jorge Villar, S.E. and Benning, L.G., 2014. Variations of algal communities cause darkening of a Greenland glacier. *FEMS Microbiology Ecology*, *89*(2), pp.402-414.

Lyons, W.B., Welch, K.A., Fountain, A.G., Dana, G.L., Vaughn, B.H. and McKnight, D.M., 2003. Surface glaciochemistry of Taylor Valley, southern Victoria Land, Antarctica and its relationship to stream chemistry. *Hydrological Processes*, *17*(1), pp.115-130.

MacDonell, S. and Fitzsimons, S., 2008. The formation and hydrological significance of cryoconite holes. *Progress in Physical Geography*, *32*(6), pp.595-610.

Marcus, Y. and Hefter, G., 2006. Ion pairing. *Chemical reviews*, *106*(11), pp.4585-4621.

McIntyre, N.F., 1984. Cryoconite hole thermodynamics. *Canadian Journal of Earth Sciences*, *21*(2), pp.152-156.

Millero, F.J., 1992. Stability constants for the formation of rare earth-inorganic complexes as a function of ionic strength. *Geochimica et Cosmochimica Acta*, *56*(8), pp.3123-3132.

Millero, F.J., 1995. Thermodynamics of the carbon dioxide system in the oceans. *Geochimica et Cosmochimica Acta*, *59*(4), pp.661-677.

Mueller, D.R. and Pollard, W.H., 2004. Gradient analysis of cryoconite ecosystems from two polar glaciers. *Polar Biology*, *27*(2), pp.66-74.

Mueller, D.R., Vincent, W.F., Pollard, W.H. and Fritsen, C.H., 2001. Glacial cryoconite ecosystems: a bipolar comparison of algal communities and habitats. *Nova Hedwigia Beiheft*, *123*, pp.173-198.

Nagatsuka, N., Takeuchi, N., Nakano, T., Shin, K. and Kokado, E., 2014. Geographical variations in Sr and Nd isotopic ratios of cryoconite on Asian glaciers. *Environmental Research Letters*, *9*(4), p.045007.

Parkhurst, D.L. and Appelo, C.A.J., 1999. User's guide to PHREEQC (Version 2): A computer program for speciation, batch-reaction, one-dimensional transport, and inverse geochemical calculations.

Parkhurst, D.L. and Appelo, C.A.J., 2013. *Description of input and examples for PHREEQC version 3: a computer program for speciation, batch-reaction, one-dimensional transport, and inverse geochemical calculations* (No. 6-A43). US Geological Survey.

Pearce, D.A., Bridge, P.D., Hughes, K.A., Sattler, B., Psenner, R. and Russell, N.J., 2009. Microorganisms in the atmosphere over Antarctica. *FEMS Microbiology Ecology*, *69*(2), pp.143-157.

Pitzer, K.S., 1973. Thermodynamics of electrolytes. I. Theoretical basis and general equations. *The Journal of Physical Chemistry*, *77*(2), pp.268-277.

Porazinska, D.L., Fountain, A.G., Nylen, T.H., Tranter, M., Virginia, R.A. and Wall, D.H., 2004. The biodiversity and biogeochemistry of cryoconite holes from McMurdo Dry Valley glaciers, Antarctica. *Arctic, Antarctic, and Alpine Research*, *36*(1), pp.84-91.

Richardson, C., 1976. Phase relationships in sea ice as a function of temperature. *Journal of Glaciology*, *17*(77), pp.507-519.

Robinson, R.A. and Stokes, R.H., 2002. *Electrolyte solutions*. Courier Corporation.

Säwström, C., Mumford, P., Marshall, W., Hodson, A. and Laybourn-Parry, J., 2002. The microbial communities and primary productivity of cryoconite holes in an Arctic glacier (Svalbard 79 N). *Polar Biology*, *25*(8), pp.591-596.

Smith, A.M., Bentley, C.R., Bingham, R.G. and Jordan, T.A., 2012. Rapid subglacial erosion beneath Pine Island glacier, west Antarctica. *Geophysical Research Letters*, *39*(12).

Steinbock, O., 1936. Cryoconite holes and their biological significance. *Zeitschrift fur Gletscherkunde*, *24*, pp.1-21.

Stumm, W. and Morgan, J.J., 1970. *Aquatic chemistry; an introduction emphasizing chemical equilibria in natural waters*.

Takeuchi, N., 2000. Characteristics of cryoconite holes on a Himalayan glacier, Yala Glacier Central Nepal. *Bull. Glaciol. Res.*, *17*, pp.51-59.

Telling, J., Anesio, A.M., Tranter, M., Fountain, A.G., Nylen, T., Hawkings, J., Singh, V.B., Kaur, P., Musilova, M. and Wadham, J.L., 2014. Spring thaw ionic pulses boost nutrient availability and microbial growth in entombed Antarctic Dry Valley cryoconite holes. *Frontiers in microbiology*, *5*, p.694.

Tranter, M., Fountain, A.G., Fritsen, C.H., Lyons, W.B., Priscu, J.C., Statham, P.J. and Welch, K.A., 2004. Extreme hydrochemical conditions in natural microcosms entombed within Antarctic ice. Hydrological Processes, 18(2), pp.379-387.

Tranter, M., Fountain, A.G., Fritsen, C.H., Lyons, W.B., Priscu, J.C., Statham, P.J. and Welch, K.A., 2005. Perturbation of Hydrochemical Conditions in Natural Microcosms Entombed within Antarctic Ice. *Ice and Climate News*, pp.21-23

Wharton Jr, R.A., McKay, C.P., Simmons Jr, G.M. and Parker, B.C., 1985. Cryoconite holes on glaciers. *BioScience*, pp.499-503.

Wharton Jr, R.A., Vinyard, W.C., Parker, B.C., Simmons Jr, G.M. and Seaburg, K.G., 1981. Algae in cryoconite holes on Canada Glacier in southern Victorialand, Antarctica. *Phycologia*, *20*(2), pp.208-211.

Zhang, A.Y., Yao, Y., Li, L.J. and Song, P.S., 2005. Isopiestic determination of the osmotic coefficients and Pitzer model representation for Li2B4O7 (aq) at T= 298.15 K. *The Journal of Chemical Thermodynamics*, *37*(2), pp.101-109.

# Appendix

Appendix 1 – Factors of increase required in F-Open (Pitzer)

| Ca | DIC |
|---|---|
| 2 | 1.53 |
| 2 | 1.685 |
| 2 | 1.815 |
| 2 | 1.897 |
| 2 | 1.94 |
| 1.4 | 1.3845 |
| 1.2686 | 0.9591 |
| 1.4291 | 0.9253 |
| 1.6273 | 0.9163 |
| 1.7881 | 0.9046 |
| 1.8946 | 0.9216 |
| 1.9512 | 0.972 |
| 1.977 | 1.024 |
| 1.98868 | 1.055 |
| 1.99482 | 1.128 |
| 1.99786 | 1.18 |
| 2.0002 | 1.173 |

Appendix 2 – Factors of increase required In F-Open (Debye-Huckel)

| Ca | DIC |
|---|---|
| 2 | 1.53 |
| 2 | 1.685 |
| 2 | 1.815 |
| 2 | 1.897 |
| 2 | 1.94 |
| 1.37 | 1.355 |
| 1.271033 | 0.962924 |
| 1.424576 | 0.918992 |
| 1.61795 | 0.887 |
| 1.788405 | 0.87476 |
| 1.8959 | 0.8671 |
| 1.95235 | 0.8671 |
| 1.97877 | 0.8671 |
| 1.99052 | 0.8664 |
| 1.99555 | 0.834 |
| 1.99783 | 0.795 |
| 1.99902 | 0.903 |

Appendix 3 - Factors of increase of both Ca and DIC required in B-Closed

| Pitzer | Debye-Huckel |
|---|---|
| 2 | 2 |
| 2 | 2 |
| 2 | 2 |
| 1.025 | 1.01 |
| 1.911 | 1.91 |
| 1.878 | 1.874 |
| 1.812 | 1.801 |
| 1.767 | 1.75 |
| 1.764 | 1.741 |
| 1.792 | 1.765 |
| 1.832 | 1.805 |
| 1.875 | 1.85 |
| 1.91 | 1.891 |
| 1.937 | 1.936 |
| 1.955 | 2.005 |
| 1.965 | 2.431 |
| 1.911 | |

Appendix 4 – Factors of increase of both Ca and DIC required in F-Closed

| Pitzer | Debye-Huckel |
|---|---|
| 2 | 2 |
| 2 | 2 |
| 2 | 2 |
| 2 | 2 |
| 1.98 | 1.95 |
| 1.869 | 1.866 |
| 1.811 | 1.806 |
| 1.748 | 1.732 |
| 1.718 | 1.695 |
| 1.727 | 1.703 |
| 1.768 | 1.735 |
| 1.815 | 1.778 |
| 1.86 | 1.828 |
| 1.902 | 1.872 |
| 1.93 | 1.914 |
| 1.95 | 0.00373 |
| 1.958 | |

Appendix 5 - Factors of increase required in B-Headspace

| Ca | DIC |
|---|---|
| 2 | 1.997059 |
| 2 | 1.994729 |
| 2 | 1.991193 |
| 1.952 | 1.92769 |
| 1.726 | 1.605193 |
| 1.618 | 1.359313 |
| 1.786578 | 1.100151 |

Appendix 6 - Factors of increase required in F-Headspace

| Ca | DIC |
|---|---|
| 2 | 1.989969 |
| 2 | 1.98286 |
| 2 | 1.974195 |
| 2 | 1.967232 |
| 2 | 1.96545 |
| 1.84 | 1.765398 |
| 1.702365 | 1.087292 |